

**Атомная  
Энергия**

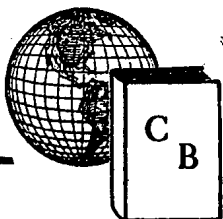
Volume 3, Number 8, 1957

*ref*

**The Soviet Journal of**

**ATOMIC  
ENERGY**

**IN ENGLISH TRANSLATION**



**CONSULTANTS BUREAU, INC.**

227 WEST 17TH STREET, NEW YORK 11, N. Y.

ATOMNAYA ENERGIYA

Academy of Sciences of the USSR

Volume 3, Number 8, 1957

EDITORIAL BOARD

A. I. Alikhanov, A. A. Bochvar, V. I. Veksler, A. P. Vinogradov,  
N. A. Vlasov (Acting Editor in Chief), V. S. Emelyanov, V. F. Kalinin,  
G. V. Kurdyumov, A. V. Lebedinsky, I. I. Novikov (Editor in Chief),  
B. V. Semenov (Executive Secretary), V. S. Fursov

---

The Soviet Journal

of

ATOMIC ENERGY

IN ENGLISH TRANSLATION

Copyright, 1958

CONSULTANTS BUREAU, INC.

227 West 17th Street

New York 11, N. Y.

Printed in the United States

Annual Subscription \$ 75.00  
Single Issue 20.00

Note: The sale of photostatic copies of any portion of this copyright translation is expressly prohibited by the copyright owners. A complete copy of any article in the issue may be purchased from the publisher for \$12.50.

THE LENIN PRIZE FOR THE CONSTRUCTION OF THE  
FIRST ATOMIC POWER STATION

By a decree of the Lenin Prize Committee of the USSR Soviet of Ministers, D. I. Blokhintsev, N. A. Dollezhal, A. K. Krasin and V. A. Malukh have been awarded the Lenin Prize for the construction of the first Soviet atomic power station.

The opening of the atomic power station has initiated a new branch of technology -- nuclear engineering. The work of the group of scientists and engineers led by D. I. Blokhintsev, N. A. Dollezhal, A. K. Krasin and V. A. Malukh, as well as that of a number of allied organizations, was very successful -- the first Soviet atomic power station already has been working without interruption for more than three years.

Turning to the history of the creation of the station, it must be noted that in 1949, at the time when its planning was started, there was already a large group of scientists and engineers in the Soviet Union familiar with the production and use of fissile materials. However, a large number of questions connected with the power engineering aspects of atomic energy remained unanswered. This situation was also present in connection with the evaluation of the physical characteristics of a reactor, the choice of new materials, the production of a sufficiently durable reactor fuel element, the development of a dependable construction for the reactor and its thermal circuit enabling safe and easy servicing, as well as a number of other problems.

At the time doubts were expressed abroad that the construction of an atomic power station was at all advantageous, since it was considered that the engineering difficulties in constructing one would be too big while the electric power produced would not be able to compete in price with the electric power produced by the burning of conventional fuels. Now such questions do not arouse doubts in anyone. The unusually swift development of the building of power reactors in the world serves as evidence for this. In the Soviet Union, as well as abroad, a large number of high-power nuclear reactors of various types and uses are being planned and constructed. Therefore, one of the chief results of the creation of the first atomic power station is that Soviet scientists and engineers were the first in the world to pave the way for the use of nuclear fission in power engineering and proved the possibility of a successful solution of those problems which appeared to be almost insurmountable.

The successes of the Soviet Union in the field of nuclear engineering would have been impossible without advances in the other branches of science and industry which directly or indirectly prepared technically the possibility for the creation of this unique establishment. The progress of nuclear engineering is due to machine construction, ferrous and non-ferrous metallurgy, electrical and radio engineering, electronics, instrument making, chemistry, geology and a large number of other branches of knowledge.

After the problem of planning and constructing a small atomic power station was set, first of all it was necessary to choose the type and output of the reactor. It was decided to settle on the heterogeneous-type reactor with tubular channels. By comparison with the pressure-vessel type, this variant has a number of advantages.\* In addition, the absence of a vessel under pressure considerably simplifies the problem of experimentally testing the construction of the various channels, control rods, the setting up of test loops for checking the behavior of coolants (with various parameters) and fuel elements.

The thermal and electric power outputs of the reactor were chosen as the result of a compromise solution since, on the one hand, it was necessary to have a station on a semi-industrial scale so that the operating experience

\* See JAE-1, 10, 1956.

gained with it could be extrapolated to some extent, in the future, to a more powerful station of the same type and, on the other hand, to plan and construct a station in the shortest possible time at minimum cost.

It must be noted that both in the planning of the first atomic power station and in the planning of more powerful atomic power stations, the main difficulties are not so much in the physical calculations, which are chiefly evaluations, however complicated and laborious, of design solutions arrived at by the constructors, but are in the choice of materials to be used and in the making of constructions satisfying the strict requirements imposed. Therefore, in the course of planning the station a considerable number of experimental investigations were carried out to check the theoretical calculations, as well as to complete the design of the various units and construction components.

The construction of the atomic power station is an instructive example of the creative cooperation of many specialists: designers, physicists, combustion engineers, technologists, chemists, fitters, builders, etc. In carrying out such a complex project, where all of the components of the atomic power station are organically interrelated so that changing one of them leads to changes in the others, it is difficult to isolate a main trend or a main problem on whose solution depended the successful completion of the work. It is only possible to record the main consecutive stages of the work leading to the construction of this unique establishment.

The chief component of an atomic power station is the reactor. The main stage of the work, consequently, consisted in choosing on the basis of the initial developmental work the most suitable form for the reactor. At the same time, this involved the choice of the method for supplying the coolant to the reactor, the arrangement of the working channels containing the fuel elements, the construction of the reactor core, the type and spacing of the lattice, the size of the control rods, etc. The design chosen, in spite of the small size of the active zone, enabled the use of uranium with fairly low enrichment, and, primarily, proved to be for sighted because starting from it a more powerful reactor, using less enriched fuel, can be developed. Such a station will be built in the Soviet Union during the sixth five-year plan.

This stage of the work was also concerned with the initial physical calculation of the reactor parameters and the aim was to evaluate in the shortest possible time the solutions chosen by the constructors. The close cooperation of the physicists and the constructors must also be pointed out here as all the problems were solved jointly.

In the second stage of the work, during the phase of technical planning, considerable difficulties were also met, in the course of surmounting which many original construction solutions were found.

Here is a far from complete list of the problems which were encountered by the constructors and which were successfully solved: the design of the reactor core, the choice of temperature limits giving the optimum working conditions, the development of the unusual working-channel design which provides an automatic compensation for nonuniform thermal expansion of the tubes, the assembly of the components and joints under conditions of small clearances, the design of the upper part of the reactor with its arrangement of pipes supplying and discharging water, the provision for the automatic functioning of the channel and easy access for removing and placing it into the reactor, the sealing of the reactor in such a way that it remains hermetically sealed during thermal expansions of its components, and a large number of other problems.

In the course of the construction work a large number of preliminary engineering calculations were made referring to the variants of the reactor, its principal components and thermal circuit and more detailed calculations referring to the reactor variant chosen. To check the results of the thermal calculations, thermocouples were placed in various locations in the reactor and their readings, after the reactor was placed on full power, confirmed the correctness of the calculations made.

As the work on planning the station progressed the methods used in the physical calculations were improved and expanded. Initially, during the first stage of the work, the calculations made (using the two-group method) were of a trial nature, while later, during the technological and operating phase, it was necessary to take into account finer details which required a considerable refinement of the methods of calculations, for example, allowing for the reactions in the intermediate energy range and, during the later stages when dealing with the reactor variant chosen, taking into account the effect of the accumulating  $\text{Pu}^{241}$ . The accuracy of the results obtained with the two-group method were checked in a number of cases by a new multigroup method. In addition, new variational methods were developed to evaluate the behavior of the compensating rods, etc.



D. I. Blokhintsev



N. A. Dollezhal



A. K. Krasin



V. A. Malukh

Considerable difficulties were also met in carrying out the physical calculations in planning the emergency reactor routines and matching the physical characteristics of the reactor with the characteristics of the thermal circuit and equipment, for example, determining the switching time of the main circulation pumps to emergency operation and determining the wearing properties of the cut-off devices which prevent the accidental filling of the core with water. The latter circumstance is of considerable importance for the safe working of the reactor since the reactor is very sensitive to the total volume of water contained in the active zone.

The difficulties of the physical calculation were also aggravated by the fact that, at the time, accurate data on a number of fundamental physical constants were absent. However, as soon as these data became available fresh calculations were made.

The starting up and the operation of the atomic power station have shown the good agreement between the experimental and theoretical data.

One of the very important problems, on which also depended the efficiency of the reactor, was the development of a reliable fuel element.

The fuel elements of a reactor must operate at a neutron flux of the order of  $\sim 10^{13}$  neutrons/cm<sup>2</sup> sec, at a temperature higher than 300° C and a thermal flux of up to  $2 \times 10^6$  kcal/m<sup>2</sup> hour. An added difficulty was the fact that at these temperatures the reaction of the uranium with the materials of the fuel elements markedly increases and this leads to their rapid breakdown.

The easiest way out could have been taken, i.e., to increase the thickness of the tubes carrying the pressurized water and the thickness of the fuel-element sheath. However, this solution was unsuitable since an increase in the amount of constructional materials in the active zone would have led to a considerable increase of the enrichment of the uranium. Further, the construction of the fuel elements must be suitable technologically since, firstly, it was necessary to develop techniques for their mass production and, secondly, the atomic power station reactor was considered as a prototype reactor for a more powerful atomic power station requiring an immense number of fuel elements.

As a result of long and mainly experimental investigations a reliable construction was finally evolved. Samples of fuel elements of various types and constructions were tested. The first stage of the testing was carried out in the laboratory where the heat produced in the fuel element was simulated by passing an electric current through it. The laboratory investigations helped in designing the fuel elements.

The second, final stage was carried out using the circuit of the experimental RFT reactor. The various types of fuel elements that had passed the laboratory tests were studied. As a result of this work preference was given to one of the fuel-element types which can be manufactured more easily than the others. During the three-years' operation of the atomic power station this choice proved to be completely justified. Only the main aspects of the work connected with the creation of the atomic power station are listed above. However, no less important was other intricate work which, in the long run, enabled the construction of the atomic power station. This included the design of the reactor control system, the development of techniques for manufacturing high-quality thin-walled tubes from stainless steel, the construction of many regulating and measuring devices, etc.

It must be understood that the work in connection with the atomic power station was not limited to designing the construction and carrying out numerous theoretical and experimental investigations. It was necessary to erect the station, to put it into operation and to learn how to operate it properly. At this stage considerable difficulties were met. It was necessary to carry out the complicated erection of the reactor (particularly of its upper part), to put the reactor into operation checking its various characteristics and, finally, to determine at full power the optimum operating conditions for the water coolant, the graphite assembly, etc. The work to improve the operating performance of the reactor is also being carried out at the present time by the group of associates of the atomic power station.

The names of those who have been honored with the Lenin Prize, of course, do not exhaust the list of all the specialists that took part in the construction of the atomic power station. The first atomic power station in the world was built in a remarkably short period of time — 4.5 years, since effectively work started at the end of 1949 — by the efforts of many scientists and engineers at whose disposal was the complete arsenal of modern technical resources.

It is hard to overestimate the significance of the atomic power station in connection with the development of nuclear engineering in the Soviet Union. Scientists and engineers constructing new power stations often make use of the experience gained during the planning and operation of the first atomic power station. In this respect it is a valuable source of information on various aspects of the operation of high-energy water-graphite reactors. However, an important point must be noted. It would be fallacious to assume that the future growth of nuclear engineering associated with the use of reactors of this type will simply consist of increasing the power output by building stations on a bigger scale and increasing the parameters of the first atomic power station. Of course, this is not the case. Firstly, because of the rapid growth of nuclear engineering and its remarkable progress in the last few years this station already cannot be regarded as ideal, satisfying modern requirements (chiefly with respect to its efficiency and the parameters of the steam produced). Secondly, in designing a more powerful atomic power station, intended to produce steam with higher parameters, not only do the difficulties increase but there also arise a number of new fundamental problems which cannot be solved by extrapolating from the first Soviet atomic power station.

Such problems, for example, are the obtaining of new construction materials, the treatment in large numbers of spent fuel elements, the fuel cycles, the removal of radioactive waste, etc.

The first Soviet atomic power station has enabled only the first page to be read from the book of endless questions and problems connected with the development of nuclear engineering. To reach the end of this book is impossible, inasmuch as it is impossible to know completely all the laws of nature. However, that which was accomplished by the large force of Soviet specialists, led by the Lenin-Prize laureates D. I. Blokhintsev, N. A. Dollezhal, A. K. Krasin and V. A. Malukh, is a valuable contribution to the solution of the problem facing mankind - to place the inexhaustible energy of the atom at the service of Man.

Yu. K.

NUCLEAR MULTIPLETS IN LIGHT ODD-ODD NUCLEI AND THEIR  
MANIFESTATION IN  $\gamma$ -TRANSITIONS OCCURRING AFTER  
THERMAL NEUTRON CAPTURE\*

L. V. Groshev and A. M. Demidov

We consider those states of odd-odd nuclei with  $A < 60$  which differ in their total angular momentum  $J$ , but whose configurations contain an odd proton and an odd neutron with given angular momenta  $j_p$  and  $j_n$ . We review the experimental data on the basis of which one may assume the existence of such nuclear multiplets lying close to the ground states. We compare the  $\gamma$ -decay schemes of those states of even-odd (odd neutron) and odd-odd nuclei with  $A < 60$  which arise as a result of the capture of thermal neutrons. The characteristics of  $\gamma$ -transitions in odd-odd nuclei are explained on the basis of multiplet concepts.

In recent years there have appeared many works [1]-[3] in which the energy and intensity of  $\gamma$ -rays emitted on capture of thermal neutrons have been measured in various ways. In addition, as a result of studies of  $\beta$ -decay and of nuclear reactions induced by charged particles, much data on the energies and other characteristics of nuclear levels has been compiled. The totality of this data makes it possible to construct sufficiently reliable  $\gamma$ -transition decay schemes for nuclei with  $A < 60$  which result from thermal neutron capture.

The  $\gamma$ -decay schemes of such nuclei were discussed by Kinsey and Bartolomew [1] in 1954. They come to the conclusion that the initial states of these nuclei, which are formed by capture of a thermal neutron, decay primarily by means of E1 and M1 transitions. Noting that in  $(n, \gamma)$  reactions on natural mixtures of isotopes, primarily even-odd (odd number of neutrons) and odd-odd nuclei are produced when  $A < 60$ , the authors go into a detailed discussion of  $\gamma$ -transitions of even-odd nuclei. They come to the conclusion that in these nuclei  $\gamma$ -transitions to  $2p_{3/2}$  and  $2p_{1/2}$  levels are the most intense.

Measurements of the  $\gamma$ -ray spectra from  $(n, \gamma)$  reactions, which were performed in our laboratory with the aid of a Compton spectrometer in a wide  $\gamma$ -energy range [2], make it possible to attain greater accuracy in the  $\gamma$ -transitions schemes in even-odd nuclei and to arrive at more reliable conclusions about these transition schemes in odd-odd nuclei. At the same time, new data on the characteristics of nuclear levels, including those of odd-odd nuclei, has appeared in the literature. A comparison of all this data makes it possible to establish certain definite rules.

Below we present the data on the lower levels of light ( $A \leq 60$ ) odd-odd nuclei and discuss the question of their  $\gamma$ -transitions.

In treating odd-odd nuclei, we shall start with the assumption that the states of these nuclei are determined by the characteristics of the odd proton and odd neutron. In addition, we shall assume that one may speak of the total angular momentum  $\vec{j} = \vec{l} + \vec{s}$  of an odd nucleon.

\* Presented at the All-Union Conference on Nuclear Spectroscopy in Leningrad (January, 1957).



It is clear that these assumptions will not be valid in all cases. One may suppose, however, that in the neighborhood of the nuclear ground state they are valid for most cases.

Let us consider some nuclear configuration with given angular momenta for the odd proton ( $j_p$ ) and the odd neutron ( $j_n$ ). For such a configuration there should exist several states differing in their total angular momentum  $J$  but having the same parity, where  $J$  must satisfy the condition  $j_p + j_n \geq J \geq |j_p - j_n|$ . The number of such states should be  $2j + 1$ , where  $j$  is the lesser of  $j_p$  and  $j_n$ . Due to the interaction between the odd nucleons, which is different for different values of  $J$ , these states will not have the same energy. We shall call a set of such states a nuclear multiplet. If such multiplets exist, the most clearly observed ones should be those including the ground states of odd-odd nuclei. In this case, the characteristics of the odd proton and odd neutron are as a rule known from the characteristics of the ground states of the neighboring odd-even and even-odd nuclei.

The existing data on this question, though far from exhaustive, nevertheless indicate the existence of nuclear multiplets quite convincingly in odd-odd nuclei. Let us now consider this data.\*

## I

If the proton or neutron in an odd-odd nucleus has angular momentum  $1/2$ , then there should be a doublet lying close to the ground state. Among such nuclei, in particular, are  $Al^{28}$  and all the isotopes of phosphorus. Doublets with small separations were established long ago for  $Al^{28}$  and  $P^{32}$ .

In Table 1 we present the doublets which can be separated out on the basis of existing level schemes. In the upper part of the Table we present nuclei whose odd proton and odd neutron have different values of  $l$ , and in the lower part of the Table we present those with equal  $l$ .

The excited state closest to the doublet in  $Al^{28}$  and  $P^{32}$  is at 0.97 and 0.57 Mev, respectively. In these cases the nuclear doublets are very clearly observed.

TABLE 1

Nucleus	Configuration		Characteristics of the state		doublet energy, kev
	p	n	ground state	first excited state	
$Al^{28}$	$d_{5/2}^{-1}$	$s_{1/2}$	$3^+$	$2^+$	29
$P^{32}$	$s_{1/2}$	$d_{3/2}$	$1^+$	$2^+$	77
$N^{16}$	$p_{1/2}$	$d_{5/2}$	$2^-$	$3^-$	300
$P^{30}$	$s_{1/2}$	$s_{1/2}$	$1^+$	$0^+$	688
$N^{14}$	$p_{1/2}$	$p_{1/2}$	$1^+$	$0^+$	2310

In the  $N^{16}$  nucleus the  $p_{1/2}$ ,  $d_{5/2}$  and  $p_{1/2}$ ,  $s_{1/2}$  states hardly differ in energy. Here the two doublets overlap creating four levels whose characteristics are  $2^-$ ,  $0^-$ ,  $3^-$ ,  $1^-$  and whose energies are 0, 113, 300, 390 kev [7].

In the  $N^{14}$  and  $P^{30}$  nuclei the energy of the excited state above the doublet is 3.95 and 1.14 Mev, respectively.

From Table 1 it is seen that the interaction between the odd proton and neutron is small if they have different  $l$ ; it is significantly greater if the odd nucleons have the same  $l$ .

If the angular momenta of the odd proton and neutron are equal to or greater than  $3/2$ , one may expect that the ground state will occur in a higher

multiplet. At present several cases are known in which there exist complex multiplets well separated from the other levels. They are observed if the odd proton and neutron have different  $l$  in the ground state.

Figure 1 gives the level schemes of  $Cl^{38}$  and  $K^{40}$ , as well as  $Ca^{41}$  for comparison.

In both  $K^{40}$  and  $Ca^{41}$  the odd neutron is in the  $1f_{7/2}$  state. As has been shown by Demidov [8], the  $2p_{3/2}$  levels in these nuclei, which can be identified from the fact that the stripping (d, p) reaction passes through them with high probability, have about the same excitation energy. The presently existing data on the (d, p) reaction shows that this assertion is valid for a larger set of nuclei. In Table 2 we present a list of nuclei whose odd neutron is in one of the states  $f_{7/2}^{\pm 1}$ ,  $f_{7/2}^{\pm 3}$ . The  $2p_{3/2}$  level in all these nuclei has about the same excitation energy.

\* References to the literature are given only if the data is not included in previous reviews [4 - 6].

TABLE 2

Nucleus	Ground state configuration	2p <sub>3/2</sub> level excitation energy, Mev
<sup>38</sup> Cl <sub>21</sub> <sup>17</sup>	d <sub>3/2</sub> <sup>-1</sup> f <sub>7/2</sub>	≥ 1.62 [9]
<sup>41</sup> K <sub>23</sub> <sup>18</sup>	d <sub>5/2</sub> <sup>2</sup> f <sub>7/2</sub> <sup>3</sup>	1.40 [10]
<sup>40</sup> K <sub>21</sub> <sup>19</sup>	d <sub>3/2</sub> <sup>-1</sup> f <sub>7/2</sub>	2.06 [11]
<sup>41</sup> Ca <sub>21</sub> <sup>20</sup>	— f <sub>7/2</sub>	1.95 [12]
<sup>43</sup> Ca <sub>23</sub> <sup>20</sup>	— f <sub>7/2</sub> <sup>3</sup>	2.05 [12]
<sup>45</sup> Ca <sub>25</sub> <sup>20</sup>	— f <sub>7/2</sub> <sup>-3</sup>	1.89 [12]
<sup>49</sup> Ti <sub>27</sub> <sup>22</sup>	f <sub>7/2</sub> <sup>2</sup> f <sub>7/2</sub> <sup>-1</sup>	1.40 [13]

multiplet. The energy levels of Cl<sup>38</sup> calculated in this way are shown in Table 3. These are compared with the Cl<sup>38</sup> level energies recently obtained [9] by magnetic analysis of the products from the Cl<sup>37</sup>(d, p)Cl<sup>38</sup> reaction. As can be seen from the Table, good agreement is obtained for the experimental and theoretical results. Similar results have recently been obtained by Pandya [15].

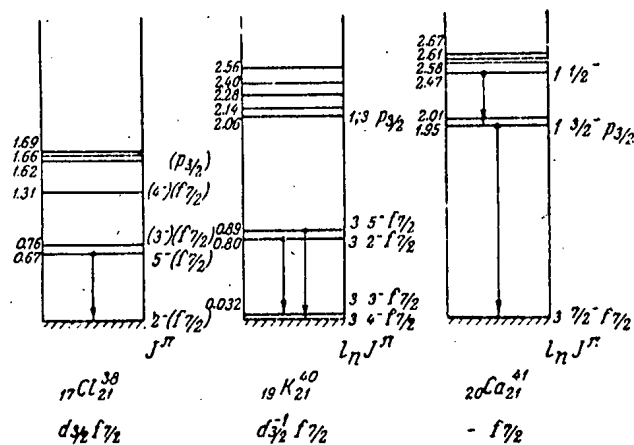


Fig. 1. Level scheme of low-lying Cl<sup>38</sup>, K<sup>40</sup>, and Ca<sup>41</sup> levels.

TABLE 3

	E Mev	J $\pi$	E Mev	J $\pi$	E Mev	J $\pi$	E Mev	J $\pi$
Calculated from K <sup>40</sup>	0	2 <sup>-</sup>	0.70	5	0.75	3	1.32	4 <sup>-</sup>
Experimental data	0	2 <sup>-</sup>	0.672	5 <sup>-</sup>	0.762	—	1.312	—

In Ca<sup>41</sup> this level corresponds to the first excited state, with energy 1.95 Mev. As opposed to Ca<sup>41</sup>, the odd-odd nucleus K<sup>40</sup> has three lower lying levels. Experiments on the (d, p) reaction on K<sup>39</sup> show that these levels and the ground state have the same parity, and that the total angular momentum J lies in the interval j<sub>p</sub> + j<sub>n</sub> ≥ J ≥ |j<sub>p</sub> - j<sub>n</sub>| (see Fig. 1).

Thus the group of four K<sup>40</sup> levels may be treated as a multiplet of the d<sub>3/2</sub><sup>1</sup> f<sub>7/2</sub> configuration. An analogous d<sub>3/2</sub> f<sub>7/2</sub> configuration occurs in Cl<sup>38</sup>. Recently Goldstein and Talmi [14], assuming that the radial functions in these two configurations are the same, have established a linear dependence between the energy intervals ΔE for the multiplets of the d<sub>3/2</sub><sup>1</sup> f<sub>7/2</sub> and d<sub>3/2</sub> f<sub>7/2</sub> configurations. Taking the experimental value of ΔE for the K<sup>40</sup> multiplet, they obtained the corresponding values of ΔE for the Cl<sup>38</sup>

The levels of the odd-odd nuclei Na<sup>24</sup> and Cl<sup>36</sup> have been studied rather thoroughly; their ground state configurations are (d<sub>5/2</sub><sup>3</sup>)<sub>3/2</sub> d<sub>5/2</sub><sup>-1</sup> and d<sub>3/2</sub> d<sub>3/2</sub><sup>1</sup>.

In the production of these nuclei as a result of the (d, p) reaction, however, a neutron with orbital angular momentum l<sub>n</sub> = 2 is captured only into the first excited or ground state. In the second and third excited states, l<sub>n</sub> = 0 so that the neutron is captured in the s rather than in the d state. This may be related to the fact that due to the strong interaction between the odd proton and neutron for equal l (the energy of the first excited state is 470 kev in Na<sup>24</sup>, and 770 kev in Cl<sup>36</sup>) the multiplet overlaps other levels and its other two components lie much higher.

A similar pattern emerges for multiplets of six components, such as in Al<sup>26</sup> whose ground state configuration is d<sub>5/2</sub><sup>-1</sup> d<sub>5/2</sub><sup>-1</sup>. We shall consider this nucleus in Section III.

II

Let us note yet another property in the level distribution of odd-odd nuclei which seem to be related to the existence of nuclear multiplets. Among the levels of a given complicated multiplet belonging to a single configuration there may occur states whose angular momenta differ by 3, 4, or 5. This may lead to the occurrence of isomerism which differs from

ordinary isomerism in which the transitions are between levels with widely differing  $l$ . Such isomers, as is well known, are located in "islands" just below the magic numbers. The first such island occurs when  $N$  or  $Z \geq 39$  ( $A \geq 69$ ). Table 4 presents the level characteristics of light odd-odd nuclei with  $A \leq 60$  among which isomer transitions take place. All these nuclei are located in the low  $A$  direction from the first island of isomerism. From Table 4 it can be seen that the angular momenta of all states taking part in isomer transitions agree with the condition  $j_p + j_n \leq J \leq |j_p - j_n|$ , and that all transitions occur without parity changes.

No isomerism is observed in  $Al^{28}$  or phosphorus isotopes, which have nuclear doublets with  $\Delta J = 1$ . With a suitable level distribution, it may also be absent in the case of a complex multiplet, as for instance in  $K^{40}$  (see Fig. 1).

TABLE 4

Nucleus	Ground state configuration [16]		Level characteristics	
	$p$	$n$	isomer level	ground state
$11 Na^{22}_{11}$	$d_{5/2}^3$	$d_{5/2}^3$	$(0^+)$	$3^+$
$11 Na^{24}_{13}$	$d_{5/2}^3$	$d_{5/2}^{-1}$	$1^+$	$4^+$
$13 Al^{26}_{13}$	$d_{5/2}^{-1}$	$d_{5/2}^{-1}$	$0^+$	$5^+$
$17 Cl^{31}_{17}$	$d_{3/2}$	$d_{3/2}$	$3^+$	$0^+$
$17 Cl^{38}_{21}$	$d_{3/2}$	$f_{7/2}$	$5^-$	$2^-$
$19 K^{38}_{19}$	$d_{3/2}^{-1}$	$d_{3/2}^{-1}$	$3^+$	$0^+$
$21 Sc^{44}_{23}$	$f_{7/2}$	$f_{7/2}^3$	$6, 7^+$	$2, 3^+$
$21 Sc^{46}_{25}$	$f_{7/2}$	$f_{7/2}^5$	$7^+$	$4^+$
$25 Mn^{52}_{27}$	$f_{7/2}^5$	$f_{7/2}^{-1}$	$2^+$	$6^+$
$27 Co^{58}_{27}$	$f_{7/2}^{-1}$	$p_{3/2}^{-1}$	$5^+$	$2^+$
$27 Co^{60}_{33}$	$f_{7/2}^{-1}$	$p_{3/2}^{-1}$	$2^+$	$5^+$

III

Let us consider separately the question of multiplets in odd-odd nuclei with  $N = Z$ . Table 5 contains data on nuclei belonging to this category. The second column gives the ground state configurations. The next column gives the level characteristics of the ground state and the closest lying excited states.

It has often been noted [18] that odd- $J$  levels in odd-odd nuclei with  $N = Z$  have even isotopic spin  $T$ , and vice versa. It is also known [19] that in odd-odd nuclei with  $T_z = 0$ , the energy difference between the lowest states with  $T = 1$  and  $T = 0$  is much less than in even-even nuclei with  $A = 4n$ . As  $A$  increases this difference decreases.

Figure 2 shows the difference  $\Delta E = E_{\uparrow\uparrow} - E_{\downarrow\downarrow}$  in the binding energy as a function of the atomic number for the two states in which the angular momenta  $j_p$  and  $j_n$  are parallel ( $J = 2j$ ,  $T = 0$ ) or anti-parallel ( $J = 0$ ,  $T = 1$ ). In all cases except that of  $Li^6$ ,  $\Delta E = E_{\uparrow\uparrow} - E_{\downarrow\downarrow}$  agrees with the energy separation of low states with  $T = 0$  and  $T = 1$  ( $-\Delta E = E_{T=0} - E_{T=1}$ ). It is seen from Fig. 2 that  $\Delta E$  changes sign at  $A \sim 34$ . When  $A > 34$  the ground state is that in which  $T = 1$  (see Table 5). In addition to the nuclei included in the Table ( $Cl^{34}$ ,  $K^{38}$ ,  $Sc^{42}$  [20] and  $Co^{54}$  [21]),  $Mn^{50}$  and possibly  $V^{46}$  [21] have a ground state whose angular momentum is  $J = 0^+$ .

From the examples of complex multiplets presented in Table 5, it is seen that all their lower components have odd  $J$  or  $J = 0^+$ . The missing even components lie much higher, which is related to the charge-independence of nuclear forces. Let us compare an odd-odd nucleus for which  $N = Z$  with a neighboring even-even nucleus with  $T_z = \pm 1$  ( $N' - Z' = \pm 2$ ). The ground states of such nuclei are  $0^+$  states and have  $T = 1$ . These states and the component of a multiplet with  $J = 0^+$  and  $T = 1$  in one of the nuclei being considered comprise an isobaric triplet. Therefore the  $2^+$  component of the multiplet should lie no

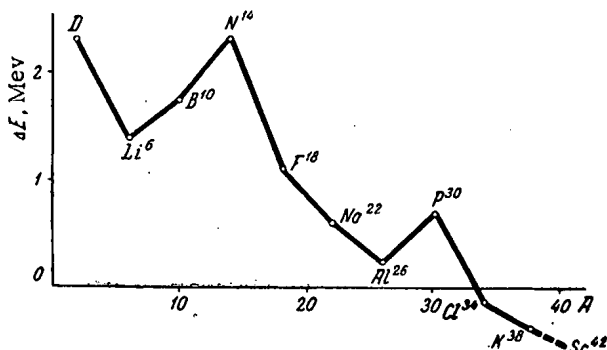


Fig. 2. The dependence of  $\Delta E = E_{\uparrow\uparrow} - E_{\downarrow\downarrow}$  on atomic weight for odd-odd nuclei with  $N = Z$ .

further below the  $0^+$  state than the first  $2^+$  level in a neighboring even-even nucleus with  $T_z = \pm 1$ . If the  $2^+$  component of a multiplet arises in the same way as in an odd-odd nucleus, it will either coincide with this level,

or it will lie above it if the latter arises in some other way. A similar conclusion may be reached also for the  $4^+$  component in more complex nuclear multiplets.

TABLE 5

Nucleus	ground state configuration		Level characteristics					
	p	n	$J^\pi$	ground state	first excited state	second excited state	third excited state	
D	$s_{1/2}$	$s_{1/2}$	$J^\pi$ $T$	$1^+$ 0	$0^{+*}$ 1			
Li <sup>6</sup>	$p_{3/2}$	$p_{3/2}$	$J^\pi$ $T$	$1^+$ 0	$3^+$ 0	$0^+$ 1		$2^+$ higher ***
B <sup>10</sup>	$p_{3/2}^{-1}$	$p_{3/2}^{-1}$	$J^\pi$ $T$	$3^+$ 0	$1^+$ 0	$0^+$ 1		$2^+$ higher
N <sup>14</sup>	$p_{1/2}$	$p_{1/2}$	$J^\pi$ $T$	$1^+$ 0	$0^+$ 1			
F <sup>18</sup>	$s_{1/2}$	$s_{1/2}$	$J^\pi$ $T$	$1^+$ 0	$0^+$ 1			
Na <sup>22</sup>	$d_{5/2}^3$	$d_{5/2}^3$	$J^\pi$ $T$	$3^+$ 0	$0^+$ 1	**		
Al <sup>26</sup>	$d_{5/2}^{-1}$	$d_{5/2}^{-1}$	$J^\pi$ $T$	$5^+$ 0	$0^+$ 1	$3^+$ 0	$1^+$ 0	$2, 4^+$ higher
P <sup>30</sup>	$s_{1/2}$	$s_{1/2}$	$J^\pi$ $T$	$1^+$ 0	$0^+$ 1			
Cl <sup>34</sup>	$d_{3/2}$	$d_{3/2}$	$J^\pi$ $T$	$0^+$ 1	$3^+$ 0			$2^+$ higher
K <sup>38</sup>	$d_{3/2}^{-1}$	$d_{3/2}^{-1}$	$J^\pi$ $T$	$0^+$ 1	$3^+$ 0			$2^+$ higher
Sc <sup>42</sup>	$f_{7/2}$	$f_{7/2}$	$J^\pi$ $T$	$0^+$ 1				
Co <sup>54</sup>	$f_{7/2}^{-1}$	$f_{7/2}^{-1}$	$J^\pi$ $T$	$0^+$ 1				

\* Virtual state.

\*\* The first excited state would seem to be  $1^+$ ,  $T = 0$ , not far from which lies the state with  $J = 0^+$ ,  $T = 1$ , as shown in the Table [17].

\*\*\* The state with this characteristic lies higher than the state shown in the previous columns.

Figures 3 and 4 show the level schemes of B<sup>10</sup> and Al<sup>26</sup> compared with their isobars with  $T_z = \pm 1$ , whose ground states are made to coincide with the  $0^+$  state of the odd-odd nucleus. It is seen from Fig. 3 that the 5.16 Mev level with  $J = 2^+$ ,  $T = 1$  in B<sup>10</sup> coincides approximately with  $2^+$  level of Be<sup>10</sup> and C<sup>10</sup>, and therefore this level (rather than the first excited  $2^+$  level with 3.58 Mev energy) should be included in the multiplet. In the case of Al<sup>26</sup> (Fig. 4), the  $2^+$  component would seem to be the 1.76 Mev level coinciding with the  $2^+$  level of Mg<sup>26</sup>. According to the latest data [22] the level with  $E = 1.76$  Mev actually has  $T = 1$ . The  $4^+$  component of the multiplet lies somewhere higher.

IV

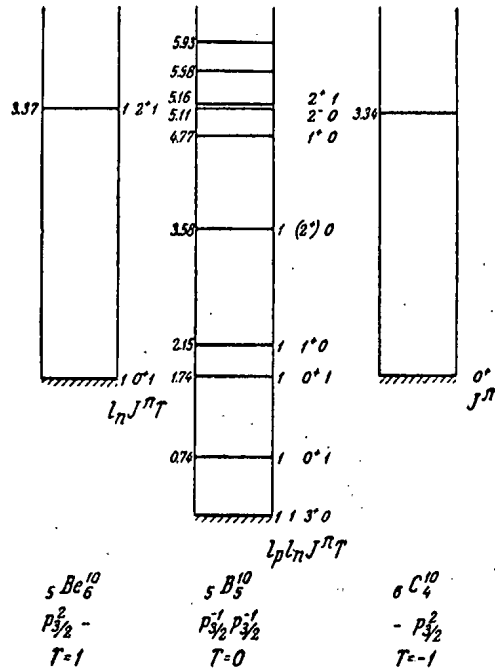


Fig. 3. Level scheme of  $\text{Be}^{10}$ ,  $\text{B}^{10}$ , and  $\text{C}^{10}$  in the isobaric triplet with  $A = 10$ .

As has already been noted, multiplet components with odd  $J$  and  $J = 0^+$  in odd-odd nuclei with  $N = Z$  lie below the  $2^+$ ,  $4^+$ , etc., states. In all other odd-odd nuclei ( $N \neq Z$ ), a different pattern emerges. Table 6 gives the ground state characteristics of such nuclei (except those in which  $N$  or  $Z$  are equal to 7, 9, or 15, for which  $j_p$  or  $j_n = 1/2$ ). It is seen from the Table that in almost all cases the ground state has even angular momentum. The only doubt occurs in the case of  $\text{Sc}^{44}$ , a nucleus which has not yet been sufficiently well studied. The only clear exception is  ${}_{27}\text{Co}_{33}^{60}$ , whose ground state angular momentum is  $5^+$  [22]. It may be that the reason for this exception is the fact that  $N = 33$  is the first case in which a nuclear shell starts to be filled before the previous one has been filled.

We note one other property of nuclear multiplets. In Table 7 we present several groups of odd-odd nuclei in which one may expect four-component multiplets. We also give the characteristics of the known multiplet components. Nuclei with given  $j_p$  and  $j_n$  for the odd proton and neutron are separated into groups. The configurations of these nuclei can be obtained from each other by replacing a particle by a hole, or vice versa. From the examples presented it is seen that performing only one such replacement causes the highest component of the multiplet (see the last column of Table 5;  $2^+$  in  $\text{Cl}^{34}$ ,  $4^-$  in  $\text{Cl}^{38}$ ,  $6^+$  in  $\text{Sc}^{42}$ , and  $4^+$  in  $\text{Sc}^{50}$ ) to become the ground state. Repeating this replacement (for instance  $\text{Cl}^{36} \rightarrow \text{K}^{38}$ ,  $\text{Sc}^{48} \rightarrow \text{Co}^{54}$ , or  $\text{Co}^{56} \rightarrow \text{Co}^{58}$ ) leads to the original picture.

V

Nuclear multiplets would seem to be manifested in the  $\gamma$ -ray spectra emitted on capture of a thermal neutron when the result of such capture is an odd-odd nucleus.

In order to verify this assertion, let us compare such  $\gamma$ -spectra for even-odd (odd number of neutrons) and odd-odd radiating nuclei. Figure 5 shows such comparison for the three pairs of nuclei

$${}_{14}\text{Si}_{15}^{29} - {}_{13}\text{Al}_{15}^{28}; {}_{20}\text{Ca}_{21}^{41} - {}_{19}\text{K}_{21}^{40} \text{ and } {}_{26}\text{Fe}_{31}^{57} - {}_{25}\text{Mn}_{31}^{56}.$$

Each pair of nuclei has the same number of neutrons. It is seen from Fig. 5 that the spectra of the even-odd nuclei are relatively simple. Those of the odd-odd nuclei have many more lines. This is directly related to the increase in the level density of odd-odd nuclei, as compared with even-odd ones.

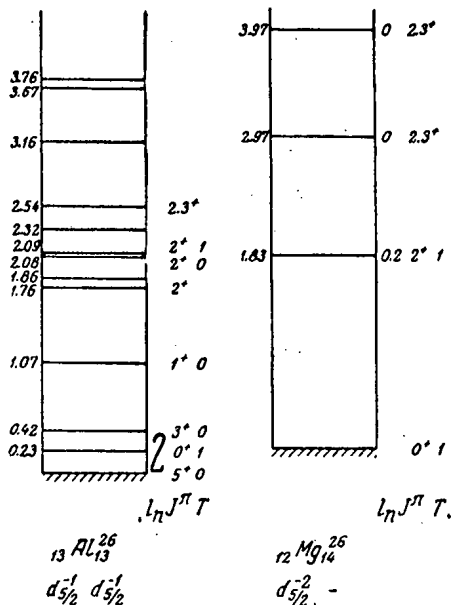


Fig. 4. The level schemes of  $\text{Al}^{26}$  and  $\text{Mg}^{26}$  in the isobaric triplet with  $A = 26$ .

TABLE 6

Nucleus	Ground state characteristics	Nucleus	Ground state characteristics
Li <sup>8</sup>	2 <sup>+</sup>	Sc <sup>48</sup>	6 <sup>+</sup>
B <sup>8</sup>	2 <sup>+</sup>	V <sup>48</sup>	4 <sup>+</sup>
Na <sup>24</sup>	4 <sup>+</sup>	Sc <sup>50</sup>	2 <sup>+</sup>
Al <sup>24</sup>	4 <sup>+</sup>	V <sup>50</sup>	6 <sup>+</sup>
Cl <sup>36</sup>	2 <sup>+</sup>	V <sup>52</sup>	2 <sup>+</sup>
Cl <sup>38</sup>	2 <sup>-</sup>	Mn <sup>52</sup>	6 <sup>+</sup>
Cl <sup>40</sup>	2 <sup>-</sup>	Mn <sup>54</sup>	2 <sup>+</sup>
K <sup>40</sup>	4 <sup>-</sup>	Mn <sup>56</sup>	2 <sup>+</sup>
Sc <sup>40</sup>	4 <sup>-</sup>	Co <sup>56</sup>	4 <sup>+</sup>
K <sup>42</sup>	2 <sup>-</sup>	Co <sup>58</sup>	2 <sup>+</sup>
Sc <sup>44</sup>	2 <sup>+</sup> , 3 <sup>+</sup>	Cu <sup>60</sup>	2 <sup>+</sup>
Sc <sup>46</sup>	4 <sup>+</sup>	Co <sup>60</sup>	5 <sup>+</sup>

Let us consider the relative probabilities for gamma transitions from the initial state resulting from thermal neutron capture to various levels of the even-odd and odd-odd light nuclei ( $A < 60$ ). The levels of interest to us have been identified on the basis of presently accepted  $\gamma$ -ray transition schemes.

The relative probability of a given transition was taken as the number  $p_i$  of photons per captured neutron divided by  $(h\nu_i)^3$ . This division by  $(h\nu_i)^3$  eliminates the energy dependence, since it is known [1] that the most intense transitions are of the dipole type. The results obtained are shown in Fig. 6. The horizontal axis gives the excitation energy of the nucleus (the nuclear levels are indicated by points), and the lengths of the vertical lines are proportional to the relative transition probabilities from the initial state to the given level. For each nucleus separately, the largest value of  $p_i / (h\nu_i)^3$  is taken as the unit of probability. The circled numbers next to some of the lines give the number of  $\gamma$ -quanta per hundred neutron captures. The data of Kinsey and Bartolomew [1] was used for Mg<sup>25</sup>, P<sup>32</sup>, Sc<sup>46</sup> and Cr<sup>53</sup>; that of Groshev, Ad'iasevich and Demidov [2] was used for Si<sup>29</sup>, S<sup>33</sup>, Ca<sup>41</sup>, Ti<sup>49</sup>, Fe<sup>57</sup>, Ni<sup>59</sup>, Na<sup>24</sup> and K<sup>40</sup>; that of Groshev, Demidov, Lutsenko and Pelekhov [24] was used for Al<sup>28</sup>, V<sup>52</sup> and Mn<sup>56</sup>.

From experiments on the (d, p) reaction, the angular momentum  $L_n$  given to the nucleus by the neutron can be found in many cases. The values of  $L_n$  are given below the horizontal axis. The left side of the figure refers to even-odd nuclei, and the right side to odd-odd nuclei. Characteristic of the decay of even-odd nuclear initial states is the fact that the transition probability to the lowest  $L_n = 1$  level (this level being clearly identified by the high probability for the (d, p) reaction in all the even-odd nuclei shown) is the highest, and varies between 25 and 70% depending on the nucleus. As has often been noted in the literature, this level is due to transition of the odd neutron into the  $2p_{3/2}$  state. Examination of the left side of the diagram shows that in addition to transitions to levels in which the neutron is in the  $2p_{3/2}$  state, there exist other  $\gamma$ -transitions whose relative probabilities are comparable. Usually these transitions are to levels lying about 2 Mev above the  $2p_{3/2}$  level. Holt and Marsham [25] have suggested that in Si<sup>29</sup> and S<sup>33</sup> this level corresponds to the transition of the odd neutron to the  $2p_{1/2}$  state. In other nuclei, the characteristics of these levels have not yet been found.

The figure clearly shows the gradual suppression of the  $2p_{3/2}$  level as the atomic weight  $A$  increases. In

TABLE 7

Nucleus	Configura-tion		Level characteris-tics of the ground state and lowest excited states				Remarks
	<i>p</i>	<i>n</i>	1	2	3	4	
Cl <sup>34</sup>	$d_{3/2}$	$d_{3/2}$	0 <sup>+</sup>	3 <sup>+</sup>			2 <sup>+</sup> higher *
Cl <sup>36</sup>	$d_{3/2}$	$d_{3/2}^{-1}$	2 <sup>+</sup>				0 <sup>+</sup> higher
K <sup>38</sup>	$d_{3/2}^{-1}$	$d_{3/2}^{-1}$	0 <sup>+</sup>	3 <sup>+</sup>			2 <sup>+</sup> higher
Cl <sup>38</sup>	$d_{3/2}$	$f_{7/2}$	2 <sup>-</sup>	5 <sup>-</sup>	3 <sup>-</sup>	4 <sup>-</sup>	
K <sup>40</sup>	$d_{3/2}^{-1}$	$f_{7/2}$	4 <sup>-</sup>	3 <sup>-</sup>	2 <sup>-</sup>	5 <sup>-</sup>	
Sc <sup>40</sup>	$f_{7/2}$	$d_{3/2}^{-1}$	4 <sup>-</sup>				2 <sup>-</sup> higher
Sc <sup>42</sup>	$f_{7/2}$	$f_{7/2}$	0 <sup>+</sup>				2 <sup>-</sup> , 4 <sup>+</sup> , 6 <sup>+</sup> higher
Sc <sup>48</sup>	$f_{7/2}$	$f_{7/2}^{-1}$	6 <sup>+</sup>				0 <sup>+</sup> higher
Co <sup>51</sup>	$f_{7/2}^{-1}$	$f_{7/2}^{-1}$	0 <sup>+</sup>				2 <sup>+</sup> , 4 <sup>+</sup> , 6 <sup>+</sup> higher
Sc <sup>50</sup>	$f_{7/2}$	$p_{3/2}$	2 <sup>+</sup>				4 <sup>+</sup> higher
Co <sup>56</sup>	$f_{7/2}^{-1}$	$p_{3/2}$	4 <sup>+</sup>				2 <sup>+</sup> higher
Co <sup>58</sup>	$f_{7/2}^{-1}$	$p_{3/2}^{-1}$	2 <sup>+</sup>				4 <sup>+</sup> higher

\* The state with this characteristic lies above the states given in the previous columns.

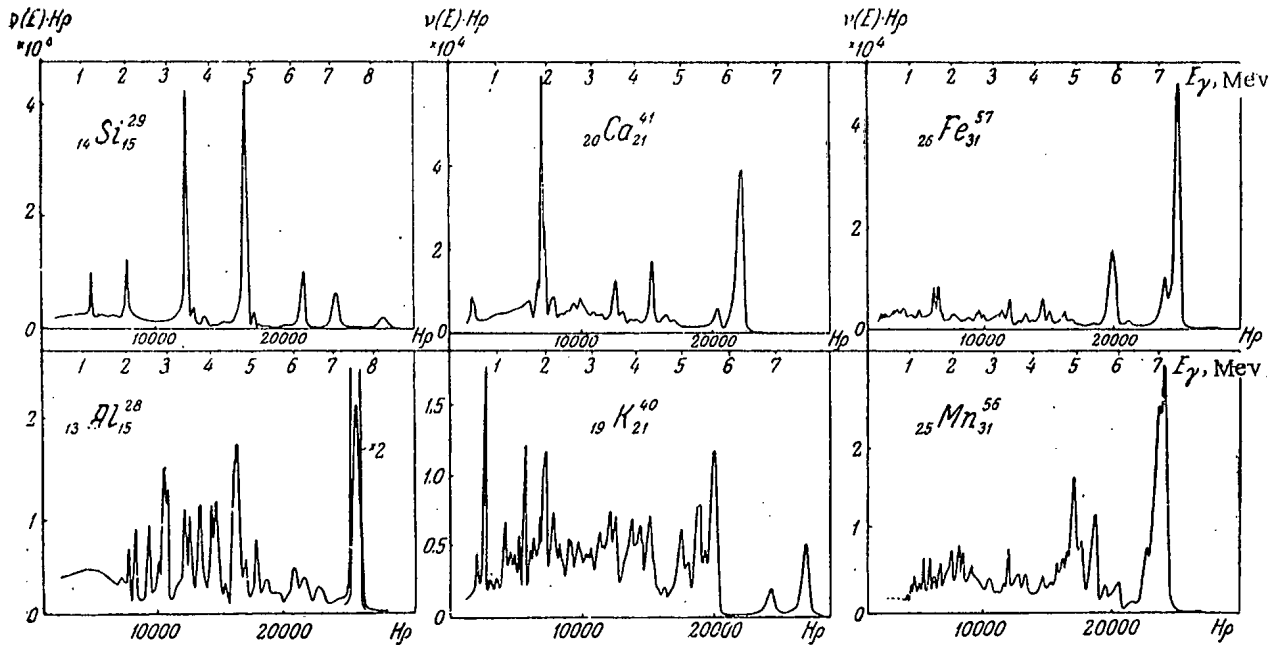


Fig. 5.  $\gamma$ -ray spectra emitted on thermal neutron capture by nuclei with N values of 15, 21, and 31.

$\text{Cr}^{53}$ ,  $\text{Fe}^{57}$ , and  $\text{Ni}^{59}$  this level becomes the ground state.\* Thus in these nuclei there exists an intense  $\gamma$ -transition to the ground state.

Thus for even-odd nuclei,  $\gamma$ -transitions are most probable only to a few levels. For those cases in which the characteristics of these levels have been found, they turn out to be  $p_{3/2}$  or  $p_{1/2}$  levels. On examining the right side of the figure (odd-odd nuclei), we see that the number of lines of comparable intensity increases (on the average, of the order of 10 photons per 100 captures). It should also be noted that these intense  $\gamma$ -transitions occur in groups whose entire structure has not yet been successfully determined. It is, however, of interest that a group of lines in the neighborhood of the ground state is observed for  $\text{V}^{52}$ ,  $\text{Mn}^{56}$ , and  $\text{Co}^{60}$  [1], [24] (the latter is not shown in the figure), whose neutron ground state is  $p_{3/2}$ . In lighter nuclei, whose ground states contain neutrons in other than the  $p_{3/2}$  state, the intense line groups are displaced towards higher energies, and in several cases it has been found from the (d, p) reaction that  $l_n = 1$  for these levels.

If one compares even-odd and odd-odd nuclei with the same number of neutrons ( $_{12}\text{Mg}_{13}^{25}$  -  $_{11}\text{Na}_{13}^{24}$ ;  $_{14}\text{Si}_{15}^{29}$  -  $_{13}\text{Al}_{15}^{28}$ ;  $_{20}\text{Ca}_{21}^{41}$  -  $_{19}\text{K}_{21}^{40}$ ;  $_{24}\text{Cr}_{29}^{53}$  -  $_{23}\text{V}_{29}^{52}$ ;  $_{26}\text{Fe}_{31}^{57}$  -  $_{25}\text{Mn}_{31}^{56}$ ) it is easily established that in the odd-odd nuclei the first group of intense transitions is to levels located at about the same energy as the  $2p_{3/2}$  level in the corresponding even-odd nuclei.

This property of the  $\gamma$ -ray spectra of odd-odd nuclei, it seems to us, can be understood in terms of nuclear multiplets in such nuclei. It is assumed here that one may speak of multiplets both of the ground and excited states.

If we consider thermal neutron capture by a light nucleus to be a direct interaction process taking place without formation of a compound nucleus, then from the results obtained for even-odd nuclei it follows that when an s-neutron is captured, the most probable transition is the electric dipole, in which the neutron goes to a p-state. If an odd-odd nucleus has a configuration containing, let us assume, a  $p_{3/2}$ -neutron, then according to what has already been said, a nuclear multiplet may be produced. If this is the case, transitions with  $\Delta J = 0, \pm 1$  to levels with a  $p_{3/2}$ -neutron in odd-odd nuclei should be of about equal intensity (in odd-odd nuclei these transitions should also be electric dipoles, since it is assumed that the level is due essentially to transition of the neutron to the p-state, without a proton transition).

On the basis of such an assumption, it is simple to explain the occurrence of groups of lines of comparable intensity in the case of odd-odd nuclei, as well as the displacement of these line groups into different regions

\* According to the latest data [26], the ground state of  $\text{Fe}^{57}$  is  $1/2^-$ , and it is the first excited level, whose energy is 14 keV, which is  $3/2^-$ .

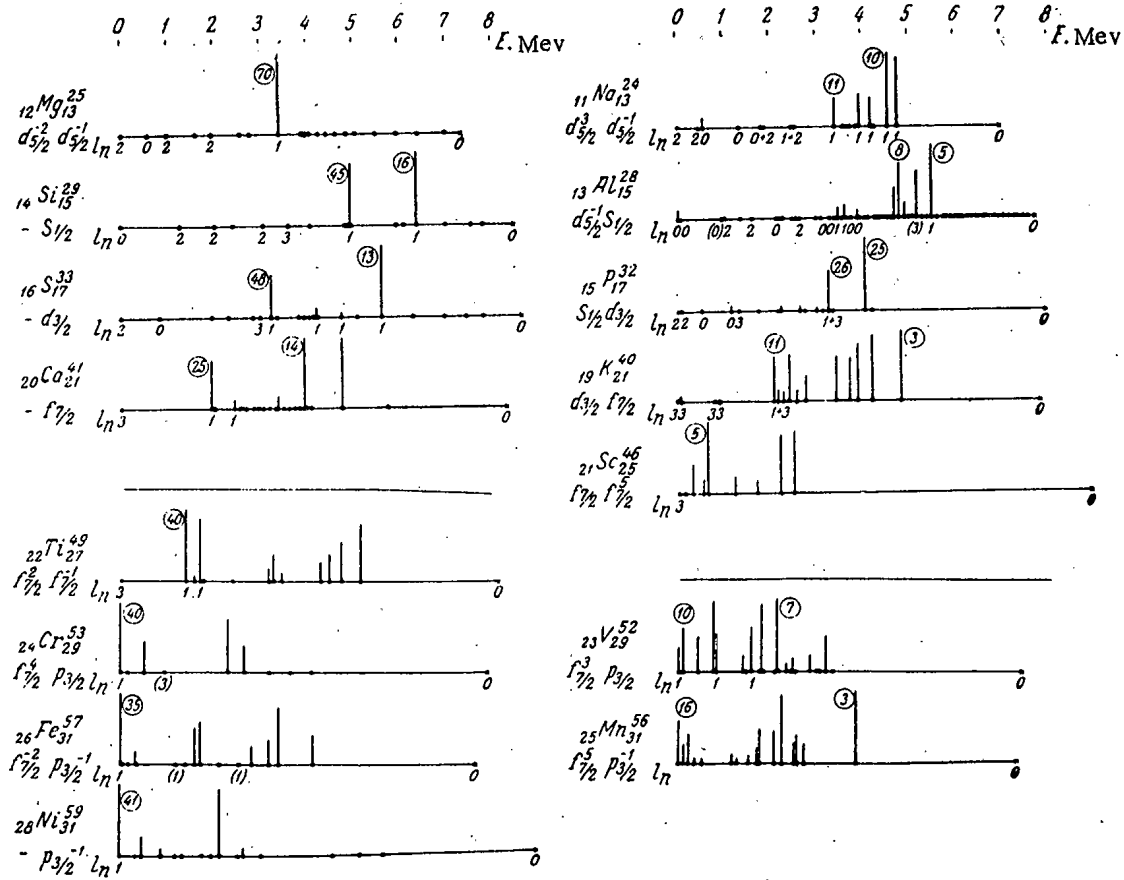


Fig. 6.  $\gamma$ -decay diagrams for states produced in thermal neutron capture for even-odd and odd-odd nuclei.

1) In the case of Mg, two isotopes contribute comparably to the thermal neutron capture cross section ( $Mg^{24}$  - 44% and  $Mg^{25}$  - 46%,  $Mg^{26}$  - 10%). This complicates the interpretation of the spectrum, and  $\gamma$ -transitions only to levels with energy less than 4 Mev are reliably established in  $Mg^{25}$ .

2) In the case of Cr, three isotopes contribute comparably to the capture cross section ( $Cr^{50}$  - 27.5%,  $Cr^{52}$  - 20.5%,  $Cr^{53}$  - 55%). The analysis of this spectrum is thus also somewhat difficult. Using the fact that the neutron binding energy of  $Cr^{51}$  is known (9.07 Mev), it can be shown that no transition to the ground state occurs for this isotope. This is related to the fact that the neutron in the  $Cr^{51}$  ground state is in an  $f_{7/2}^{-1}$  state, rather than in a  $p_{3/2}$  state as in  $Cr^{53}$ .

3) The overwhelming majority (92%) of neutron captures by iron leads to the production of the  $Fe^{57}$  nucleus, whose neutron has a binding energy of 7.65 Mev. The  $Fe^{55}$  nucleus is produced 5% of the time, and in this case the binding energy is 9.34 Mev. The last neutron of  $Fe^{55}$  is in the  $p_{3/2}$  state. As a result, transition to the ground state is observed, with 40 quanta per 100 capture events of this isotope belonging to this transition.

4) A similar pattern is observed for  $Ni^{61}$  (the neutron is  $p_{3/2}^{-1}$ ), which is produced 16% of the time and has a highly intense transition to the ground state.



of the spectrum, approximately as happens with the  $2p_{3/2}$  level in the corresponding even-odd nuclei.

Received February 28, 1957

#### LITERATURE CITED

- [1] B. B. Kinsey and G. A. Bartolomew, Phys. Rev. 93, 1260 (1954); 83, 519 (1951); 85, 1012 (1952); 89 375, 386 (1953).
- [2] L. V. Groshev, B. P. Adyasevich and A. M. Demidov, Physical Investigations (Reports of the Soviet Delegation to the International Conference on the Peaceful Uses of Atomic Energy), Izd. AN SSSR 1955, p. 252; J. Atomic Energy 2, 28, 40 (1956).\*
- [3] T. H. Braid, Phys. Rev. 102, 1109 (1956); M. Reier and M. H. Shamos, Phys. Rev. 100, 1302 (1955).
- [4] F. Ajzenberg and T. Lauritsen, Rev. Mod. Phys. 27, 77 (1955).
- [5] P. M. Endt and J. C. Klyuver, Rev. Mod. Phys. 26, 95 (1954).
- [6] B. S. Dzhelepov and L. K. Peker, Decay Schemes of Radioactive Isotopes, Izd. AN SSSR, 1957.
- [7] E. K. Warruton and J. N. Gruer, Bull. Amer. Phys. Soc. II, 1, 325 (1956).
- [8] A. M. Demidov, Bull. Acad. Sci. USSR (ser. Phys.) 8, 962 (1956).
- [9] C. H. Paris, W. W. Buechner and P. M. Endt, Phys. Rev. 100, 1317 (1955).
- [10] H. B. Burrows, T. S. Green, S. Hinds and R. Middleton, Proc. Phys. Soc. 69 A, 310 (1956).
- [11] I. Teplov, Dissertation MGU, 1954.
- [12] J. B. French and B. J. Raz, Phys. Rev. 104, 1410 (1956).
- [13] G. F. Pieper, Phys. Rev. 88, 1299 (1952).
- [14] S. Goldstein and I. Talmi, Phys. Rev. 102, 589 (1956).
- [15] S. P. Pandya, Phys. Rev. 103, 956 (1956).
- [16] M. Goeppert-Mayer and J. H. D. Jensen, Elementary Theory of Nuclear Shell Structure (1955).
- [17] D. H. Wilkinson, Phil. Mag. 11, 1031 (1956).
- [18] A. De-Shalit, Phys. Rev. 91, 1479 (1953); S. A. Moszkowski and D. C. Peaslee, Phys. Rev. 93, 455 (1953).
- [19] A. Baz and Ya. Smorodinsky, Prog. Phys. Sci. LV, 215 (1955).
- [20] H. Morinaga, Phys. Rev. 100, 431 (1955).
- [21] R. W. King, Rev. Mod. Phys. 26, 327 (1954).
- [22] L. L. Green, J. J. Singh and J. C. Willmott, Proc. Phys. Soc. 69 A, 335 (1956).
- [23] W. Dobrowolski, R. V. Jones and C. D. Jeffries, Phys. Rev. 101, 1001 (1956).
- [24] L. V. Groshev, A. M. Demidov, V. N. Lutsenko and V. I. Pelekhov, J. Atomic Energy (to be published).
- [25] J. R. Holt and T. N. Marsham, Proc. Phys. Soc. A 66, 258 (1953).
- [26] T. Lindqvist and E. Heer, Nucl. Phys. 2, 680 (1957).

\*[See C. B. translation.]

## DETERMINATION OF THE INTENSITY OF SHORT FAST-NEUTRON PULSES

V. M. Gorbachev and Yu. S. Zamyatnin

A quantitative method has been developed for determining yields of pulses; the method is based on the detection of the  $\gamma$ -rays produced in the capture of neutrons slowed down in paraffin. The detectors used in this scheme have a sensitivity of  $0.1 \text{ neut/cm}^2$ . The scheme presented here makes it possible to carry out measurements in the presence of electrical disturbances and the  $\gamma$ -rays which accompany the neutron radiation; the method can also be used with controlled-detector operation.

## INTRODUCTION

In investigating the operation of pulsed neutron sources it is of interest to measure the time characteristics of the neutron pulse (initial portion of the pulse, length of the pulse, slope of the leading edge, etc.) and the nature of the neutrons generated during the pulse.

Existing methods of determining neutron yields in single neutron pulses\* can be divided into two groups. On the one hand we have "fast" methods, in which detection of the neutron pulse occurs at the instant the neutrons are produced. Of these methods the highest efficiency and best resolving power can be obtained through the use of organic-crystal scintillation counters and an oscilloscope with high writing speed. The other method is the well-known activation method.

If the pulse amplifier used in the first method has adequate band width it is possible to distinguish pulses produced by individual neutrons [1]. However, if the scintillator loading is high and the resolving time of the detection circuit is longer than the neutron pulse, it is impossible to distinguish pulses due to individual neutrons because of pile-up effects.

In cases of this kind neutron pulse intensity must be determined by an integration method; in this method the pulses produced by the individual neutrons incident on the crystal are added in such a way that the pulse at the output of the detector is proportional to the sum of the individual effects. If the photomultiplier is operated in a voltage region such that the output pulse amplitude is proportional to the intensity of the scintillation and if the amplifier is linear, we can estimate the number of neutrons which have contributed from the area of the resultant pulse; thus, the neutron yield can be evaluated.

A basic advantage of the "fast" method is the high efficiency for detection of neutrons with energies of approximately 1 Mev; this efficiency reaches 10% per centimeter of crystal thickness. Furthermore, using these methods, we can determine the moment at which the pulse starts and its shape; this is of great advantage in a number of experiments. On the other hand, the detection of neutron radiation by "fast" methods entails a number of disadvantages. One of these is the fact that at the instant the pulse is initiated in the neutron-production apparatus there is a high likelihood of the production of rapidly-varying electric and magnetic fields which give rise to strong interference in the detection circuits. It is also extremely difficult to analyze the results in cases in which the neutron output is accompanied by  $\gamma$ -radiation. In addition the use of "fast"

\* Here and in what follows we shall be concerned with single or periodic pulses of fast neutrons with energies greater than 1 Mev.

methods entails rather complicated electronic units if high resolution is to be achieved.

The determination of neutron yield by the activation method (cf. for example, Ref. [2]) is extremely simple; however, the sensitivity of this method is poor – in the best geometry it is impossible to detect neutron pulses with yields of less than  $10^5$  neutrons per pulse ( $> 5$  neut/cm<sup>2</sup>).

An important disadvantage of the activation method is the fact that it is impossible to determine the instant at which the neutron pulse starts.

In the present paper we describe a convenient method for determining yields from pulsed neutron sources; this method was developed by A. I. Veretennikov and one of the authors. This method provides high neutron-detection efficiency and also makes it possible to carry out quantitative measurements on very short neutron pulses. Also the instant at which the neutron pulse starts can be determined with relatively high accuracy.

### Method and Apparatus

In the "detection-stretching" method described here the neutron yield is determined from the  $\gamma$ -rays which are produced in the capture of neutrons which have been slowed down in paraffin which surrounds the scintillation-counter crystal.

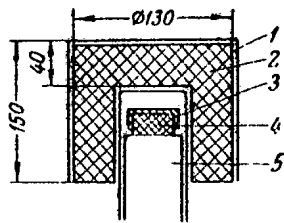


Fig. 1. Diagram of the neutron detector (the dimensions are in millimeters).

- 1) Lead casing; 2) paraffin block;
- 3) cadmium cover; 4) scintillator;
- 5) photomultiplier.

In Fig. 1 is shown a schematic diagram of the neutron detector. Neutrons from the pulsed source, after striking the paraffin block, are slowed down and then captured by the hydrogen. If the dimensions of the paraffin block are chosen properly the majority of neutrons slowed down in the paraffin are detected. The  $\gamma$ -rays produced in these events are recorded by the scintillation counter. The lifetime of thermal neutrons in paraffin is approximately  $200 \mu$  sec. Thus, instead of examining the neutrons in a short period of time (duration of the pulse  $0.1-1.0 \mu$  sec) using the paraffin-block detector it is possible to extend the detection period to  $100-300 \mu$  sec; using this scheme the requirements on the resolving power of the electronic units can be reduced considerably. Furthermore, a detector of this type is relatively insensitive to the details of the original neutron spectrum.

The pulses from the scintillation counter are fed to an amplifier with a bandwidth of approximately 3 Mc/sec, and then to the cathode of the oscilloscope tube. In the present experiments an oscilloscope with spiral sweep was used; this was a standard type IV-13M time-measuring system in which some simple modifications had been made. The use of this oscilloscope turns out to be especially convenient since its sweep length, which is approximately  $250-300 \mu$  sec, corresponds to the mean neutron lifetime in paraffin.

The oscilloscope sweep was synchronized with the pulsed neutron source to within an accuracy of  $10 \mu$  sec.

Pulses appearing at the cathode of the cathode-ray tube blank the beam for a time equal to the pulse width at the blanking threshold (approximately 15 v). Thus, the arrival of a pulse is indicated by a break in the sweep. The intensity modulation of the beam, produced by pulses of sufficient amplitude, results in the production of a clear pattern.

If a large number of neutrons are recorded by the detector a considerable fraction of the spiral will be blanked out because of pile-up. The resulting "breaks" make it difficult to analyze the oscillograms. To reduce pile-up effect rather narrow blanking pulses are desirable. In the present experiments the pulses applied to the cathode-ray tube were less than  $0.2-0.4 \mu$  sec in width at the blanking level. Using these pulses it was possible to interpret oscilloscope pictures in which more than 300 individual neutron pulses were recorded. Further width reduction of the pulses is undesirable because of the small circumference of the inner spirals. In Fig. 2 is shown a sample of the pattern obtained when the detector is irradiated by pulsed neutrons.

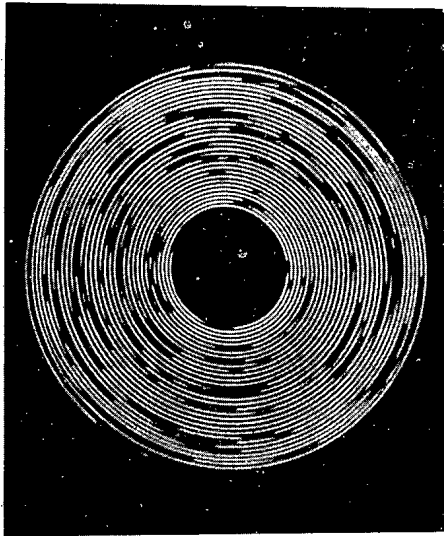


Fig. 2. Sample of a neutron pulse trace obtained by "detection-stretching."

In addition to using the oscilloscope record, the pulses from the detector can be recorded by a high-speed scaler. In this case the scaler is operated only during the neutron pulse. Thus it is possible to eliminate pulses due to the inherent background in the scintillation counter.

Using scalars with a resolving time of 0.2-0.3  $\mu$  sec the high resolution inherent in the oscilloscope can be maintained, thereby simplifying an analysis of the results considerably.

An analysis of "detection-stretching" indicates that the scheme is insensitive to  $\gamma$ -radiation and to any type of electromagnetic or other disturbance which occurs during the neutron pulse. Furthermore, it is possible to determine the instant at which the neutron pulse appears since there are always neutrons striking the scintillator which have not been first slowed down. If an oscilloscope such as that used in the IV-22 time-measuring device is used,

the accuracy with which the appearance of the pulse can be determined is 0.03  $\mu$  sec.

### Detector Efficiency

The efficiency of the detection-stretching neutron detector was determined for the following scintillator materials: stilbene, naphthalene with anthracene, thallium-activated sodium and caesium iodide. All crystals were of the same dimension: diameter 35 mm, height 20 mm.

A diagram of the experiment is shown in Fig. 3.

To calibrate the detector a pulsed accelerator with a pulse length of approximately 1  $\mu$  sec was used as a neutron source. The neutrons were a product of the reaction



The neutron yield was monitored by a  $\beta$ -counter enclosed in a silver foil and placed in the paraffin block. The neutron yield was determined from the activity in the silver. The beta-counter was first calibrated against the accelerator tube. The detector was shielded with a lead casing to eliminate x-ray radiation from the neutron source. The detector was adjusted using  $\gamma$ -rays from a radioactive cobalt source. The inherent background of the scintillation counter was so low that there were virtually no pulses at the oscilloscope due to this source.

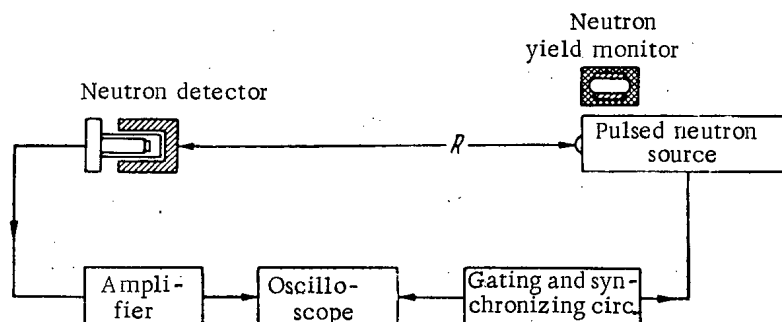


Fig. 3. Diagram of the experiment in which the detector efficiency was measured.

The efficiency of the detector for slowed-down neutrons was increased by adding cadmium covers to the scintillation crystals. Because of the increased number of  $\gamma$ -rays produced in the capture of thermal neutrons in the cadmium\* and because of the high probability for detection of these  $\gamma$ -rays the efficiency of the detector was increased by approximately a factor of two.

It should be noted, however, that in cases in which large scintillators are covered by cadmium (approximately  $100 \text{ cm}^3$ ) the cadmium absorber was somewhat less effective because of volume-shielding effects in the scintillator which reduced the number of thermal neutrons which could be captured in the scintillator.

The efficiency measurements are given in the Table.

Crystal	Total neutron yield during the time of measurement, N	Number of pulses recorded by the detector, n	Neutron flux in $1 \text{ cm}^2$ giving 1 pulse in the detector: $N/4\pi R^2n$	Relative efficiency
Stilbene	$26.8 \cdot 10^7$	603	1.57	1.00
Naphthalene	$22.2 \cdot 10^7$	579	1.35	1.16
NaI	$16.8 \cdot 10^7$	1016	0.58	2.60
CsI	$16.0 \cdot 10^7$	1464	0.38	4.12

It is apparent from the Table that the most efficient detectors are those in which the inorganic scintillators NaI and CsI were used. This fact indicates that the most important effect is the detection of  $\gamma$ -rays produced when neutrons pass through the detector.

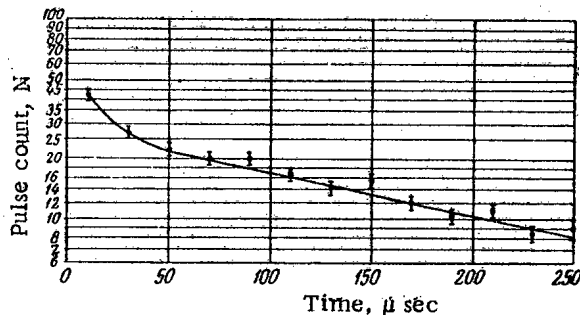


Fig. 4. Time distribution of detector pulses.

#### Time Distribution of Detector Pulses

The authors have examined the time distribution of pulses recorded in a detector consisting of 5 scintillation counters connected in parallel (FEU-19M photomultiplier and a stilbene crystal). The number of pulses in each turn of the spiral sweep was counted (the length of a turn corresponds to  $10 \mu \text{ sec}$ ).

The experimental results are shown in Fig. 4.

The straight line indicates that the time distribution of the pulses is exponential. The mean neutron lifetime, as determined from the slope of the line, is  $\lambda = 190 \mu \text{ sec}$ .

This value of  $\lambda$  is in satisfactory agreement with the generally accepted diffusion time for neutrons in paraffin. The fact that it is somewhat lower would seem to be explained by the additional absorption of slowed-down neutrons in the cadmium. The results which have been obtained also indicate that the basic contribution to the detection process is that due to  $\gamma$ -rays produced in thermal-neutron capture in the hydrogen in the paraffin. The sharp rise in the initial part of the curve is apparently due to fast neutrons.

\* The mean number of  $\gamma$ -quanta produced in thermal-neutron capture in cadmium is 4.1 [3].

The measurement of the time distribution of detector pulses is a convenient way of checking the operation of the detector.

The author wishes to express his gratitude to Doctor of Physico-Mathematical Sciences V. A. Davikenko for many valuable discussions and for his interest in this work.

Received March 15, 1957

#### LITERATURE CITED

- [1] A. I. Veretennikov, Dissertation, 1955.
- [2] N. A. Vlasov, Neutrons. (State Tech. Press, 1955).
- [3] C. O. Muehlhause, Phys. Rev. 79, 277 (1950).

ANGULAR DISTRIBUTION OF ELASTIC AND INELASTIC SCATTERING OF  
2.34 Mev NEUTRONS FROM CHROMIUM, IRON, AND LEAD\*

O. A. Salnikov

Spectra are obtained for neutrons with initial energy  $E_0 = 2.34$  Mev scattered by chromium, iron, and lead nuclei, and the corresponding differential cross sections for elastic and inelastic scattering are measured for angles from  $30^\circ$  to  $135^\circ$ . The neutrons were obtained from the  $D(d, n)He^3$  reaction with an initial deuteron energy of 1 Mev and a neutron emission angle of  $110^\circ$ . Nuclear photographic emulsion was used as the detector-spectrometer and as the monitor of the incident neutron flux. The scatterers were 2.8 cm diameter spheres. In calculating the cross sections for elastic and inelastic scattering, corrections for self-absorption and multiple scattering were introduced to the incident neutron flux in the scatterer. The angular distribution of inelastically scattered neutrons from chromium and iron, as well as from lead when the 0.53 Mev level was excited, was found to be isotropic within the limits of the experiment. Inelastic scattering from lead when the 0.805 and 0.890 Mev levels are excited cannot be considered isotropic.

Method of Measurement and Apparatus

The neutron source was the  $D(d, n)He^3$  reaction with an incident deuteron energy  $E_d = 1$  Mev. The target for this reaction was ice in which the hydrogen had been replaced by deuterium. In order to obtain the lowest energy spread in the incident neutron beam, the scatterer was irradiated by neutrons leaving the target at an angle of  $110^\circ$  with respect to the deuteron beam.

Under these conditions the incident neutron energy  $E_0$  was 2.34 Mev.

The energy spectrum of these neutrons is shown in Fig. 1.

The detector-spectrometer of the scattered neutrons, and the monitor of the incident neutron flux was "Ilford C-2" photographic emulsion  $200\mu$  thick, which registers the scattered neutrons by the recoil protons. The range-energy relation for recoil protons in this emulsion is known for a wide energy range.

In order to collimate the neutron beam incident on the scatterer, as well as to shield the photographic plates from the incident neutron flux, the target was placed into a cavity within a large water tank, a channel in which served as the collimator. Locating the target within the tank also decreases the background of neutrons scattered from surrounding objects.

Figure 2 shows a diagram of the experiment. The scatterers were cast in the form of 2.8 cm diameter spheres. The distance between the center of the scatterer and the center of the photographic plate was 8 cm. The scatterers were located 57 cm from the target. This geometry gave an angular resolution of  $\pm 10^\circ$ .

In inspecting the plates, tracks were counted whose horizontal projections made an angle no greater than  $10^\circ$  with the projection axis (the projection axis is the line connecting the center of the scatterer to the center of the photographic plate), and whose vertical projections were no greater than 0.1 times their lengths. After

\* This work was carried out during 1953-1955; the results were partially reported at the International Conference on the Peaceful Uses of Atomic Energy in Geneva, 1955.

accounting for the shrinkage of the developed emulsion, this corresponds to a maximum vertical angle of  $14^{\circ}30'$ .

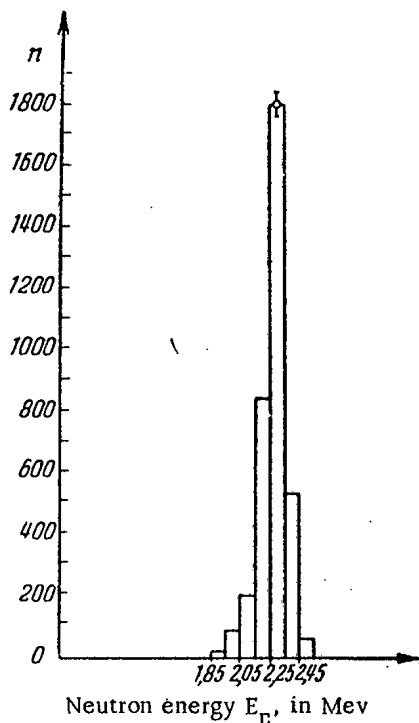


Fig. 1. Incident neutron spectrum.

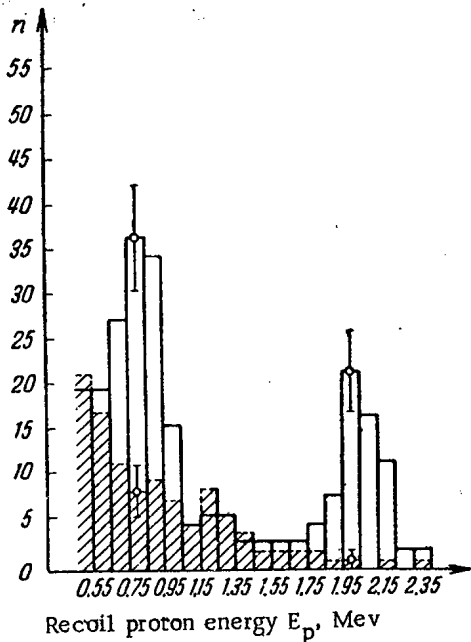


Fig. 3. Recoil proton spectrum due to neutrons scattered by chromium nuclei at an angle of  $90^{\circ}$ . The shaded region gives the scattered neutron background.

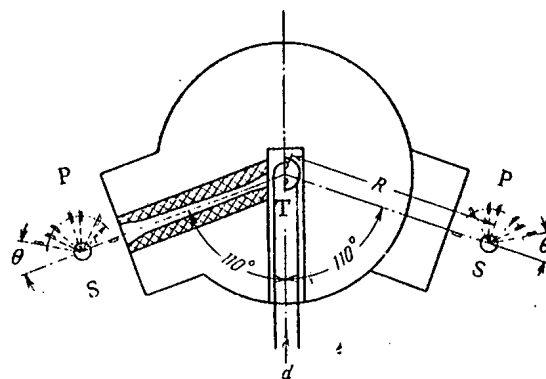


Fig. 2. Diagram of the experiment. T) target; S)scatterer; P) photographic plates;  $\theta$  ) scattering angle; R) distance from target to scatterer; r) distance from scatterer to photographic plates; d) deuteron beam.

Histograms of the recoil proton spectra were constructed by using energy intervals of 100 kev. The histograms were constructed with corrections to normalize the scattered and background neutron flux to a common value and to a common volume of emulsion.

The energy of a neutron recorded is related to that of the recoil proton by the expression

$$E_n = \frac{E_p}{\cos^2 \gamma}$$

where  $E_n$  is the neutron energy,  $E_p$  is the recoil proton energy,  $\gamma$  is the angle between the neutron direction and recoil proton track, and  $\overline{\cos^2 \gamma}$  is the mean square value of the cosine of  $\gamma$ . With the geometry chosen and the indicated values of the maximum horizontal and vertical angles,  $\overline{\cos^2 \gamma} = 0.94$ .

The elastic and inelastic scattering cross sections for chromium, iron, and lead were calculated after account was taken of the difference in the efficiencies for counting scattered neutrons and neutrons of the incident flux.

In calculating the cross-section for elastic scattering, a correction was introduced to account for the decrease in the incident flux in the scatterer due to self-absorption. Multiple scattering was accounted for by the method of Blok and Jonker [1], as refined by Meier and co-workers [2].

Corrections were calculated for double and triple scattering. In calculating the inelastic scattering cross



section, decrease of the incident flux was accounted for only due to inelastic scattering, since the neutron energy and mean free path in the scatterer hardly change as a result of elastic collision. Multiple inelastic scattering may be neglected, since a second inelastic collision has low probability due to the decrease of the inelastic neutron cross section after the first inelastic collision.

### Results

The histograms of the recoil proton spectra due to neutrons scattered by chromium, iron and lead show separate groups with good energy resolution. The most typical histograms are shown in Figs. 3, 4 and 5.

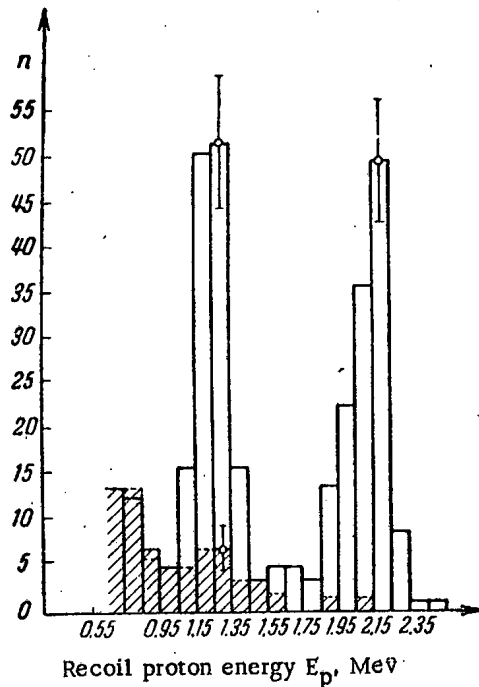


Fig. 4. Recoil proton spectrum due to neutrons scattered by iron nuclei at an angle of  $90^\circ$ . The shaded region gives the scattered neutron background.

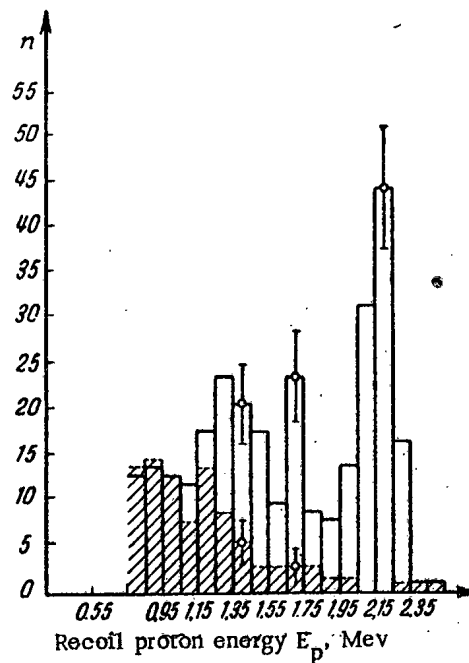


Fig. 5. Recoil proton spectrum due to neutrons scattered by lead nuclei at an angle of  $90^\circ$ . The shaded region gives the scattered neutron background.

The highest energy proton groups (2.3 Mev) are due to elastically scattered neutrons. The remaining proton groups are due to neutrons whose scattering has excited various energy levels of the nuclei.

The mean energy of these neutrons from iron is 1.5 Mev, corresponding to the 0.85 Mev level. The mean energy of the inelastically scattered neutrons from chromium is 0.9 Mev, for a level energy of 1.44 Mev. There are two such groups in lead: one, with an energy of 1.8 Mev, corresponds to the 0.53 Mev level, and the other, with a mean energy of 1.5 Mev, corresponds to excitation of the two levels at 0.805 and 0.890 Mev, which were not resolved in this work.

In some of the histograms there appears also a fourth, barely noticeable neutron group (with an energy of 1.2 Mev), corresponding to an energy level at 1.1 Mev.

The differential elastic scattering cross sections of 2.34 Mev neutrons by chromium, iron, and lead are given in the Table.

The angular distributions of 2.34 Mev neutrons inelastically scattered by these nuclei are shown in Figs. 6 and 7.

The total inelastic scattering cross sections for chromium and iron are:

for chromium  $\sigma_{in} = 0.93 \pm 0.08$  barns;

for iron  $\sigma_{in} = 0.90 \pm 0.07$  barns.

The total inelastic scattering cross section with excitation of the 0.53 Mev level in lead is  $\sigma_{in}^{0.53} = 0.80 \pm 0.08$  barns.

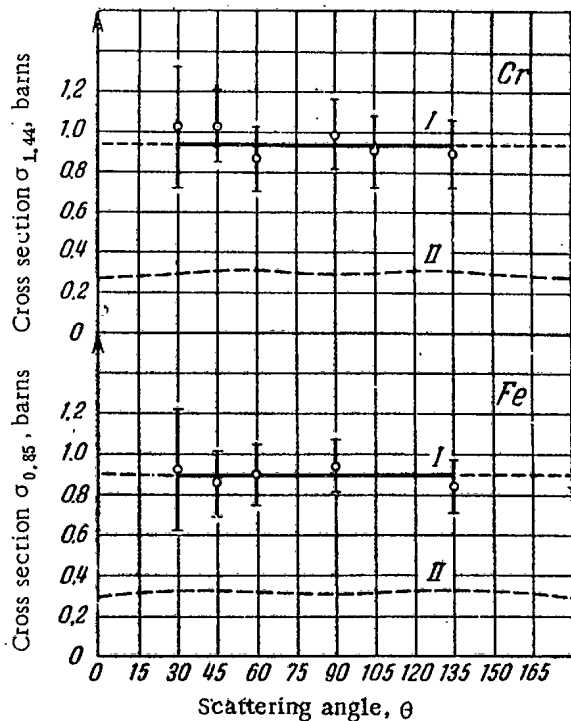


Fig. 6. Inelastic scattering cross section of 2.34 Mev neutrons by chromium and iron. All cross sections are calculated for a solid angle of  $4\pi$  I) experimental data; II) calculated curve.

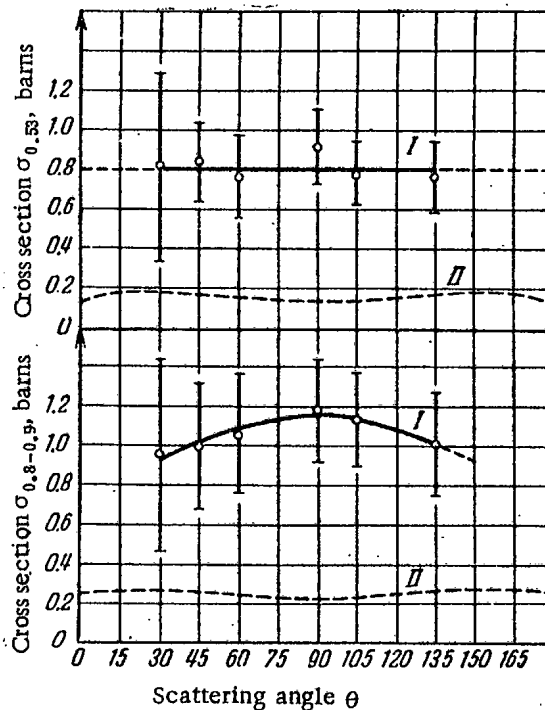


Fig. 7. Inelastic scattering cross section of 2.34 Mev neutrons by lead. All cross sections are calculated for a solid angle of  $4\pi$ . I) experimental data; II) calculated curve.

Scattering with excitation of the unresolved lead levels (with energies of 0.805 and 0.890 Mev) cannot, according to the present author, be considered isotropic. The total inelastic scattering cross section with excitation of these levels is  $\sigma_{in}^{0.8-0.89} = 1.08 \pm 0.10$  barns.

#### DISCUSSION OF RESULTS

All the neutron groups seen in the histograms correspond to well known levels of the given elements.

Another level at 1.74 Mev is known for lead, but it would seem that with an incident neutron energy of 2.34 Mev it is only weakly excited. The energy of the neutrons scattered by excitation of this level is insufficient for reliable registration in the photographic emulsion.

The differential elastic scattering cross sections of neutrons by iron and lead nuclei, as obtained in the present work, are in agreement with those of Walt [3] within the limits of experimental error.

The differential elastic scattering cross section of neutrons on chromium nuclei is here published for the first time. The total cross sections obtained by adding the total elastic and inelastic cross sections have been compared with the total cross sections obtained by a transmission method [4]. The results agree within the limits of experimental error.

## Elastic Scattering Cross Section (in Barns).

Angle \ Element	30°	45°	60°
Chromium	10.2±1.1	6.3±0.5	1.9±0.3
Iron	6.2±0.8	2.9±0.3	1.4±0.2
Lead	20.4±1.7	7.7±0.7	2.6±0.4

Angle \ Element	90°	105°	135°
Chromium	1.3±0.1	1.8±0.2	1.6±0.2
Iron	2.0±0.3	—	1.4±0.2
Lead	4.3±0.5	3.6±0.4	2.4±0.2

Note: All cross sections are calculated for a solid angle of  $4\pi$ .

section of 2.5 Mev neutron scattering by lead. The effective fission threshold of  $U^{238}$  is 1.35 Mev. Bondarenko obtained  $\sigma_{in} = 0.52 \pm 0.15$  barns.

For the same energy, with a threshold detector using the  $P^{31}(n, p)Si^{31}$  reaction, Pasechnik [8] obtained the value  $\sigma_{in} = 1.69 \pm 0.32$  barns for the cross section. The effective threshold for the (n, p) reaction on phosphorus is 1.7 Mev. The increase of the cross section can be explained only by the presence of levels with high cross sections within the interval by which the effective thresholds of these two detectors differ, that is the 0.53 and 0.805-0.890 Mev levels. A particularly large effect is produced by the 0.53 Mev level, since one of the detectors, the  $U^{238}$  chamber, misses it almost completely, and the other, that using the  $P^{31}(n, p)Si^{31}$  reaction, observes it entirely.

It would seem that such an anomalously high inelastic scattering cross section can be explained by the high probability for forming the compound nucleus  $Pb^{208}$ , which is magic both in the number of protons and neutrons. As for the unresolved 0.805 and 0.890 Mev levels, it is seen from Fig. 7 that the differential cross section for inelastic scattering on these levels lies on a smooth curve symmetric about 90°. It is true that the anisotropy is less than the experimental error, but the smooth form of the curve and the agreement between our data and that of Yurova [6] (who measured at angles of 40° and 100°) verifies the anisotropy.

The inelastic neutron scattering cross sections were compared with the differential cross sections calculated according to the theory of Hauser and Feshbach [9]. The calculations were performed using the optical model of Porter, Feshbach, and Weisskopf [10]. The potential used was of the form

$$U(r) = -V_0(1 + i\xi) \text{ for } r < a,$$

$$U(r) = 0 \text{ for } r > a,$$

where  $a = 1.45 A^{1/3} 10^{-13}$  cm is the nuclear radius,  $V_0 = 42$  Mev, and  $\xi = 0.03$ .

This choice of parameters for the potential well leads to the best agreement between the experimental and theoretical cross sections.

As can be seen from Figs. 6 and 7, all the measured inelastic cross sections are from 3 to 10 times greater than the calculated ones. This divergence is explained by the form chosen for the potential and the small value of  $\xi$ .

The angular distribution of the inelastically scattered protons predicted by the theory is almost isotropic.

As is seen from Fig. 6, within the limits of our experiment inelastic scattering from chromium and iron is isotropic. Cranberg and Levin [5] have observed a weak anisotropy of the inelastic scattering from iron. Our points agree very well with the curves suggested by these authors, though the experimental error will not allow conclusions as to the anisotropy.

There exists no data on the angular distribution of inelastically scattered neutrons from chromium. There is likewise no data on the angular distribution of inelastically scattered protons from lead, with the exception of two points obtained by Yurova [6]. Inelastic scattering with excitation of the 0.53 Mev level in lead is isotropic within the limits of our experiment. The value we have obtained for the inelastic scattering cross section for this level would seem to be too high, since after calculating the results for the  $Pb^{207}$  isotope, to which this level belongs, we obtain a cross section of  $3.8 \pm 0.4$  barns. This result is, however, verified by other authors.

Bondarenko [7] has used a threshold detector, a  $U^{238}$  fission chamber, to measure the inelastic cross

This does not contradict the results of the present work, except for the inelastic scattering from the 0.805 and 0.890 Mev levels in lead. It would seem that this results from the inapplicability of the statistical theory to the compound nucleus  $Pb^{207}$  ( $Pb^{206} + n$ ).

It would seem that the statistical theory is applicable to the  $Pb^{208}$  compound nucleus, since it is excited to a much higher degree than  $Pb^{207}$ .

The author expresses his gratitude to Acting Member of the Academy of Sciences of the Ukrainian SSR A. I. Leipunsky for constant interest in the work, and to Candidates of Physical-Mathematical Sciences O. D. Kazachkovsky and I. I. Bondarenko for valuable discussion of the results.

Received February 13, 1957

#### LITERATURE CITED

- [1] J. Blok and C. Jonker, *Physica* 18, 809 (1952).
- [2] R. Meier, P. Scherrer and G. Trumphy, *Helv. Phys. Acta* 27, 577 (1954).
- [3] M. Walt, *Proceedings of the International Conference on the Peaceful Uses of Atomic Energy, Geneva 1955*, vol. 2, U.N., N.Y., 1956, p. 18.
- [4] D. J. Hughes and J. A. Harvey, *Neutron Cross Sections*, McGraw-Hill Comp., 1955.
- [5] L. Cranberg and J. Levin, *Phys. Rev.* 103, 343 (1956).
- [6] L. N. Yurova, private communication.
- [7] I. I. Bondarenko, private communication.
- [8] M. V. Pasechnik, *Physical Investigations (Reports of the Soviet delegation to the International Conference on the Peaceful Uses of Atomic Energy)*, Izd. AN SSSR, 1955, p. 319.
- [9] W. Hauser and H. Feshbach, *Phys. Rev.* 87, 366 (1952).
- [10] H. Feshbach, C. Porter and V. Weisskopf, *Phys. Rev.* 96, 448 (1954).

\*[The discrepancy in spelling between [9] and [10] is in the Russian original — Publisher's note.]

SPECTROSCOPIC QUANTITATIVE ANALYSIS OF THE ISOTOPIC COMPOSITION  
OF GAS MIXTURES CONTAINING HYDROGEN, DEUTERIUM, AND TRITIUM

M. N. Oganov and A. R. Striganov

A detailed experiment is carried through to construct a calibrating curve in the concentration interval from 0.7 to 97%  $H_2$  in  $D_2$ . The results obtained are in good agreement with theory. It is shown that it is possible to perform an isotopic analysis of tritium in mixtures with hydrogen and deuterium. An investigation is performed of the relative intensity of the isotope lines as a function of the pressure in a discharge tube.

Attempts have long ago been made to apply spectroscopic methods to the quantitative analysis of gas mixtures of hydrogen isotopes. It was only in 1952, however, that reliable experiments on this problem were published. Broida and co-workers [1] developed a photoelectric method for spectroscopic analysis of gas mixtures of hydrogen and deuterium in the concentration interval from 85 to 99% of deuterium.\* At the same time, and independently from the above authors, Veinberg and co-workers [3], as well as one of the present authors, developed photographic methods of spectroscopic analysis over a wider concentration interval. Our experiments were performed on mixtures of light hydrogen and deuterium, and the method was then applied to the isotopic analysis of tritium.

### 1. Experimental Apparatus

The spectroscopic apparatus was constructed of a three-prism glass ISP-51 spectrograph with a self-collimating UF-85 camera ( $F = 1300$  mm). This apparatus has a dispersion of about  $9.5 \text{ \AA/mm}$  in the region of  $6500 \text{ \AA}$ , which was found to be entirely sufficient for resolving the isotope lines  $H_{\alpha}$  and  $D_{\alpha}$ . The  $D_{\alpha}$  and  $T_{\alpha}$  lines are not then entirely resolved, although it was found possible to perform an isotopic analysis of deuterium-tritium mixtures with the aid of the ISP-51 spectrograph. The slit was illuminated by a condenser, for which  $f = 1200$  mm, located so as to place a sharp image of the source on the spectrograph objective. In order to compare lines of very different intensities, we used a platinum three-stage attenuator with transmission coefficients of 100, 46.2, and 11.8% in the region of  $6500 \text{ \AA}$  (we shall denote these three stages by 1, 2, and 3 respectively). In several cases, in order to decrease the intensity of one of the lines an additional gelatin filter with a transmission coefficient of 25.8% was placed in front of the photographic plate.

The light source was a quartz discharge tube with a capillary of length 50 mm and a diameter of 1-1.5 mm. Illumination was excited by an electrodeless high-frequency discharge from an 800 w oscillator at a frequency of 10 Mc. The discharge current was 400 ma. The coupling circuit was tuned to resonance with the oscillator by means of a variable capacitor.

Standard gas mixtures of hydrogen and deuterium were prepared in a special vacuum system by the method of partial pressures at constant volume. A diagram of this system is shown in Fig. 1. It consists of a mixing chamber 1 with a large oil U-manometer 2, two palladium tubes 3 and 4 for purifying the hydrogen and deuterium, a mercury U-manometer for measuring the hydrogen pressure, an electrolyzer 6, 7, 8 for obtaining

\* This work is discussed in detail in the review by Striganov [2].

deuterium from heavy water, a tank of ordinary hydrogen 9, liquid nitrogen traps, 10, 11, and 12 for removing water vapor, a diffusion pump 13 with a trap 14, a thermocouple tube 15, and a quartz discharge tube 16.

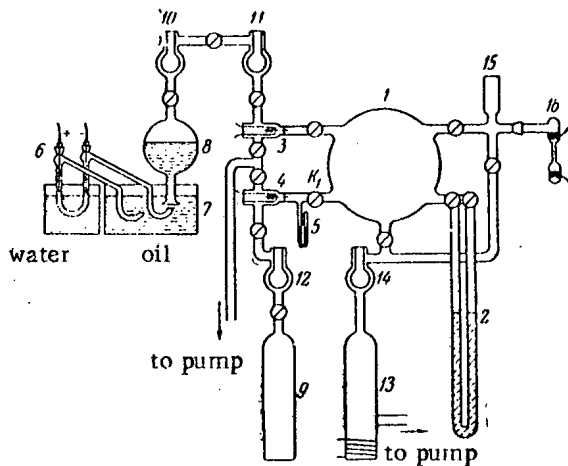


Fig. 1. Diagram of vacuum systems for preparing standards.

## 2. Preparing the Standards

The deuterium for the standards was collected in a gas tank 8 (see Fig. 1). It then passed through two liquid nitrogen traps 10 and 11. After this the gas passed through a palladium tube into an evacuated and degassed mixer 1, where the gas pressure was measured by the manometer 2.

The hydrogen from tank 9 passed through trap 12 and the palladium tube 4 into the volume in front of the valve  $k_1$ , where the gas pressure was measured by the mercury manometer 5. The hydrogen was admitted into the mixing chamber in small portions until the desired total pressure was reached. After a ten-hour delay the gas mixture was admitted into the discharge tube 16. The accuracy with which the standards are prepared by this method depends on the purity of the initial gases and the accuracy with which the partial pressures are measured in the mixing tank.

Deuterium was obtained from heavy water whose concentration was 99.5%  $D_2O$ . About  $8 \text{ cm}^3$  of 10% alkaline solution of heavy water ( $LiOD$ ) was admitted into the U-tube 6 of the electrolyzer, which was cooled by water. It was established spectroscopically [4] that the isotopic composition of the alkaline electrolyte corresponds exactly to the isotopic composition of heavy water. The tank 7 and the gas collector 8 were filled with vacuum grease. The deuterium and hydrogen were cleaned of water vapors by means of liquid nitrogen traps, in each of which the gas remained no less than twenty minutes. Palladium tubes were used to clean the gas of other impurities, as well for leads.

The pressure in the mixing chamber was measured by an oil manometer 1000 mm long with a cathetometric indicator and a vernier making it possible to read accurately to 0.1 mm. Special experiments showed that the oil manometer has practically no effect on the isotopic content of the samples being analyzed.

Since the standard samples were prepared from the partial pressures of hydrogen and deuterium ( $P_H$  and  $P_D$ ), the atomic concentrations of hydrogen and deuterium can be written

$$C_H = \frac{P_H}{P_H + P_D} 100. \quad (1)$$

The relative error in the prepared sample will be

$$\frac{\Delta C_H}{C_H} = \frac{\Delta P_H}{P_H} + \frac{\Delta P_H + \Delta P_D}{P_H + P_D}. \quad (2)$$

Since the pressures were measured by the same manometer,  $\Delta P_H = \Delta P_D$ , so that

$$\frac{\Delta C_H}{C_H} = \frac{\Delta P_H}{P_H} + \frac{2\Delta P_H}{P_H + P_D}. \quad (3)$$

For small concentrations (up to 10%) with  $P_H \ll P_D$ , we have

$$\frac{\Delta C_H}{C_H} \approx \frac{\Delta P_H}{P_H}, \quad (4)$$

and for medium concentrations (from 10 to 90%) when  $P_H \approx P_D$ , we have

$$\frac{\Delta C_H}{C_H} \approx \frac{2\Delta P_H}{P_H} \quad (5)$$

It follows that in preparing standard samples with low  $H_2$  concentrations, the relative error  $\Delta P_H / P_H$  in the pressure measurements should be no greater than the relative error  $\Delta C_H / C_H$  in the preparation of the standards, and that for medium concentrations, this error should be about two times lower.

Knowing the absolute error in pressure measurements, one can find the lowest pressure (in millimeters of oil) at which a given accuracy is attained in preparing the standard. According to Equations (4) and (5):

$$\text{for low concentrations } P_H = \Delta P_H C_H / \Delta C_H \quad (6)$$

$$\text{for medium concentration } P_H = 2\Delta P_H C_H / \Delta C_H \quad (7)$$

The other component is calculated also from Equation (1), so that

$$P_D = \frac{100 - C_H}{C_H} P_H \quad (8)$$

Table 1 gives the allowable errors in preparing standard samples of various concentrations.

TABLE 1

Concentration $H_2$ , % . . . . .	1	5	10	20	30	50	70	80
Allowable error in preparation. $\Delta C_H / C_H$ , % . .	2	1	0.5	0.4	0.3	0.2	0.1	0.1

We note that the above calculated data for preparing the standard samples can only be used roughly, since in admitting deuterium and hydrogen into the mixing chamber it is in practice hard to obtain specified pressures. Therefore the per cent concentrations of the components in the standard must be recalculated according to Equation (1) using the actually obtained pressures of  $H_2$  and  $D_2$ . The apparatus makes it possible to use a relatively high pressure, which in turn increases the accuracy of the standards. Preparation of the standards at high pressure eliminates the influence of gases absorbed in the walls of the mixing chamber.

### 3. Choice of Spectral Line

The line most suitable for isotopic analysis is the  $H_\alpha$  Balmer line ( $6562.79 \text{ \AA}$ ), which is ten times as intense as the  $H_\gamma$  line, and unlike the  $H_\beta$  line lies in a region in which there are no lines of the molecular spectrum. A disadvantage of this line is that it lies in the red region of the spectrum where the dispersion of prism spectrographs is relatively low.

Figure 2 shows a microphotogram of the isotopic  $H_\alpha$ ,  $D_\alpha$  and  $T_\alpha$  lines, obtained by photometry of a three-isotope sample whose spectrum was photographed by means of the ISP-51 spectrometer. From the microphotogram it is seen that the  $H_\alpha$  and  $D_\alpha$  lines are entirely resolved, whereas the  $D_\alpha$  and  $T_\alpha$  lines overlap somewhat.

For the spectral analysis of  $D_2 + T_2$  mixtures, it is better to use an apparatus with high dispersion (of the order of  $5 \text{ \AA/mm}$ ). Figure 3 shows the  $H_\gamma$  line as an example of the resolution of isotopic lines at a dispersion of  $2.8 \text{ \AA/mm}$ . The upper spectrum corresponds to pure hydrogen, the center one to a  $H_2 + D_2$  mixture, and the lowest one to a  $H_2 + D_2 + T_2$  mixture. Figure 4 gives a microphotogram of the  $H_\gamma$  line of a three-component sample, showing complete resolution of the isotopic lines.

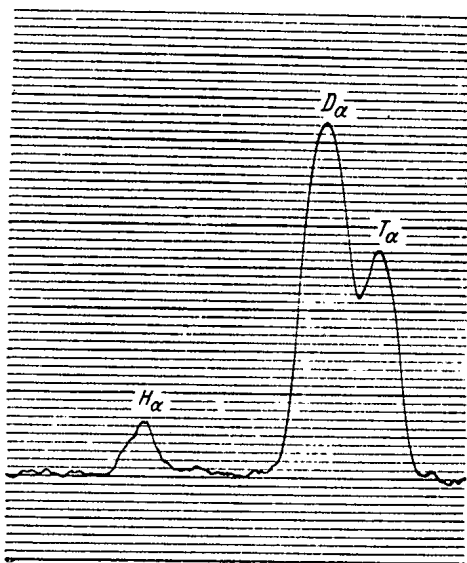


Fig. 2. Microphotogram of the  $H_{\alpha}$  line in a three-component sample.

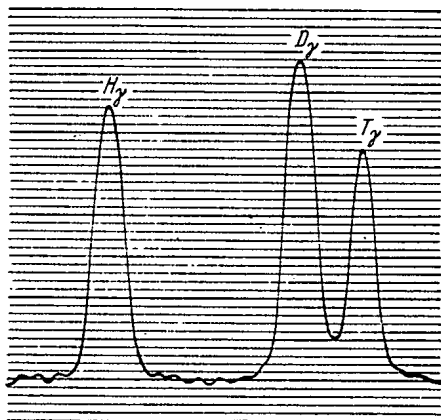


Fig. 4. Microphotogram of the  $H_{\gamma}$  line in a three-component sample.

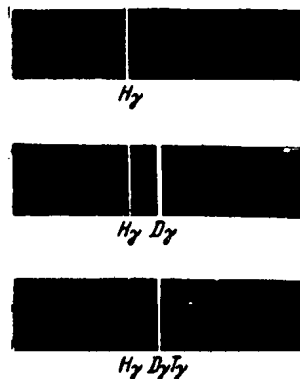


Fig. 3. Isotopic structure of the  $H_{\gamma}$  line.

#### 4. Photography and Treatment of the Spectra

Before starting operation, the discharge tube was carefully degassed by baking in a vacuum. It was then subjected several times to the mixture being investigated, and was aged five times for thirty minutes by discharge. Figure 5 shows the effect of aging the discharge tube.

When the spectra were photographed, the discharge tube was filled to a pressure of 0.4 mm Hg with the gas mixture being investigated. Five successive measurements were made on different portions of gas for the standard samples. For samples being analyzed, three portions of gas were used. The discharge tube was cooled by a stream of water during the experiments. The spectra were photographed on panchromatic photographic plates. At average concentrations (20-80%) the exposure lasted three seconds, and at low (1-20%) and high (80-95%) concentrations it lasted six seconds.

The quantity  $\log(I_H/I_D)$  was found at mean concentrations by photometry and using stages 1/1, whereas at low and high concentrations stages 1/3 and 3/1 were used. From the photometry data of the isotopic  $H_{\alpha}$  and  $D_{\alpha}$  lines, we obtained

$$\log \frac{I_H}{I_D} = \frac{W_H - W_D}{\gamma_W}, \quad (9)$$

where  $W_H$  and  $W_D$  are the transformed blackenings of the  $H_{\alpha}$  and  $D_{\alpha}$  lines as given by the microphotometer. The contrast factor  $\gamma_W$  was found by photometry of analytic lines with stages 1/2 and 2/3.



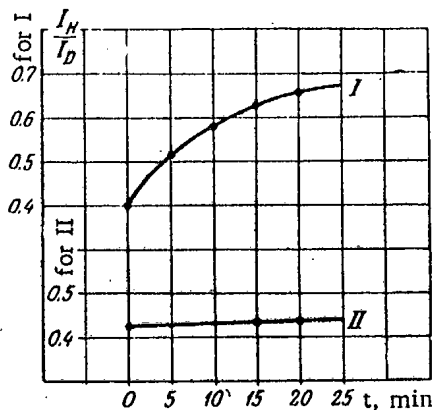


Fig. 5. The effect of aging the discharge tube.

I) Variation of the intensity ratio for an unaged tube; II) variation of the intensity ratio for an aged tube.

## 5. Calibration Curve

Figure 6 shows a calibration curve constructed from twenty standard  $H_2 + D_2$  mixtures and broken into four concentration regions. The abscissa gives values of  $\log(I_H/I_D)$ , and the ordinate values of  $\log(C_H/C_D)$ . To go over from the reduced concentration  $C_H/C_D$  to ordinary atomic concentrations  $C_H$ , an additional  $C_H$  scale is given on the ordinate axis in terms of per cent; one could also construct a table. The formula used to convert from one to the other is

$$C_H = \frac{\frac{C_H}{C_D} \cdot 100}{1 + \frac{C_H}{C_D}} \quad (10)$$

Curve I includes the lowest hydrogen concentrations (from 0.7 to 3.5%) and is constructed with the 1/1 stage, with the additional 25.8% attenuator used for the deuterium line. Curves II, III, and IV include the con-

centration ranges 3.5-25%, 25-75%, and 75-97%, respectively, and were obtained using stages 1/3, 1/1, and 3/1.

In a large concentration interval (from 5 to 95%) the calibration curve is a straight line making an angle of  $44.6^\circ$  with the concentration axis, and is bent at both ends (at concentrations of 5 and 95%  $H_2$ ); this straight line is displaced to the left of the origin by an amount  $\log(I_H/I_D) = -0.055$ . This displacement shows that when  $C_H = C_D = 50\%$ , the intensities of the  $H_\alpha$  and  $D_\alpha$  lines are not the same, so that at equal molecular concentrations of  $H_2$  and  $D_2$  in the discharge tube, the intensity of the hydrogen line will be 0.88 times that of the deuterium line. The intensities become equal when the  $H_2$  concentration is 53.3%, which corresponds to a reduced relative concentration of  $C_H/C_D = 1.13$ . Thus the  $H_\alpha$  and  $D_\alpha$  lines have the same intensity when the number of hydrogen molecules is 1.13 times that of deuterium molecules in  $H_2 + D_2$  mixtures.

The reason for these deviations, it would seem, is the different Doppler broadenings of the  $H_\alpha$  and  $D_\alpha$  lines at different association energies of  $H_2$  and  $D_2$  (4.47 and 4.53 ev). Indeed, the intensity ratio of the  $H_\alpha$  and  $D_\alpha$  lines at the maximum of the distribution curve is given by [5]

$$\frac{I_H}{I_D} = \frac{\alpha_H}{\alpha_D} \frac{C_H}{C_D} \sqrt{\frac{A_H}{A_D}} \quad (11)$$

where  $\alpha_H$  and  $\alpha_D$  are proportionality constants which reflect the physical properties of the isotopes, and  $\sqrt{A_H/A_D}$  is a correction due to Doppler broadening.

For hydrogen and deuterium,

$$\sqrt{A_H/A_D} = 0.71.$$

It follows that Doppler broadening decreases the normal intensity ratio of the  $H_\alpha$  and  $D_\alpha$  lines by a factor of 0.71. In order to evaluate  $\alpha_H/\alpha_D$ , it is necessary to account for the difference in hydrogen and deuterium molecule dissociation energies. Since the hydrogen molecule dissociation energy is less than that of deuterium, there will be more dissociated hydrogen molecules in the discharge tube when the dissociation is not complete. The number of dissociated molecules is given by the expression

$$N = N_0 e^{-\frac{E}{KT}} \quad (12)$$

where  $N_0$  is the total number of molecules.  $E$  is the dissociation energy,  $K$  is Boltzmann's constant, and  $T$  is the absolute temperature. From this we obtain

$$\frac{\alpha_H}{\alpha_D} \approx e^{-\frac{E_H - E_D}{KT}}, \tag{13}$$

where  $E_H$  and  $E_D$  are the dissociation energies of  $H_2$  and  $D_2$ , respectively. If we take the temperature of our source to be  $T = 2500^\circ K$ , then  $\alpha_H / \alpha_D = 1.30$ . This means that the normal intensity ratio for the isotopic lines will be increased by a factor of 1.30. The total effect is then the product of these two, namely  $0.71 \times 1.30 = 0.92$ . This quantity is greater than the experimentally found value of 0.88.

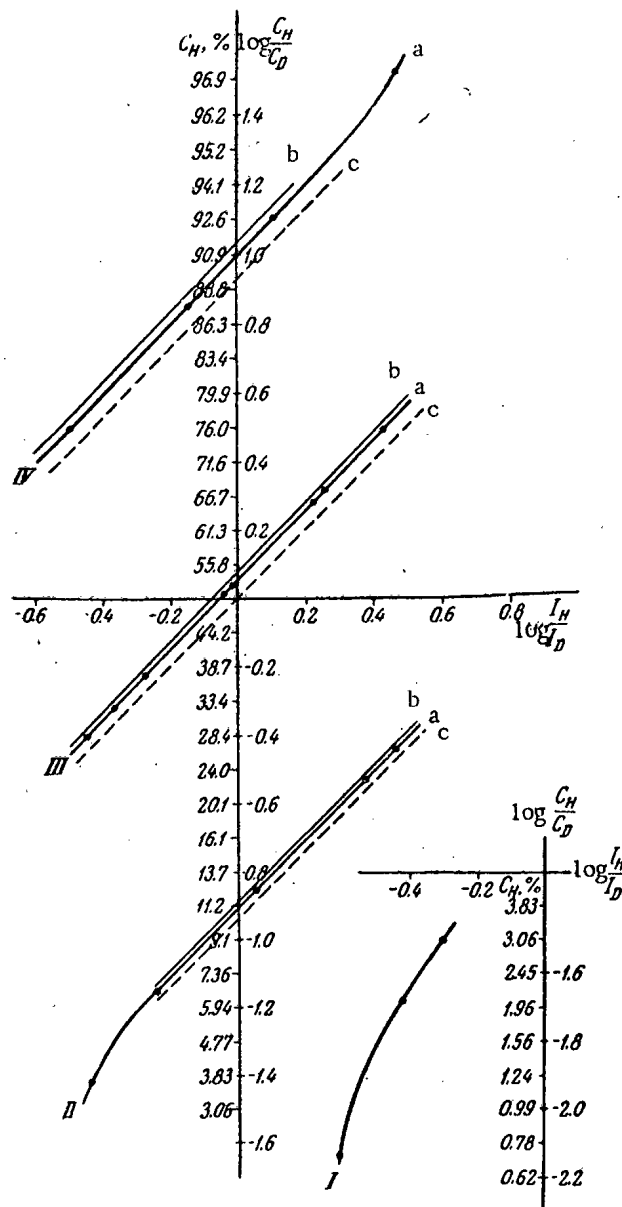


Fig. 6. Calibration curve.  
 a) Experimental curve for finding  $H_2$  in  $D_2$ ; b) auxiliary curve for finding  $H_2$  in  $T_2$ ; c) a graph of the equation  $I_H/I_D = C_H/C_D$ .

Our explanations do not claim to be complete, but are merely qualitative. It would seem that to account for all the effects would be quite difficult.

All the properties here noted of the calibration curve for the  $H_2 + D_2$  mixtures are in complete agreement with the theoretical relation obtained between the relative intensities of isotopic lines and relative isotope concentrations [5]. The deviation of the angle of slope from  $45^\circ$ , as well as the bend at the ends of the line are explained by the presence of a low background in the spectrum.

## 6. The Effect of Pressure

In performing the experiments it was found that the intensity ratio  $I_H/I_D$  varies depending on the gas pressure in the discharge tube. Figure 7 shows the intensity ratio of the  $H_\alpha$  and  $D_\alpha$  lines as a function of gas pressure for various concentrations. The results obtained show that at a concentration of about 10.2% the intensity ratio  $I_H/I_D$  remains about constant under pressure variation, whereas for lower and higher concentrations it increases with the pressure. Broida and Morgan[1] have shown that for pressures less than 0.4 mm Hg this increase is approximately inversely proportional to the pressure; at higher pressures, as in our case, it is approximately linear. This latter results from the more rapid decrease of the intensity of the  $D_\alpha$  line compared to that of the  $H_\alpha$  line.

There exists as yet no complete explanation of the pressure dependence of  $I_H/I_D$ . Veinberg et al. [3] have shown that an important factor influencing  $I_H/I_D$  is the fractionation which takes place when the  $H_2 + D_2$  gas passes through a capillary in the circulation system. In our apparatus, however, there are no capillaries, so that fractionation cannot alter the composition of the gas mixture in the closed discharge tube. It would seem that Doppler broadening and the different dissociation energies of  $H_2$  and  $D_2$  play important roles here. Of course one may assume that when the pressure is increased the kinetic energy of the particles is decreased, causing a drop in the temperature of the discharge column. This leaves the correction for Doppler broadening invariant, since it is temperature independent. However the correction due to the different dissociation energies will increase as the temperature is decreased, since the latter enters into the exponent in Equation (13). As a result of these simultaneous effects, a pressure increase will cause  $I_H/I_D$  to become larger. Since these effects act in opposite directions on the intensity ratio, at some pressure they will cancel each other. In this case  $I_H/I_D$  will correspond to the expression obtained in the absence of these effects (for instance at a concentration of 50.8% and pressure of 1.6 mm Hg, shown in Fig. 7).

There probably exist also other factors which compensate the effect of the difference in dissociation energies, as for instance at a concentration of 10%  $H_2$ , where  $I_H/I_D$  hardly varies.

From a practical point of view, the pressure dependence of the intensity ratio shows that it is necessary to maintain a given pressure in the discharge tube in performing analysis.

## 7. Analysis of Two- and Three-Component Samples

The analysis was performed in the vacuum system shown in Fig. 8. It consists of a quartz tube 1, an oil manometer 2 for measuring the pressure, an ampoule 3 with a valve, a tube 4 with by-pass valves, a thermocouple manometer tube 5, and a liquid nitrogen trap 6. The dimensions of the discharge tube must correspond to those of the tube with which this method was standardized. The ampoule with the gas to be investigated is attached to the tube with two or three by-pass valves. After careful degassing and aging of the vacuum system (see Section 4), small portions of the gas to be analyzed were admitted into the discharge tube up to pressures of 0.4 mm Hg. The spectra were then photographed.

The isotopic composition was analyzed with the aid of a constant calibration curve. The calibration curve for  $H_2 + D_2$  mixtures is shown in Fig. 6. As has already been noted, this calibration curve is displaced by an amount  $\log(I_H/I_D) = -0.055$  from the origin. Using this as a basis, we constructed an additional calibration curve for  $H_2$  and  $T_2$ , displacing it by an amount  $\log(I_H/I_D) = -0.08$ , in agreement with the difference in mass numbers (see Fig. 6). In exactly the same way, the concentration of  $D_2$  in  $T_2$  can be found from a calibration curve displaced by an amount  $\log(I_H/I_D) = -0.04$ .

The spectroscopic method makes it possible to obtain directly the reduced relative isotope concentrations, which can then be transformed to per cent concentrations relative to the total sum of the two isotopes, by using

Equation (10). In practice, however, for three-component samples, it is usual to express the concentration relative to the sum of the three isotopes. Below we show how to transform from the reduced relative concentrations obtained from the calibration curves to per cent concentrations relative to the total amount of three isotopes.

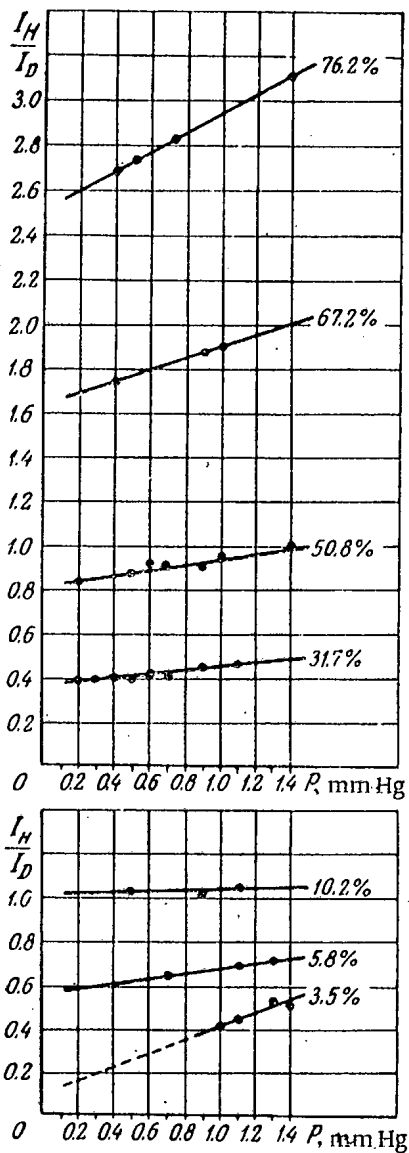


Fig. 7. Pressure variation of the intensity ratio.

These two equations and

$$C_H + C_D + C_T = 100 \text{ (\%)}, \tag{17}$$

is a set of three equations in three unknowns, whose solution is

$$C_H = \frac{100}{\left(1 + \frac{1}{C_{II}'} + \frac{1}{C_{II}''}\right)}, \quad C_D = \frac{100}{C_{II}'' \left(1 + \frac{1}{C_{II}'} + \frac{1}{C_{II}''}\right)}, \quad C_T = \frac{100}{C_{II}'' \left(1 + \frac{1}{C_{II}'} + \frac{1}{C_{II}''}\right)}. \tag{18}$$

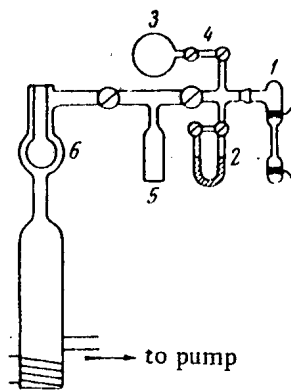


Fig. 8. Vacuum system for analyzing the isotopic composition of hydrogen, deuterium, and tritium.

Letting  $P_H$ ,  $P_D$  and  $P_T$  be the partial pressures of the three isotopes, the reduced relative concentrations are given by

$$C_H' = \frac{P_H}{P_D}, \quad C_H'' = \frac{P_H}{P_T}. \tag{14}$$

The concentrations relative to the total amount of the three components are given by

$$C_H = \frac{P_H \cdot 100}{P_H + P_D + P_T}, \quad C_D = \frac{P_D \cdot 100}{P_H + P_D + P_T}, \tag{15}$$

$$C_T = \frac{P_T \cdot 100}{P_H + P_D + P_T}.$$

The relations between  $C_H'$ ,  $C_H''$  and  $C_H$ ,  $C_D$ ,  $C_T$ , are

$$C_H' = \frac{C_H}{C_D}, \quad C_H'' = \frac{C_H}{C_T}. \tag{16}$$

Thus in order to find the concentrations relative to the total amount of the three isotopes in a three-component mixture, we must know the reduced concentrations  $C_H'$  and  $C_H''$ . These can be found with the aid of the calibration curves. It is more convenient to use the first of equations (18) for  $C_H$ , and then find the concentrations of the other two isotopes from the equations

$$C_D = \frac{C_H}{C_H'}, \quad C_T = \frac{C_H}{C_H''} \quad (19)$$

The accuracy of this method was established by many analyses of fourteen gas mixtures containing  $H_2 + D_2$ .

TABLE 2

Concentration $H_2$ , %	Mean square error, %	
	Absolute	Relative
4-5.5	± 0.25	± 5.5
18-30	± 0.77	± 3.5
38-61	± 0.33	± 0.6
71-89	± 0.50	± 0.6

In Table 2 we give the mean square error over four concentration regions. Qualitatively, the variation of the error with concentration is in good agreement with theory [2].

## SUMMARY

It has been shown that there exists no simple equality between  $I_H/I_D$  and  $C_H/C_D$  for hydrogen isotopes in the conditions of our experiment. Equality can be obtained only at certain definite gas pressures in the discharge tube, this pressure depending on the concentration. Therefore in order to avoid systematic errors, it is necessary to standardize a method in order to establish the relation between  $I_H/I_D$  and  $C_H/C_D$ . It is, however, possible to choose such experimental conditions that the factor  $\frac{\alpha_H}{\alpha_D} \sqrt{A_H/A_D}$  in Equation (11) will be close to unity; then the intensity ratio  $I_H/I_D$  uniquely determines the relative concentration ratio in the sample investigated. It is of course clear that this requires detailed preliminary experiments with standard mixtures.

Received July 20, 1956

## LITERATURE CITED

- [1] H. P. Broida and I. W. Moyer, *J. Opt. Soc. Am.* 42, 37 (1952); H. P. Broida and G. H. Morgan, *Anal. Chem.* 24, 799 (1952).
- [2] A. R. Striganov, *UFN* LVIII, No. 3, 365 (1956).
- [3] G. V. Veinberg, A. N. Zaidel, and A. A. Petrov, *Optics and Spectroscopy* 1, No. 8, 972 (1956).
- [4] Yu. P. Dontsov and A. R. Striganov, *Analytical Chemistry* XII, No. 1, 5 (1957).
- [5] A. R. Striganov, *Factory Lab.* No. 12, 1476 (1955).

ANALYSIS OF NATURAL RADIOACTIVE ELEMENTS BY MEANS OF  
LABORATORY RADIOMETRIC MEASUREMENTS

I. M. Nazarov

Radiometric methods are described for determining the amount of natural radioactive elements in rocks, ores, minerals, etc. The presently existing methods are based on a) measuring various types of radiation, b) discrimination of one type of radiation, c) using in addition to the measurement of one type of radiation, additional emanation measurements, and d) combinations of the first two methods. Equations are given in general form for the determination of the amounts of separate radioactive elements, and these are analyzed for the specific conditions involved in determining the amount of uranium, radium, thorium, and potassium.

At the present time radiometric methods for determining the amount of natural radioactive elements are replacing the more expensive chemical analyses and are becoming the fundamental method in industrial measurements. When detecting radioactive elements, however, the determination of their amount is not always sufficiently accurate. Although in simple ores containing only equilibrium uranium or thorium, radiometric measurements are often even of higher accuracy than the chemical ones, in nonequilibrium and complex ores, and particularly in low concentrations, radiometric measurements may involve errors that are greater than one can allow.

The problem of increasing the accuracy of radiometric determinations can be solved successfully in each particular case at the least expenditure of effort by a deep study of the physical processes determining the results of measurement.

Thus the author considers it useful to investigate the problem of the quantitative analysis of radioactive elements in a general form and to show that all existing methods reduce to simple mathematical relations.

Let us denote the counting rate from 1%  $j$ -th radioactive element by  $n_{ij}$ , where the index  $i$  defines the conditions of measurement, that is whether one is counting  $\alpha$ ,  $\beta$ , or  $\gamma$  particles, the discriminator setting, screening thickness, etc. Then the counting rate from a radioactive sample containing  $m$  radioactive elements can be written

$$\sum n_{ij} q_j = n_i - \phi_i, \quad (1)$$

where  $q_j$  is the content of the  $j$ -th element in per cent,  $\phi_i$  is the background counting rate, and  $n_i$  is the counting rate from the sample and the background, together.

To determine the content of each element, we need  $m$  linearly independent first order algebraic equations such as (1). In practice the results are more often given in equivalent uranium units, which means that one finds the counting rate relative to that from a sample containing 1% of equilibrium uranium under the same conditions of measurement:

$$A_i = (n_i - \phi_i) c_i, \quad (2)$$



3) methods which use, in addition to measurements of a single type of radiation, measurements of additional emanations;

4) combined methods, involving a combination of the first two above.

A method for determining the uranium and radium content in nonequilibrium ores from measurements of  $\beta$  and  $\gamma$  radiation was proposed by V. L. Shashkin in 1947.\* A similar method was developed in France in 1949 by Tommeret [1].

The  $\beta$  and  $\gamma$  measurements were performed using Geiger counters. The  $\beta$  and  $\gamma$  radiation was separated by metallic screens whose thickness was of the order of 1-2 gm/cm<sup>2</sup>. Circuits consisting of many counters were used in order to increase the sensitivity.

The most successful method for increasing sensitivity to  $\gamma$  radiation involves using scintillation counters [2].

In all modifications of the method, the measurements were performed in saturation layers for  $\beta$ -rays. Depending on its content, the weight of the sample varied between 20 and 600 gm. The weight was usually between 50 and 150 gm.

The degree of granulation of the material plays no role, except for extreme cases (greater than 1 mm or less than 100 mesh).

The fundamental assumption of the method is that  $UI/UX_2 = \text{const}$ . Then neglecting  $\gamma$  radiation from  $UX_2$  and  $UZ$ , one obtains the following two equations from Equation (3) in equivalent uranium units:

$$\left. \begin{aligned} a_{11}U + a_{12}Ra &= A_{\beta}, \\ Ra &= A_{\gamma}. \end{aligned} \right\} \quad (7)$$

In order to calculate the coefficients, let us use the formula for determining the intensity of  $\beta$  radiation from a thin layer [3], extrapolating it to the thickness of a saturation layer for  $\beta$  radiation. Then making the rough approximation that when measuring with an end counter the counting efficiency is independent of the  $\beta$ -ray energy, from Equation (7) we obtain

$$a_{11} = \frac{\Delta_{UX_2}}{\Delta_{UX_2} + \Delta_{RaB} + \Delta_{RaC} + \Delta_{RaE}}, \quad (8)$$

$$a_{12} = 1 - a_{11} = \frac{\Delta_{RaB} + \Delta_{RaC} + \Delta_{RaE}}{\Delta_{UX_2} + \Delta_{RaB} + \Delta_{RaC} + \Delta_{RaE}}, \quad (9)$$

where  $\Delta$  is the half-value thickness for  $\beta$  radiation.

Since the  $\beta$ -radiation from  $UX_1$  and  $RaD$  is of low energy, its influence may be neglected.

Using the data on  $\beta$ -energies [4] and a graph relating the maximum energy to the half-value thickness [3], the author found that

$$\begin{aligned} \Delta_{UX_2} &= 130 \text{ mg/cm}^2 & \Delta_{RaB} &= 20 \text{ mg/cm}^2 \\ \Delta_{RaC} &= 110 \text{ mg/cm}^2 & \Delta_{RaE} &= 44 \text{ mg/cm}^2 \end{aligned}$$

Inserting these values into (8) and (9), we obtain  $a_{11} = 0.43$  and  $a_{12} = 0.57$ .

These results are in agreement with the experimentally obtained values for the coefficients using an end counter with a window thickness of 3 mg/cm<sup>2</sup> [2].

\* Unpublished work.



In order to go over to counters with wall thickness  $l$ , we may assume that the total efficiency is equal to the product of the counting efficiency, which is almost energy independent, and a function which gives the absorption in the counter walls. One can easily calculate the necessary corrections if one assumes that the absorption in the walls of a cylindrical counter varies exponentially, but that the effective thickness depends on the experimental geometry and may be twice as great as the true thickness of the counter walls [3]. When the wall thickness is  $l = 30 \text{ mg/cm}^2$  and  $l_{\text{eff}} = 2l$ , we obtain  $a_{11} = a_{12} = 0.5$ . For AS-2 and STS-6 counters (with approximately equal wall thicknesses)  $a_{11}$  is 0.52 and 0.515, and  $a_{12}$  is 0.48 and 0.485, respectively.

If the effective wall thickness is taken to be between 1.2 and 1.5 times  $l$ , the results obtained will be about the same.

As follows from Equation (6), the relative error in the determination of the uranium content, due to fluctuations in the counting rate, is given by

$$\epsilon_U = \frac{\sqrt{c_\beta^2 \left( \frac{n_\beta}{l_\beta} + \frac{\phi_\beta}{l_{\phi\beta}} \right) + c_\gamma^2 a_{12}^2 \left( \frac{n_\gamma}{l_\gamma} + \frac{\phi_\gamma}{l_{\phi\gamma}} \right)}}{A_\beta - a_{12} A_\gamma} \quad (10)$$

Thus for a given duration of measurement and a given background rate, the relative error depends both on the total sensitivity of the apparatus and on its sensitivity to the  $\beta$  radiation from radium. All other conditions being equal, the error will be smaller as  $a_{12}$  is made smaller, the latter determining the amount of radium radiation in the equilibrium series.

Since the radium content is determined from the  $\gamma$  radiation from RaC, an accurate determination of the radium content necessitates a knowledge of the emanation coefficient. If the emanation coefficient  $k$  is known, the radium content can be found from

$$\text{Ra} = \frac{A_\gamma}{1 - k} \quad (11)$$

In addition to an equilibrium shift between uranium and radium, or radium and short-lived decay products of radon, an equilibrium shift may occur between radon with its short-lived decay products and RaE. The amount of short-lived decay products is found from the emanation of the sample; thus when the sample, screened from the untouched ore, is ground, there may occur an additional amount of RaE due to an increase in the emanation. It is not difficult to see that this additional amount of  $\beta$ -radiation will lead to an increase in the observed uranium content. Denoting the increase in the RaE content over the amount of short-lived decay products by  $\Delta q_{\text{RaE}}$ , the increase obtained in the uranium content will be

$$\frac{\Delta U}{U} = \frac{a_{\text{RaE}} \frac{\Delta q_{\text{RaE}}}{A_\gamma}}{\frac{A_\beta}{A_\gamma} - a_{12}} \quad (12)$$

For an end counter,  $a_{\text{RaE}} = 0.14$ . When the equilibrium shift is destroyed only by 30% emanation, the error in the determination of the uranium content is about 7%. For an equilibrium shift by a factor of 5 towards radium, 30% emanation causes the error to increase to 50%.

When using AS and STS counters,  $a_{\text{RaE}} = 0.084$ . For this reason, as well as because of the decrease in  $a_{12}$ , the influence of RaE on the accuracy of the uranium determination is reduced roughly by a factor of 2.

In order to remove the influence of RaE, one introduces an aluminum filter of thickness between 240 and 270  $\text{mg/cm}^2$  [5], which almost entirely absorbs the  $\beta$  radiation.

In this case, if the  $\gamma$  counter registers part of the hard  $\beta$  radiation from  $\text{UX}_2$  or the  $\gamma$  radiation from  $\text{UX}_2$  and  $\text{UZ}$ , the second equation of (7) must be rewritten

$$a_{21}\text{U} + a_{22}\text{Ra} = A_\gamma \quad (13)$$

After some simple operations, one obtains a formula for finding the uranium content, namely

$$U = \frac{1}{a_{11}} A_{\beta} - \frac{a_{12}}{a_{11}} A_{\gamma} + \left[ \frac{a_{12} a_{21}}{a_{11}^2 a_{22}} A_{\beta} - \frac{a_{12} a_{21}}{a_{11}} \left( 1 + \frac{a_{12}}{a_{11}} \right) A_{\gamma} \right], \quad (14)$$

where the expression in square brackets is a correction to the radiation from uranium recorded in the  $\gamma$  measurements.

Let us evaluate this correction term when  $a_{11} = a_{12} = 0.5$ ,  $a_{21} = 0.06$  and  $a_{22} = 0.94$ , which is approximately the situation when measuring with AS and STS counters without screening and with a screen whose thickness is  $800 \text{ mg/cm}^2$ . As  $\text{Ra}/\text{U} \rightarrow 0$ , the correction term approaches 6% of the uranium content obtained. For approximately equilibrium conditions, the correction is about 1%. Finally, as  $\text{U}/\text{Ra} \rightarrow 0$ , the correction approaches  $-0.05 A_{\gamma}$ , so that if there is no uranium at all, it will give a "negative" amount.

The influence of thorium on the accuracy with which the uranium content is determined depends strongly on the radiation measuring devices. Very often [2, 5] it is found that about 1% of thorium gives off  $\beta$  and  $\gamma$  radiation about equivalent to radium in equilibrium with 0.5% uranium. In this case the presence of thorium is treated as additional radium, and the uranium can be accurately determined.

If the  $\beta$  and  $\gamma$  radiation of thorium and radium are not equivalent, it is impossible to determine the exact amount of uranium when thorium is present.

The sensitivity of  $\gamma$ -radiation methods with Geiger counters is seldom greater than 0.005% uranium with low equilibrium shifts; when the equilibrium shift is large in the direction of radium, however, the sensitivity may be several times lower.

The use of scintillation counters for measuring the  $\gamma$  radiation can increase the sensitivity to 0.001% uranium, and even better.

The errors in the determination of the uranium content are usually between 5 and 20%.

A method for determining the equilibrium uranium and thorium content from  $\beta$  and  $\gamma$  radiation was suggested by V. I. Baranov and N. N. Shashkina [6] in 1947. Outside the USSR a description has been given by Franklin and Barnes [7].

From the technical point of view this method is no different than that for the determination of the separate contents of uranium and radium.

In this case the equations are

$$\left. \begin{aligned} U + a_{12} \text{Th} &= A_{\beta}, \\ U + a_{22} \text{Th} &= A_{\gamma}. \end{aligned} \right\} \quad (15)$$

The coefficient  $a_{12}$  was calculated on the basis of  $\beta$  radiation energy data presented by Baranov [6]. The half-value thicknesses were obtained in the same way as for elements of the uranium series, and are

$$\begin{aligned} \Delta_{\text{MSTh}_2} &= 68 \text{ mg/cm}^2 & \Delta_{\text{ThB}} &= 9 \text{ mg/cm}^2 \\ \Delta_{\text{ThC}} &= 82 \text{ mg/cm}^2 & \Delta_{\text{ThC}'} &= 27 \text{ mg/cm}^2 \end{aligned}$$

If we take into account the different decay rates of uranium and thorium [8], for an end counter it is found that  $a_{12}$  is equal to 0.22. Almost the same value ( $a_{12} = 0.215$ ) is obtained for AS and STS counters. For MST-17 counters we obtain  $a_{12} = 0.26$ , and for a counter with a window thickness of  $3 \text{ mg/cm}^2$  Eicholz [2] gives a value of 0.25. For AS-2 and STS-6 counters,  $a_{12} = 0.23$ .

The value of  $a_{22}$  can be found for a counter with a copper cathode, since the efficiency of such a counter is almost directly proportional to the  $\gamma$ -ray energy [9]. Using the data on radium and thorium  $\beta$  radiation [6],

one is led to a value of 0.49 for  $a_{12}$ . This result does not account for self-absorption of the  $\gamma$  radiation.

Common values of  $a_{22}$  lie between 0.43 and 0.60, depending on the type of recording apparatus [5, 10-15]. For counters with copper cathodes, the experimental value of  $a_{22}$  lies usually between 0.45 and 0.47. The lowest values of  $a_{22}$  are obtained in ionization measurements, and the highest in measurements at which the low-energy lines are cut off.

The sensitivity and accuracy of the method is approximately the same as in determining uranium and radium in nonequilibrium ores.

A practical convenience of the method using  $\beta$  and  $\gamma$  measurements is the relative simplicity of the apparatus and the fact that it is possible to perform both measurements simultaneously on a single sample. This method is sufficiently sensitive for surveying and exploiting deposits of radioactive elements, but its accuracy is often insufficient for solving special problems. The determination of uranium and thorium contents by discriminating only one type of radiation is only possible in the absence of an equilibrium shift, since it is the radiation of the daughter elements which is measured.

The first discrimination methods for  $\alpha$  radiation were developed by Evans [8, 16, 17] in the middle thirties. He performed his measurements in pulse ionization chambers with screens whose thickness was of the order of 5 to 6 cm air equivalent, and without such screens. When  $\alpha$  scintillation counters first appeared, two equations were used which were obtained by measuring the distance from the source to the scintillator [18] or the discriminator threshold [19].

In all the above-mentioned works the results of measurements were expressed not in equivalent uranium units, but directly in terms of the counting rate, and the set of equations was of the form

$$\left. \begin{aligned} \mu d (n'_{11}U + n'_{12}Th) &= n_1 - \phi_1, \\ \mu d (n'_{21}U + n'_{22}Th) &= n_2 - \phi_2, \end{aligned} \right\} \quad (16)$$

where  $\mu d$  is the product of the density  $d$  of the substance by its stopping power  $\mu$ , which was found as the ratio of the range of an  $\alpha$ -particle in the substance to its range in air [8];  $n'_{11}$ ,  $n'_{21}$  and  $n'_{12}$ ,  $n'_{22}$  are the counting rates from 1% uranium and thorium at  $\mu d = 1$ .

In the second measurement only  $\alpha$ -particles from ThC' are recorded, with all the other  $\alpha$  radiation being cut off.

The product  $\mu d$  is calculated separately, since for various ores it may vary by as much as 10 to 15%, and for various minerals by as much as several times a hundred per cent.

If the chemical composition of the substance is known,  $\mu d$  can be calculated by Bragg's rule. If the chemical content is not known, however,  $\mu d$  can be calculated by measuring the variation of the counting rate when a known amount of uranium or thorium is added to the sample and thoroughly mixed with it. When the standard and the sample have similar compositions, Equations (16) expressed in terms of equivalent uranium units are independent of the sample composition, as has been shown by the author:

$$\left. \begin{aligned} U + a_{12}Th &= A_1, \\ U + a_{22}Th &= A_2. \end{aligned} \right\} \quad (17)$$

The form of (17) is no different than that of Equations (15) obtained for  $\beta$  and  $\gamma$  measurements.

The coefficients  $a_{12}$  and  $a_{22}$  can be calculated using Evans' formula [8] for a saturated layer.

For bulk material, the thickness of the saturation layer is about  $50 \mu$ . In order to avoid possible intergranular openings in the source, the thickness is taken of the order of 1 mm when performing measurements with a porous ground sample. Even when using the largest pans with an area of the order of  $150 \text{ cm}^2$ , the weight of the sample is not greater than several grams.

The material is usually ground down to 100 mesh, although if it is experimentally established that the

counting rate for a given ore hardly depends on the grain size, one may use a coarser grind.

For the  $\alpha$ -particles with the lowest recorded range, namely  $\rho = 0.45$  cm of air, the calculated value of  $a_{12}$  is 0.324. For measurements on a Da-49 apparatus with a cutoff corresponding to  $\rho = 0.45$  cm, the author obtained  $a_{12}$  equal to 0.320.

The sensitivity of the apparatus for measurements in aged nitrogen atmospheres (that is, with a background of 5-15 counts per hour), using pulse chambers with electrode areas up to 150 cm<sup>2</sup>, lies between 1 and  $5 \cdot 10^{-4}$ ‰ uranium and thorium, if one uses a screen of the order of 5-6 cm air equivalent. The limit of sensitivity is given by the second equation, since due to the reduced counting rate it is in the measurements with the screen that the practical minimum of sensitivity is reached; this minimum is due to statistical fluctuations in the background counting rate. At the lowest concentrations, the duration of measurement for a single sample may be as much as 10-20 hours.

The use of  $\alpha$  scintillation counters is more highly developed than that of pulse counters. However in performing measurements at low concentrations, which is the fundamental region of application for  $\alpha$  radiation measurements, the background limits the usefulness of  $\alpha$  scintillation counters.

The sensitivity of scintillation counter measurements is almost an order and a half lower than that of ionization chambers.

The accuracy of  $\alpha$  measurements depends strongly on the chemical composition and physical state of a sample, and particularly on the emanation. In addition, at low concentrations a very important, and often decisive role, is played by the statistical fluctuations in the counting rate. For hardly converted igneous rock the errors are often of the order of 10-20‰, and only in very favorable cases will they be lower.

A method for determining the equilibrium uranium content by  $\gamma$ -ray discrimination has recently been suggested by Withan [20] in connection with recent developments in  $\gamma$  spectroscopy. The form of the equations is then similar to (15) and (17).

For a sample weighing 100 gm, Withan's apparatus can be used to measure activities up to 0.004 ‰ uranium equivalent, but detection of uranium and thorium could be attained only at activities no lower than 0.04‰ uranium equivalent.

A special set of methods is that employing time discrimination in something akin to a reversal of the Geiger-Nuttall law. A description of the theoretically possible modifications of these methods is given in the work of Franklin and Barnes [7]. Peirson [19] has suggested a similar method for determining equilibrium uranium and thorium.

As is well known, RaC is transformed to RaC' by  $\beta$  decay, and this latter is an  $\alpha$  emitter with a half-life of 160  $\mu$ sec; on the other hand, ThC decays to ThC', which has a half-life of 0.3  $\mu$ sec. The duration of sensitivity of the  $\alpha$  detector is determined by a time discriminator triggered by Geiger counters. The discriminator is set so that it can record the  $\alpha$  particles of RaC' and ThC' with a large sensitivity time, or those of ThC' with a small one. Subtracting the number of chance coincidences calculated from the total  $\alpha$  and  $\beta$  counts, Peirson obtained two equations similar to (16). However the extremely complicated apparatus and the low sensitivity caused him not to use this method in practice, in spite of the fact that it is reasonable in principle.

Errors in the determination of uranium and thorium due to statistical fluctuations in the counting rate, in view of the similar form of the equations, are in all cases given by the same expressions:

$$\epsilon_U = \frac{\sqrt{a_{22}^2 c_1^2 \left( \frac{n_1}{t_1} + \frac{f_1}{t_{f_1}} \right) + a_{12}^2 c_2^2 \left( \frac{n_2}{t_2} + \frac{f_2}{t_{f_2}} \right)}}{|a_{22}A_1 - a_{12}A_2|}, \quad (18)$$

$$\epsilon_{Th} = \frac{\sqrt{c_1^2 \left( \frac{n_1}{t_1} + \frac{f_1}{t_{f_1}} \right) + c_2^2 \left( \frac{n_2}{t_2} + \frac{f_2}{t_{f_2}} \right)}}{|A_2 - A_1|}. \quad (19)$$

In Equations (18) and (19) the sign in the denominator is dropped, since it does not matter which equation is first and which is second. It is not difficult to see that though the accuracy in the thorium determination depends explicitly on the total sensitivity of the apparatus, the accuracy in the uranium determination depends on the relation between  $a_{12}$  and  $a_{22}$ . All other conditions being equal, this accuracy is greatest when the difference between these coefficients is largest.

Thorium and uranium determination by  $\alpha$  measurements with auxiliary emanation measurements is used for activities between  $10^{-4}$  and  $5 \cdot 10^{-5}\%$  equilibrium uranium equivalent.

The uranium content is determined from emanation measurements on the assumption that it is in equilibrium with radium, and the thorium content is determined from the total  $\alpha$  count.

When the radium is reduced in a solution, it is in principle possible to use the solution to determine the thorium from the thoron.

But such a pure emanation method for determining the above concentrations is admittedly inapplicable in practice, both due to the complexity of the thoron measurements and to the decreased accuracy.

Radon measurements can be performed with the aid of electrometers and pulse methods.

The emanation is introduced into the chamber by a vacuum system. In measuring the lowest concentrations, the chamber is filled with nitrogen or carbon dioxide, which are first stored for about a month so that any possible radon impurity may decay.

At very low concentrations it is not desirable to reduce the samples in a solution, due to many effects related both to loss of radium in the chemical vessels, as well as to alteration of the results by radium impurities from the chemicals themselves. These difficulties can be avoided by baking the sample in an oven to temperatures sufficient to separate out the radon [21, 22]. The weight of the sample from which the radon is separated is usually no greater than 10-30 gm.

The accuracy in measuring extremely low concentrations is almost completely determined, if one takes measures which warn of loss or introduction of additional radon, by statistical fluctuations, and errors between 5 and 15% can become very much larger, even as large as several times a hundred percent.

An attempt to design a method using  $\gamma$  and emanation measurements [13] was not successful due to the low sensitivity of the Geiger counters and due to the fact that such a method was subject to the influence of potassium  $\gamma$ -rays.

A disadvantage of the above methods is their restriction by certain conditions placed at the basis of the equations. For industrial use or for specific concrete problems they are usually satisfactory. Thus, if one is even able to determine only the radium in the presence of thorium and an equilibrium shift, this is entirely sufficient. In solving more complex problems it is convenient to know all of the components independent of their inter-relations.

In recent years, several Soviet investigators [5] have suggested a method for the determination of separate uranium, radium, and thorium contents (if one can neglect the radiation from potassium), based on a combination of  $\gamma$  discrimination and  $\beta$  measurements:

$$\left. \begin{aligned} a_{11}\dot{U} + a_{12}\text{Ra} + a_{13}\text{Th} &= A_{\beta}, \\ \text{Ra} + a_{23}\text{Th} &= A_{\gamma_1}, \\ \text{Ra} + a_{33}\text{Th} &= A_{\gamma_2}. \end{aligned} \right\} \quad (20)$$

These equations are formally the same as those of Whithan, but it is not assumed that the radium is in equilibrium with the uranium. The magnitudes of the coefficients of Equations (20) are similar to those of the methods described above.

Using a ring scaler with Geiger counters for discrimination of the  $\gamma$  radiation, Golbek and co-workers [5] obtained  $a_{23} = 0.51$  and  $a_{33} = 1.11$  (the calculation of these coefficients was performed on the basis of their own

data [5], since the authors equations were not expressed in equivalent uranium units, but directly in counting rates). The coefficient for thorium increases by about a factor of two when the counting rate from radium drops by a factor of 90 and that from thorium by a factor of 41.5.

With a CsI scintillation counter (designed by the author and P. I. Solonkov), the thorium coefficient changes from 0.7 to 1.7 when the counting rate from radium has decreased by a factor of 41 and that from thorium by a factor of 17.

By decreasing the thorium counting rate by a factor of 40 and using a specially chosen photomultiplier, it was possible to cut off completely the radiation from radium, so that the last equation of (20) becomes

$$\text{Th} = A_{\gamma_2} \quad (21)$$

where  $A_{\gamma_2}$  is expressed directly in per cent of thorium.

To date this method has not yet found wide industrial application, and it is therefore difficult to speak of its accuracy and sensitivity; in any case, these should be roughly of the same order as for other methods using similar apparatus.

The expression for the relative error in uranium determination can be written

$$\epsilon_U = \frac{\sqrt{(a_{33} - a_{23})^2 c_{\beta}^2 \left( \frac{n_{\beta}}{t_{\beta}} + \frac{g_{\beta}}{t_{g_{\beta}}} \right) + (a_{12}a_{33} - a_{13})^2 c_1^2 \left( \frac{n_1}{t_1} + \frac{g_1}{t_{g_1}} \right) + (a_{12}a_{23} - a_{13})^2 c_2^2 \left( \frac{n_2}{t_2} + \frac{g_2}{t_{g_2}} \right)}}{(a_{33} - a_{23}) A_{\beta} - (a_{12}a_{33} - a_{13}) A_{\gamma_1} + (a_{12}a_{23} - a_{13}) A_{\gamma_2}} \quad (22)$$

The relative errors in the radium and thorium determinations are given by expressions (18) and (19), except that the coefficient  $a_{22}$  in the radium formula should be replaced by  $a_{33}$ , and  $a_{12}$  should be replaced by  $a_{23}$ . The indices 1 and 2 now refer to the numbers associated with the  $\gamma$  measurements.

It is clearly seen that not one of the methods accounts for the influence of potassium, which may be found in measurable quantities in the samples investigated. This is explained not only by the difficulty in the potassium determinations due to its low activity, but also by the fact that in very many specific problems its presence causes no difficulties.

Therefore most investigators restrict themselves to the most general remarks on the influence of potassium in radiometric measurements, and successful potassium determinations have been performed only in special investigations in which the potassium was either first chemically separated or in which special apparatus was used and the influence of other radioactive elements was small [23, 24].

The use of  $\gamma$  scintillation counters, which sharply increase the sensitivity of the methods and make it possible to measure activities of the order of thousandths or even ten-thousandths of a per cent uranium equivalent, has made the problem of accounting for potassium radiation, as well as that of obtaining quantitative potassium determinations, entirely possible to handle.

The further development of methods for the separate determination of natural radioactive elements depends primarily on the design of highly sensitive analyzers, since the use of such analyzers would make it possible to increase sharply the statistical accuracy with which these elements are determined.

Received January 22, 1957

#### LITERATURE CITED

- [1] J. Tommeret, J. Phys., et Radium 10, 249 (1949).
- [2] G. Eicholz, J. Hilborn and C. McMachon, Can. J. Phys. 31, 613 (1953).

[3] V. Bochkarev et al., "Measurement of the Activity of Beta and Gamma Sources," Izd. AN SSSR (1953).

[4] A. N. Murin. "Introduction to Radioactivity." Izd. LGU [Leningrad State U. Press] (1955).

[5] G. R. Golbek, V. V. Matveev and R. S. Shlyapnikov, Investigations in the Fields of Geology, Chemistry, and Metallurgy (Reports of the Soviet Delegation to the International Conference on the Peaceful Uses of Atomic Energy), Izd. AN SSSR, p. 40 (1955).

[6] V. I. Baranov. "Radiometry," Izd. AN SSSR (1956).

[7] E. Franklin and R. Barnes, AERE EL/R, No. 1175 (1953).

[8] G. Finney and R. D. Evans, Phys. Rev. 48, 503 (1935).

[9] V. Veksler, L. Groshev and B. Isaev, "Ionization Methods for Studying Radiation," Gostekhizdat (1950).

[10] R. D. Evans and R. O. Evans, Rev. Mod. Phys. 20, 305 (1948).

[11] N. P. Starovarov and G. V. Gorshkov, Geophysics VII, No. 5 (1937).

[12] H. McCoy and L. Henderson, J. Am. Chem. Soc. 40, 1316 (1918).

[13] R. D. Evans and R. A. Mugele, Rev. Sci. Instr. 7, 441 (1936).

[14] R. D. Evans and W. Raitt, Phys. Rev. 48, 171 (1935).

[15] A. Czalay and E. Csongor, Science 109, 146 (1949).

[16] R. D. Evans, Phys. Rev. 45, 29 (1934).

[17] R. D. Evans, Phys. Rev. 45, 38 (1934).

[18] Ch. Santimay and Dh. Sobhana, Ind. J. Phys. 24, 346 (1951).

[19] D. Peirson, Proc. Phys. Soc., Sec. B 64, 876 (1951).

[20] K. Whithan, Trans. Am. Geophys. Un. 33, 902 (1952).

[21] J. Joly, Phil. Mag. 22, 134 (1911).

[22] R. D. Evans, Rev. Sci. Instr. 4, 222 (1934).

[23] A. Gandin and J. Pannel, Anal. Chem. 20, 1154 (1948).

[24] E. C. Anderson, R. L. Schuch, J. D. Perrings and W. H. Langham, Nucleonics 14, No. 1, 26 (1956).

PHOSPHATE-HYDROXYQUINOLINE METHOD FOR SEPARATION AND  
VOLUMETRIC DETERMINATION OF ZIRCONIUM

A. V. Vinogradov and V. S. Shpinel

The proposed method consists of a combination of the well-known phosphate method for separation of zirconium, and determination of zirconium as the hydroxyquinolate. The separation of zirconium hydroxyquinolate from an oxalate medium after solution of the phosphate precipitate in oxalic acid has been used for the first time. The conditions of separation of zirconium from titanium and thorium in the phosphate precipitation, and from niobium and tantalum in precipitation of the hydroxyquinolate, have been studied. By this method it is possible to separate zirconium in practice from all accompanying elements (except hafnium), and to determine small amounts of zirconium (2-5 mg) by a volumetric method to an accuracy of  $\pm 2-4\%$ .

The principal defect of most of the gravimetric methods described in the literature [1-5] is the need for using large samples, so that milligram quantities of zirconium cannot be determined.

It is therefore desirable to find a rapid volumetric method for determination of small amounts of zirconium.

Most of the volumetric methods described in the literature are not suitable for practical use owing to their nonspecific nature. For example, the methods of Sawaya and Yamashita [6], Bezier [7], Uspenskaya, Guldina, and Zverkova [8], based on the use of a fluoride complex of zirconium, Zolotukhin's method [9] based on the formation of a zirconium complex with tartaric acid, and certain complexometric methods, are evidently only suitable for solutions which do not contain other elements capable of forming complexes with the reagents.

The method of Chernikhov and Uspenskaya [10], based on the formation of zirconium iodate, is inapplicable if the solution contains titanium, thorium, lead, silver, or large amounts of iron.

Other authors [11-13] have developed the chemistry of selective separation of zirconium from accompanying impurities. However, such schemes are either complex or insufficiently sensitive. We adopted the following route: precipitation of zirconium as phosphate, conversion of phosphate into hydroxyquinolate, and titration of the latter with bromate.

Precipitation of zirconium as phosphate is a well-known method by which it is possible to separate zirconium from nearly all accompanying elements. Zirconium hydroxyquinolate is rarely used for analytical purposes.

Sue and Wetloff [14] obtained compounds of zirconium with hydroxyquinoline from an acetate medium containing tartaric acid.

Balanescu [15] stated that when zirconium is precipitated by hydroxyquinoline from chloride or sulfate solution (with ammonium acetate buffer), or from ammonium tartrate solution, precipitates of variable composition are obtained. He recommended the precipitation of zirconium hydroxyquinolate from nitrate solutions in presence of large amounts of ammonium acetate. Titration of hydroxyquinolate dissolved in 50% sulfuric acid



with 0.1 N bromide-bromate solution gives satisfactory results in titration of not more than 12 mg of zirconium. With larger amounts of the metal the results are 5-6% too low.

All subsequent publications on zirconium hydroxyquinolate are of a fragmentary character [15-18].

### EXPERIMENTAL RESULTS

The possibility of separating zirconium hydroxyquinolate from an oxalate medium and titrating the hydroxyquinolate in hydrochloric acid with 0.05 N bromide-bromate solution was first investigated. The excess  $\text{KBrO}_3$  after addition of KI was titrated with  $\text{Na}_2\text{S}_2\text{O}_3$  solution.

To a solution of zirconium sulfate excess 10% oxalic acid solution was added; hydroxyquinoline was added first, and then ammonia until the hydroxyquinolate was precipitated. The solution was titrated in the usual way with potassium bromide-bromate. The results are given in Table 1.

TABLE 1  
Separation of Zirconium Hydroxyquinolate from an Oxalate Medium  
(Weight of Zr = 3.44 mg)

0.05 N $\text{KBrO}_3$ taken by hydroxy- quinolate, ml	Zr found, mg	Error, %
12.30	3.51	+2.04
12.24	3.49	+1.45
12.08	3.44	0.0
12.02	3.43	-0.29
12.22	3.48	1.16
11.82	3.37	-2.04
11.88	3.39	-1.45
11.76	3.35	-2.62
11.76	3.35	-2.62
Mean	3.42	

Root mean square error  $\pm 0.064$  mg, or  $\pm 1.86$  rel. %.

TABLE 2  
Separation of Zirconium as Phosphate with Subsequent Conversion into Hydroxyquinolate  
(Weight of Zr = 1.72 mg)

0.05 N $\text{KBrO}_3$ taken by hydroxy- quinolate, ml	Zr found, mg	Error, %
5.93	1.69	-1.7
5.98	1.70	-1.2
5.91	1.68	-2.3
6.06	1.73	+0.6
5.94	1.69	-1.7
5.94	1.69	-1.7
6.04	1.72	-0.0
6.09	1.74	+1.2
6.04	1.72	0.0
6.16	1.76	+2.3
Mean	1.71	

Root mean square error + 0.0265 mg, or  $\pm 1.55$  rel. %.

All the tables give the actual consumption of bromate by the hydroxyquinolate, i.e., without the excess of  $\text{KBrO}_3$ , determined iodometrically.

After it had been shown that complete separation of zirconium from oxalate solutions by means of hydroxyquinoline is possible, definite amounts of zirconium were precipitated by ammonium phosphate, the phosphate precipitates were dissolved in 10% oxalic acid solution, the hydroxyquinolate was precipitated as described above, and titrated in the usual way.

As Tables 1 and 2 show, completely satisfactory results are obtained in determinations of 1.7-3.5 mg of zirconium.

For establishing the lower applicability limit of this method, 0.34 mg of zirconium was precipitated by phosphate from 10%  $\text{H}_2\text{SO}_4$ , the precipitate was converted into oxalate solution, the hydroxyquinolate was precipitated, and titrated with 0.01 N  $\text{KBrO}_3$  solution.

A systematic negative error is obtained in separation of small amounts of zirconium (Table 3); this is readily explained by losses in precipitation and washing of small amounts of precipitates (phosphate and hydroxyquinolate).

A method was then developed for determination of zirconium in presence of elements forming phosphates dissolving with difficulty in an acid medium, namely: titanium, thorium, niobium, and tantalum.

TABLE 3

Separation of Zirconium as Phosphate and Hydroxyquinolate

(Weight of Zr = 0.39 mg)

0.01 NK BrO <sub>3</sub> solution taken by hydroxyquinolate, ml	Zr found, mg	Error, %
5.66	0.32	-6.0
5.10	0.29	-14.7
5.76	0.33	-3.0
5.37	0.31	-9.0
5.59	0.32	-6.0
6.00	0.34	-0.0
5.72	0.33	-3.0
Mean	0.32	

TABLE 4

Determination of Zirconium in Presence of Titanium  
(Weight of Zr = 3.44 mg)

Titanium added, mg	0.05 NK BrO <sub>3</sub> taken by hydroxyquinolate, ml	Zr found, mg	Error, %
5.0	12.08	3.44	±0
5.0	11.83	3.36	-2.3
5.0	12.16	3.47	±0.9
5.0	11.89	3.39	-1.45
20.0	11.93	3.40	-1.20
20.0	11.98	3.41	-0.9
20.0	12.03	3.43	-0.3
20.0	12.03	3.43	-0.3
Mean		3.42	

Determination of Zirconium in Presence of Titanium

As is known, titanium forms a sparingly soluble phosphate which is precipitated together with zirconium phosphate. The Hillebrand procedure was therefore followed, 3 ml of 30% hydrogen peroxide being added when zirconium was precipitated in presence of titanium. The results are given in Table 4.

Thus, the presence even of sixfold amounts of titanium does not interfere with the determination of zirconium. With 80 mg of titanium present, its entrapment does not exceed 0.1 mg if the wash liquid used for washing the phosphate precipitate contains hydrogen peroxide.

Determination of Zirconium in Presence of Thorium

Experiments on determination of zirconium in presence of thorium show that when the concentration of sulfuric acid is increased to 20% (by volume) practically no thorium is precipitated as phosphate (Table 5).

TABLE 5

Determination of Zirconium in Presence of 40.0 mg ThO<sub>2</sub>(H<sub>2</sub>SO<sub>4</sub> Concentration 20% (by volume); (weight of Zr = 3.44 mg)

0.05 N K BrO <sub>3</sub> taken by hydroxyquinolate, ml	Zr found, mg	Error, %
11.68	3.33	-3.20
11.76	3.35	-2.62
11.68	3.33	-3.20
12.22	3.48	-1.16
12.60	3.59	+3.78
12.04	3.43	-0.29
12.08	3.44	-0.0
Mean	3.42	

Determination of Zirconium in Presence of Niobium and Tantalum

Zirconium cannot be separated from niobium and tantalum by precipitation as the phosphate; these elements are precipitated together. The possibility of separating zirconium from these elements by means of hydroxyquinoline was studied.

To determine zirconium in presence of tantalum, to a solution of 25 mg of tantalum in 3-4% oxalic acid (volume about 100 ml) 2 ml of zirconium solution (2.88 mg of zirconium) and 3 ml of 3% hydroxyquinoline solution was added; this was followed by addition of 60-70 ml of 20% ammonia, and the solution was heated to 70-80°. A white precipitate (tantalum hydroxide ?), insoluble in hydrochloric acid, was formed simultaneously with a yellow precipitate of zirconium hydroxyquinolate. The washed hydroxyquinolate precipitate was dissolved in HCl and titrated by the usual method. The results are given in Table 6.

In contrast to zirconium hydroxyquinolate, which is completely precipitated over a wide pH range (8.5-12.0), niobium hydroxyquinolate is not precipitated from strong ammoniacal solutions (pH 10.7-11.5). Therefore the precipitation of zirconium in presence of niobium was carried out under exactly the same conditions

as the precipitation in presence of tantalum. The results are given in Table 7.

TABLE 6

Determination of Zirconium in Presence of Tantalum

(Weight of Ta = 25 mg; of Zr = 2.88 mg)

0.05 N bromate taken by hydroxyquinolate, ml	Zr found, mg	Error	
		mg	%
10.02	2.86	-0.02	-0.69
10.28	2.93	+0.05	+1.74
10.30	2.94	+0.06	+2.08
10.06	2.87	-0.01	-0.35
9.68	2.76	-0.12	-4.17
9.42	2.68	-0.20	-6.94
10.00	2.85	-0.03	-1.04
10.26	2.92	+0.04	+1.39
10.28	2.93	+0.05	+1.74
Mean	2.86		

TABLE 7

Determination of Zirconium in Presence of Niobium

(Weight of Zr = 2.88 mg)

Nb taken mg	0.05 N KBrO <sub>2</sub> taken by hydroxyquinolate, ml	Zr found mg	Error	
			mg	%
8.74	10.14	2.89	+0.01	+0.35
8.74	10.38	2.96	+0.08	+2.78
8.74	10.04	2.86	-0.02	-0.69
8.74	9.60	2.74	-0.14	-4.86
12.5	10.22	2.91	+0.03	+1.04
17.48	10.68	3.04	+0.16	+5.55
17.48	9.60	2.74	-0.14	-4.86
Mean		2.90		

#### General Analytical Procedure

The weight of the material for analysis is so chosen that the zirconium content is not less than 1 mg and not more than 10-12 mg. With higher zirconium contents aliquot portions containing 2-5 mg of zirconium are used. The manner of dissolving the material depends on its properties, and various methods can be used, but the resulting solution should contain about 10% sulfuric acid (by volume).

Precipitation of zirconium phosphate. To the solution, 50-60 ml in volume (if the presence of titanium is suspected) 3-5 ml of 30% hydrogen peroxide and 10% ammonium phosphate  $(\text{NH}_4)_2 \text{HPO}_4$  are added, the latter in 10 to 100-fold excess over the presumed amount of zirconium.

The solution is heated to 80-90° and left to settle. If the amount of precipitate is very small, it is left overnight.

The zirconium phosphate precipitate is filtered off on a paper filter and washed with cold 5% solution of ammonium phosphate in 5% sulfuric acid until turbidity is no longer formed on neutralization with ammonia.

If titanium is present in the material, 1-2 ml of 30% hydrogen peroxide (perhydrol) is added to the wash liquor. The precipitate is then washed 3-4 times with a solution without hydrogen peroxide, and dissolved on the filter in 10% oxalic acid solution.

Precipitation of hydroxyquinolate. To the oxalic acid solution, first 3-5 ml of 3% hydroxyquinoline solution in 1% acetic acid is added, and then ammonia to complete precipitation of zirconium hydroxyquinolate.

If niobium or tantalum are presumed to be present, a large excess of ammonia is added at once to the solution, or the solution is poured into excess ammonia (60-70 ml of strong ammonia). The mixture is then heated to 70-80° to coagulate the precipitate, cooled, and filtered. The precipitate is washed 3-4 times with hot (70-80°) 5% solution, and then with a warm solution of  $\text{NH}_4\text{Cl}$  of the same concentration until the wash waters are completely colorless.

Titration of hydroxyquinolate. The precipitate is dissolved on the filter in hot hydrochloric acid (20% by volume), and the filter is washed with the same acid. The hydrochloric acid solution is cooled and, after addition of about 2 g of potassium bromide and 3-4 drops of methyl red indicator, titrated with 0.05-0.01 N  $\text{KBrO}_2$  solution, depending on the presumed zirconium content, until the color changes from orange to pure yellow; this is followed by the addition of a further 2-3 ml of bromate solution and 5 ml of 20% potassium iodide solution. After 3-5 minutes the liberated iodine is titrated with 0.05-0.01 N thiosulfate solution, starch being added at the end, until the blue color disappears.

Calculation of the Zirconium Content

$$\% \text{ Zr} = \frac{(n-aK)T}{m} \cdot 100$$

where  $n$  is the amount of  $\text{KBrO}_3$  taken for the titration, in ml;  $a$  is the amount of  $\text{Na}_2\text{S}_2\text{O}_3$  taken for the back titration, in ml;  $K$  is the factor of the  $\text{Na}_2\text{S}_2\text{O}_3$  solution for conversion to bromate solution;  $m$  is the weight of the sample in mg;  $T$  is the titer of the bromate solution for zirconium.

The factor for calculation of  $\text{Na}_2\text{S}_2\text{O}_3$  as  $\text{KBrO}_3$  is determined by addition, to a definite volume of bromate solution, of 5 ml of 20% potassium iodide solution, and titration with thiosulfate solution. 1 ml of 0.05 N  $\text{KBrO}_3$  solution corresponds to 0.285 mg of zirconium.

The analytical scheme is given above in its most complicated form, as the presence of a number of elements precipitated by hydroxyquinoline under the same conditions as zirconium is presumed.

With a high zirconium content and in absence of interfering impurities, direct precipitation of zirconium by hydroxyquinoline and gravimetric determination as the hydroxyquinolate is possible. The factor for conversion of the weight of hydroxyquinolate to the weight of zirconium is 0.1376.

Preliminary precipitation as the phosphate is obviously also unnecessary in presence of such elements as molybdenum, tungsten, vanadium, and niobium, which do not give precipitates either of hydroxyquinolates or of hydroxides by the simultaneous action of hydroxyquinoline and excess ammonia.

It must also be noted that, instead of phosphate precipitation, precipitation by organic acids such as phenylarsinic may be used.

The method is suitable for all alloys containing zirconium, and also for zirconium ores and intermediates.

Received August 15, 1956

## LITERATURE CITED

- [1] W. Fresenius and G. Jander, *Handbuch der Anal. Chemie. Quantitative Bestimmungsmethoden IVb*, 170-287 (1950).
- [2] C. H. Bailey, *J. Chem. Soc. Trans.* 49, 481 (1886).
- [3] C. A. Kumins, *Anal. Chem.* 19, 376 (1947).
- [4] A. Purushottam, S. V. Bhadur and Raghava Rao, *Analyst* 75, 684 (1950).
- [5] P. S. Marty, S. V. Bhadur and Raghava Rao, *Z. Anal. Chem.* 141, 93-96 (1954).
- [6] Tsuguo Sawaya and Masao Yamashita, *J. Chem. Soc. Japan, Pure Chem. Sect.* 72, 356 (1951).
- [7] D. Bezier, *Chem. Anal.* 36, 175 (1954).
- [8] T. A. Uspenskaya, E. I. Guldina and M. S. Zverkova, *Factory Labs.* 9, 142 (1940).
- [9] V. K. Zolotukhin, *Trans. Voronezh State Univ. XI (Chemical Division)*, No. 2 (1939).
- [10] Yu. A. Chernikhov and T. A. Uspenskaya, *Factory Labs.* 10, 248 (1941).
- [11] P. R. Subbaraman and K. S. Rajan, *J. Sci. Ind. Research* 13B, 31-34 (1954).
- [12] G. W. C. Milner and P. I. Phennah, *Analyst* 79, 475-82 (1954).
- [13] Mulk Ray Verma and Sukh Deo Paul, *Nature* 173, 1237 (1954).
- [14] P. Sue and G. Wettruff, *Bull. Soc. Chem. France* 2, 1002-1007 (1935).

- [15] Gr. Balanescu, Z. f. Anal. Chem. 101, 101 (1935).
- [16] T. Kiba and T. Ikeda, J. Chem. Soc. Japan 60, 911 (1939).
- [17] J. Stachtchenko and Cl. Duval, Anal. Chim. Acta 5, 410 (1951).
- [18] T. A. Portcastle, Chem. Age, No. 1764, 673 (1953).

## NATROAUTUNITE

A. A. Chernikov, O. V. Krutetskaya and N. I. Organova

A new mineral is described, hydrated sodium uranyl phosphate, found in one of the granodiorite ranges of the USSR. The mineral belongs to the group of uranium micas and is similar in properties to autunite.

In 1953 a mineral very similar to autunite in external appearance was discovered in one of the granodiorite ranges of the USSR. It consists of lemon-yellow or lettuce-yellow elongated or square thin tabular plates with perfect (001) cleavage and less perfect (100) cleavage. The plates, which form scales and fanlike aggregates, and sometimes radiating bundles (Fig. 1), are brittle. Hardness 2-2.5. The luster at the (001) cleavage planes is nacreous, and glassy in other directions.

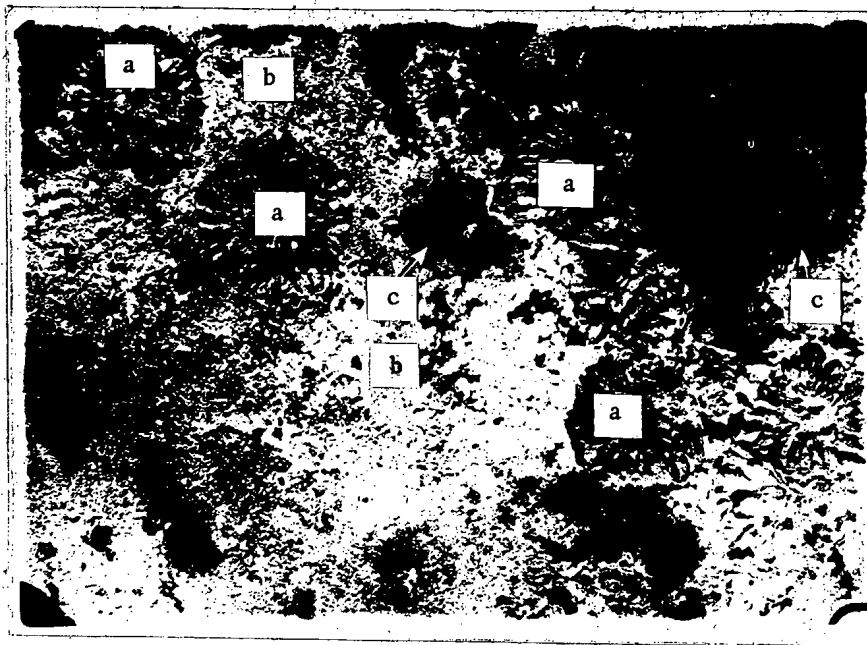


Fig. 1. a) Natroautunite formation ( $\times 5$ ); b) kaolinite; c) limonite.

The mineral is readily soluble in acids, giving greenish yellow solutions. When heated in a sealed tube it gives off water, becoming straw-yellow and loose. It gives a distinct reaction for uranium with borax and phosphate.

The mineral exhibits a bright greenish yellow luminescence under ultraviolet light. The luminescence

spectrum and microphotogram of natroautunite are very similar to those of autunite (Fig. 2). Examination under the immersion microscope shows clearly defined square crystals of greenish yellow and pale yellow color; the interference color is pale yellow.

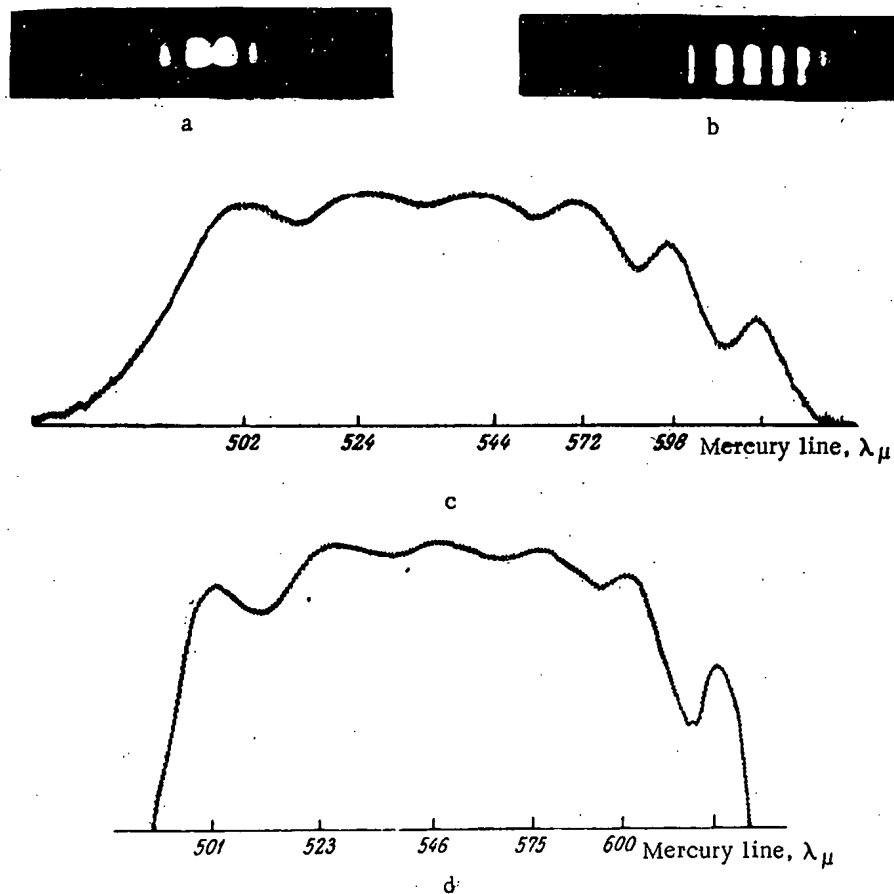


Fig. 2. a) Luminescence spectrum of natroautunite; b) luminescence spectrum of autunite; c) microphotogram of natroautunite; d) microphotogram of autunite (Taken by Senior Assistant of the IGEM, Acad. Sci. USSR, E. S. Rudnitskaya).

The freshly mined crystals are uniaxial, optically negative,  $N_0 = 1.578$ ,  $N_e = 1.559$ , weakly pleochroic, bright yellow along  $N_0$ , pale yellow along  $N_e$ . After the crystals have been kept for two days at 35-40° the refractive indices increase to 1.585 for  $N_0$  and 1.564 for  $N_e$ .

It is seen that the optical properties of natroautunite are very similar to the optical properties of autunite as given in the literature [1-3].

Spectroscopic analysis carried out in the spectroscopy laboratory of IGEM (Institute of the Geology of Ore Deposits, Mineralogy, Geochemistry, and Petrography) showed that the mineral contains large amounts of uranium and phosphorus, several percent of sodium, up to 1% iron, and small amounts of calcium, aluminum, and silicon.

On the basis of these results, the following scheme was devised for chemical analysis of two samples of natroautunite.

The weighed sample was treated with perchloric acid. Silicic acid was filtered off and determined in the usual way. For precipitation of iron, aluminum, and uranium phosphates, ammonia free from carbon dioxide was used. The precipitate was filtered off, washed, dissolved in sulfuric acid, and treated with cupferron after preliminary reduction of the uranium with sodium hydrosulfite. Uranium and iron were precipitated, while

phosphorus and aluminum remained in solution. The precipitate was ignited and fused with potassium bisulfate, dissolved in sulfuric acid, and again treated with cupferron after oxidation of uranium to the hexivalent state. The precipitated iron was ignited and weighed as  $\text{Fe}_2\text{O}_3$ . A test for titanium was performed.

The filtrate which contained phosphorus and aluminum was treated with nitric acid to decompose the cupferron present, and divided into aliquot portions. One was analyzed for phosphorus (precipitation as magnesium phosphate and ignition to pyrophosphate) and the other for aluminum (colorimetric arsenazo method).

Uranium was determined in a separate sample by P. A. Volkov's method [4]. The principle of the method is that uranium is reduced by sodium hydrosulfite to the quadrivalent state. The precipitate is dissolved in 33% sulfuric acid and titrated with potassium dichromate solution.

If not enough material is available, uranium can be determined in the cupferron solution.

Calcium and magnesium were determined in the filtrate after  $\text{R}^{3+}$  precipitation by the usual gravimetric methods: calcium as the oxalate, magnesium as the pyrophosphate.

Potassium and sodium were determined by the Smith method.

Hygroscopic water ( $\text{H}_2\text{O}^-$ ) was determined by drying a sample to constant weight at 105-110°, and bound water ( $\text{H}_2\text{O}^+$ ) was determined by the Penfield method.

The results of two chemical analyses of natroautunite are given in Table 1.

TABLE 1

	I			II			III		
	%	Molecular amounts	Molecular ratios	%	Molecular amounts	Molecular ratios	%	Molecular amounts	Molecular ratios
$\text{UO}_3$	61.9	0.209	1.91	62.53	0.215	2.1	62.18	0.218	2
$\text{P}_2\text{O}_5$	15.56	0.109	1.00	14.69	0.104	1.0	15.43	0.109	1
$\text{Na}_2\text{O}$	5.62	0.09	0.83	6.88	0.111	1.06	6.74	0.109	1
$\text{CaO}$	1.2	0.021	0.19	0.14	—	—	—	—	—
$\text{SiO}_2$	1.6	0.027	0.25	—	—	—	—	—	—
$\text{CO}_2$	0.24	0.006	0.006	—	—	—	—	—	—
$\text{MgO}$	0.43	0.01	0.01	—	—	—	—	—	—
$\text{Al}_2\text{O}_3$	0.32	0.03	0.03	—	—	—	—	—	—
$\text{Fe}_2\text{O}_3$	0.97	0.006	0.006	—	—	—	—	—	—
$\text{H}_2\text{O}^+$ 4.05	13.07	0.728	6.66	14.84	0.824	7.9	15.65	0.87	8
$\text{H}_2\text{O}^-$ 9.02									
Total	100.91			99.08			100.00		

Note: I and II) native natroautunite (I - analysis performed by Junior Assistant, IGEM Acad. Sci. USSR O. V. Krutetskaya; II - uranium, phosphorus, and water determined by Senior Laboratory Assistant, IGEM Acad. Sci. USSR V. I. Litenkova, sodium and calcium by O. V. Krutetskaya); III) theoretical composition for  $\text{Na}_2(\text{UO}_2)_2(\text{PO}_4)_2 \cdot 8\text{H}_2\text{O}$ .

In the first analysis there is not enough sodium for the formula  $\text{Na}_2(\text{UO}_2)_2(\text{PO}_4)_2 \cdot 8\text{H}_2\text{O}$ . This is possibly because the analyzed sample contained some impurity.

The analytical results for the second sample, more carefully taken, correspond fairly exactly to the formula  $\text{Na}_2(\text{UO}_2)_2(\text{PO}_4)_2 \cdot 8\text{H}_2\text{O}$ . Only the water content is somewhat lower, which is probably the result of loss in a dry atmosphere, as for most micas.

The possibility of isomorphous substitution of sodium by calcium in the first sample is not excluded.

Published analytical data on native autunite [1 - 3] show absence of sodium, but Fairchild [5] showed that in artificial autunites sodium readily replaces calcium.



TABLE 2

Photographic Conditions: Cu Radiation, Camera Diameter 57.9 mm, Specimen Diameter 0.6 mm

No.	Natroantunite			Synthesized autunite (E. N. Leonova)			Synthesized hydrogen autunite (E. N. Leonova)		
	<i>I</i>	$d_{\alpha}$	( <i>hkl</i> )	<i>I</i>	$d_{\alpha}$	( <i>hkl</i> )	<i>I</i>	$d_{\alpha}$	( <i>hkl</i> )
1	5	8.57	001	6	8.46	001	5	8.45	001
2	4	5.40	101	3	5.41	110, 101	4	5.77	110
3	5	4.32	002	1	4.91		6	4.30	111
4				5	4.168	002			
5	2	4.03		2	4.00		1	3.85	
6	10	3.67	102	10	3.65	102	3	3.71	102
7	5	3.49	200	4	3.51	200	10	3.56	200
8	7	3.23	112	6	3.25	120	10	3.28	112, 201
9	5	2.94	121	4	2.93	121	8	2.97	121
10				2	2.77	003			
11	8	2.675	103	8	2.62	103	5	2.69	103
12	4	2.54	122	3	2.53	122	4	2.57	122
13	3	2.46	113	3	2.46	113	4	2.49	113
14	4	2.36	221	2	2.40	221	7	2.39	221
15				2	2.34				
16				3	2.27	301			
17	3	2.20	130	4	2.23	130			
18				3	2.16	131			
19	3	2.16	004	7	2.11	123, 004	3	2.19	004
20	6	2.12	123				2	2.14	123
21	5	2.05	104, 302	5	2.04	104	6	2.09	104
22	5 b	1.984	114	7	1.96	230	4	2.00	114
23	2	1.899	231	1	1.90	231	4	1.908	231
24	3	1.845	204	5	1.81	303, 204	3	1.854	222
25	4	1.816	303						
26	3	1.768	124		1.78		4	1.79	124
27				5 b		400			
28	3	1.746	133, 400		1.76		2	1.745	400
29	3	1.711	005	4	1.70	005	3	1.729	
30	7	1.639	115	10	1.59	115	4	1.655	115
31	4	1.614	224				2	1.62	
32	2	1.576	304	3	1.58	304			
33	8 b	1.566	205, 134	8	1.53	134, 303	5	1.574	303
		1.540							
34	3	1.461		1	1.49				
35	3	1.449	006	1	1.487		2	1.468	006
36	4	1.420	106				1	1.435	106
37							2	1.407	
38	2	1.386		5	1.385		6	1.380	
39	7	1.364		6	1.35				
40	4	1.322		2	1.34		1	1.330	
41	3	1.298							
42	1	1.282							
43	2	1.259		4	1.260		2	1.267	
44		1.240					2	1.243	
45	2 b	1.214					2	1.224	
46		1.200					1	1.204	
47	2 b	1.187		6	1.19		1	1.193	
48	6 b	1.166		2	1.159				
		1.156							
49	1	1.141		3	1.136				
50	3	1.111		1	1.115		1	1.110	
51	3	1.097					1	1.099	
52							1	1.086	
53	5	1,074		5	1,074				
54	3	1,048					6	1,046	
55							1	1,039	
56	1	1,024		2	1,024				
57	5	0,985		1	1,008				
58				3	0,988				
59	2	0,967							
60	5	0,950							
61				3	0,902				
62				1	0,88				
63	3	0,858		1	0,87				

A comparison of x-ray powder pattern data (Table 2) for native natroautunite and artificial hydrogen and calcium autunites synthesized by Junior Scientific Assistant of IGM, Acad. Sci. USSR E. N. Leonova (data not published) shows that they have related structures. All the x-ray patterns were analyzed for tetragonal syngony by means of Hull charts by N. I. Organova. Indices of the  $n\text{OO}$ ,  $n2n\text{O}$ ,  $2n2n\text{O}$  types were not found. This indicates that all the autunites studied belong to the  $p4/nmm$  space group. The unit cell dimensions of the samples studied were also similar (Table 3).

Calculations show that the samples belong to the meta group. By analogy with calcium metaautunite reported in the literature [1, 2] it may be concluded that the unit cell of metanatroautunite contains one molecule of  $\text{Na}_2(\text{UO}_2)_2(\text{PO}_4)_2 \cdot 8\text{H}_2\text{O}$ .

TABLE 3

	Natroautunite	Synthesized calcium autunite	Synthesized hydrogen autunite
<i>a</i>	6.97Å	7.04Å	7.07Å
<i>c</i>	8.69Å	8.46Å	8.80Å
<i>c/a</i>	1.245	1.20	1.245

On this assumption the calculated density of the mineral was 3.89 g/cc. Experimental determination of the density, carried out by V. S. Amelina, gave 3.584 g/cc.

This discrepancy probably cannot be attributed only to porosity of the sample. It is probably associated with variable contents of water in autunites. The decrease in the amount of water in metaautunites by comparison with autunites is accompanied by an increase in density. As the material was powdered when prepared

for the x-ray photography, some water could have been lost from the lattice, leading to the discrepancy between the calculated and experimental densities.

It is seen from the foregoing that natroautunite is very similar to autunite in properties (color, crystal form, type of luminescence, structure, optical properties), and differs from it only in chemical composition.

Received February 25, 1957

#### LITERATURE CITED

- [1] O. M. Shubnikova, Minerals of the Rare Elements and their Identification (Moscow, 1952).
- [2] J. D. Dana, E. S. Dana, C. Palache, H. Berman and C. Frondel, System of Mineralogy, Vol. 2, part 2 (Moscow, 1954).
- [3] I. Beintema, Recueil des Fravaux chimiques des Pays-Bas. 57, No. 1, 155-175 (1932).
- [4] P. N. Palei, "Investigations in the Field of Geology, Chemistry, and Metallurgy" (Papers of the Soviet Delegation at the International Conference on the Peaceful Use of Atomic Energy) (Izd. AN SSSR, 1955)p. 21.
- [5] J. G. Fairchild, Am. Mineralogist 14, 7-8 (1929).
- [6] W. F. Hillebrand and G. E. Lundell, Applied Inorganic Analysis (Moscow, 1935).
- [7] V. I. Kuznetsov, and R. B. Golubtsova, Factory Labs. No. 2 (1956).
- [8] A. I. Ponomarev, Methods for the Chemical Analysis of Minerals and Rocks, Vol. 1 (Moscow, 1951).

INDIVIDUAL SHIELDING DURING MAINTENANCE OPERATIONS UNDER  
CONDITIONS OF RADIOACTIVE CONTAMINATION

S. M. Gorodinsky and V. L. Shcherbakov

The basic characteristics of shielding during maintenance operations under conditions of radioactive contamination are discussed, and the basic principles of organization of maintenance personnel shielding are established. A brief description of the design of individual shielding devices is given, as well as their operational characteristics. Particular attention is given to the specific areas of utility of the various devices. The article is intended for persons working directly with radioactive materials, as well as for those working in the area of radiation safety.

In the field of shielding and decontamination methods for work with radioactive substances, an important place is held by the correct execution of maintenance and repair operations.

During maintenance and disassembly of radioactively contaminated laboratory equipment, as well as during accidents that may occur in any "hot" research laboratory, the probability of radioactive contamination of the air in working areas, of equipment, floors, walls, ceilings and direct contamination of people doing the maintenance, is greatly increased. This may lead to overexposure of the people and to the particularly dangerous ingestion of radioactive substances in quantities exceeding the limits of safe dosage.

Effective shielding during maintenance and repair work under radioactive contamination, comes down to individual shielding of the maintenance people and to the prevention of dissemination of radioactive contaminants through clean establishments and territories.

The shielding of people doing the maintenance and repair work is considerably complicated by the fact that this type of work is done unsystematically, and often can not be anticipated. Therefore when designing and equipping a laboratory, completely mechanized repair work can not be provided for in most cases. Often during repair there is required the very equipment and mechanisms that are being repaired. For instance, the malfunction of various manipulators, ventilating systems and fume chambers as well as the exposure of containers or contaminated ducts leads to particularly unfavorable health safety conditions and complicates maintenance work.

While ordinarily all work with moderate to large quantities of gamma emitters is conducted from behind lead or concrete shielding with the use of remote manipulation in special chambers (cells) and chests, maintenance work entails a great number of hand operations and direct contacts of personnel with equipment that is contaminated by radioactive materials, thus making it impossible to shield through screening or separation distances between worker and the contaminated object.

It is more realistic in such cases to conduct prior deactivation of equipment and the surfaces where maintenance work must be carried out (to reduce the gamma dose rate) and to use "time shielding", that is, the reduction of working time to intervals in which the irradiation of each person does not exceed 0.05 r in one working day. The reduction of working time is often accompanied by an increase in the number of people engaged in the repair work.

A specific danger of maintenance work on contaminated equipment is the possibility of dispersal of radioactive substances to clean buildings and over clean territories and the significant contamination of the latter. This can be caused particularly by exposure of hermetically sealed containers, maintenance of fume chambers, containers, ducts and piping. Working experience has shown that considerable radioactive contamination can be carried on the protective clothing and on the hands of personnel, as well as on instruments and tools.

The question of proper planning of working areas for reduction of possibilities of dissemination of radioactive contamination is dealt with seriously in the published literature [1 - 3].

The shielding of working personnel, because of the peculiarities of maintenance work that have been enumerated, can not be usually done by general shielding devices (hermetic sealing, remote control and manipulation, etc.). Therefore the people doing the maintenance and repair work are shielded primarily by individual devices and methods, which under these conditions become the primary means.

The individual shielding of maintenance and repair personnel under conditions of radioactive contamination, reduces to the following:

- 1) shielding from gamma radiation, which is primarily effected by reduction of the working time;
- 2) protection of the respiratory passages against penetration by radioactive substances and their movement into the body;
- 3) protection against contaminants collecting on the skin.

The question of shielding from gamma radiation, in particular the regulation of allowable working time as a function of the total irradiation dose, has been fully dealt with in the works of native and foreign authors [4 - 7].

Individual means can not protect against neutron and gamma radiation, and are intended for prevention of contamination of the body surfaces and the interior organism [8, 9].

A peculiarity of individual shielding devices is the necessity of thorough subsequent decontamination of the devices after their use at exposed radioactive substances.

For this reason, a number of conditions must be imposed on the use of individual protective devices. Particular attention must be given to the correct choice of design and materials of the separate pieces of individual protective equipment. Simultaneously with working convenience and general hygienic suitability, individual protective devices must:

- 1) protect against collection of radioactive substances on the skin and within the organism, and also must completely shield the skin against external  $\alpha$  and, partly,  $\beta$  radiation;
- 2) be easy to clean and decontaminate, or must be so inexpensive that in case of contamination above allowable limits, they can be easily destroyed.

These requirements are basic, and for their observance it sometimes becomes necessary to sacrifice convenience of operation. To meet these requirements it is possible to select the proper materials and corresponding design of protective device. Protective clothing and other means of individual protection must provide dependable shielding against radioactive contamination, must be convenient for work, have a minimum number of seams, and for ease of subsequent cleaning must be made of a single type of material. The material must be impermeable, must be sufficiently inexpensive or must clean easily, since many materials when heavily contaminated with radioactive substances can be cleaned only with difficulty and cumbersome equipment.

At present, a number of Soviet researchers have created plastisols and rubberoids that are easily cleaned of radioactive contaminations: several polymer materials, plastisols and films of the polyethylene and polyvinylchloride type, separate formulations of rubber, organic glass and several others.

An extremely important question is that of the proper use of cotton-paper cloths, which, as is known, are suitable for the mass manufacture of the more high quantity types of special clothing. Experience with radioactive substances has shown that under insignificant contaminations, such as are encountered in laboratory conditions, cotton-paper cloths can be used successfully, particularly those that clean well when laundered. As protective clothing, in these conditions, use is made of lab coats, semi-coveralls, coveralls, and caps of white cotton-paper cloth.

However, under significant contamination with radioactive substances, such as can occur during maintenance and repair work, cotton paper cloth can not guarantee protection of the body surfaces, and therefore film type protective clothing is put on, over the cotton paper clothing [8, 9]. Since the film type protective clothing cleans well, its use over the cotton paper yields a significant economy. Personnel working on repair and maintenance under contaminated conditions must wear fully enclosing coveralls made of white cloth with heavy silk binding. In this type of work, contamination of underclothing is possible, and therefore protective underclothing must be issued together with the outer garments. With proper use of health physics monitors, this averts the possibility of dissemination of radioactive contamination to living quarters. The requirement for white cotton-paper cloth (for example, exterior protective clothing of "moleskin" art. 555,553, protective underclothing of cotton cloth art. 26,28) is occasioned by the fact that the introduction of pigments reduces the particle releasing properties of cloth, and it launders off radioactive contaminants significantly worse.

Hands become contaminated most often and must therefore be protected by rubber or plastic gloves (the best design must be considered that of gloves of art. 374). The gloves must be treated with special care, since careless handling may cause contamination of their interior surfaces. In case of tearing or piercing of the gloves, they must be immediately replaced by others.

An extremely important question is that of the proper foot wear for maintenance workers. Under significant contamination, common foot wear (leather and rubber) easily absorb radioactive substances and are extremely difficult to clean. In addition, clean quarters can be contaminated by foot wear. Therefore, in these cases, it is practical to use easily cleaned, plastic base foot wear, or special shoes that are removed immediately upon emergence from contaminated areas. Spence [2] recommends the use of canvas cloth covers over common foot wear for this purpose.

As indicated above, the exposure and disassembly of equipment can be accompanied by significant contamination of the air by radioactive gases and aerosols. Consequently there is the possibility of entry of these gases into the system through the respiratory passages. By general agreement, this inhalation of radioactive substances into the organism is the most dangerous to health [10 - 12], and therefore the means of individual protection of respiratory organs acquire great importance.

To the ranks of individual shielding devices for protection of respiratory organs must be added respirators, gas masks, and pneumatic suits, that have been widely adopted in domestic and foreign practice (see Figs. 1 and 2).

Pneumatic clothing made of plastisol material completely isolates the body and respiratory organs of personnel from surrounding media. For respiration and for ventilation of the space under the pneumatic suit, fresh, clean air is constantly fed to the suit. The supply of air is delivered through a special hose from plant pneumatic lines or in the case of certain maintenance operations (in exceptional cases) from portable, high pressure ventilators. Because the pneumatic suit is fed clean air constantly, the worker can remain in contaminated areas, containing radioactive aerosols and gases, for long periods of time without any danger of inhaling radioactive substances and feeling no ill effects. In this case the time in the contaminated chamber is regulated by the type of neutron and gamma fields that are present in excess of allowable levels.

Pneumatic suits can be used in the following operations: disassembly and reassembly of equipment; inspection of ventilation installations and hot cells; unpacking of powdered radioactive substances and the preparation of radioactive solutions, if these operations can not be conducted within a hermetic chest; cleanup of contaminated quarters; gathering up of spilled and dropped radioactive substances, and a whole series of other operations that entail contamination of air and surfaces. The use of pneumatic suits is limited somewhat in work involving motion over large distances, since the radius of motion is limited by the length of the hose.

At the present time, in the Soviet Union, pneumatic suits of the type LG-1 and LG-2 are in use.

Pneumatic suit LG-2 (Fig. 3) is made entirely of plastisol, and has a soft helmet with viewing glass that is integral with the coveralls.

The design of the pneumatic suit ensures air flow over the entire person, thus making normal temperature regulation possible and ensuring complete protection against any contamination.

In contrast to filtering gas masks and respirators, the respiratory organs are completely isolated from the surrounding contaminated air, good visibility is ensured, there is no pressure on the head or irritation of the

\*[This is a transliteration. The significance of the abbreviation is not known — Publisher's note.]

skin of the face, and the eyes are shielded from the action of  $\alpha$  and  $\beta$  radiation. The plastisol material of the coveralls is easily cleaned of radioactive contamination by solutions of acids and alkalis.



Fig. 1. Maintenance work in progress on heavy cells, with personnel dressed in pneumatic suits type LG-2.



Fig. 2. A type of pneumatic suit used in England for work with radioactive substances.



Fig. 3. Pneumatic suit LG-2. 1) plastic coveralls; 2) coiled "loop"; 3) hose; 4) exhaust valve, 5) viewing glass.

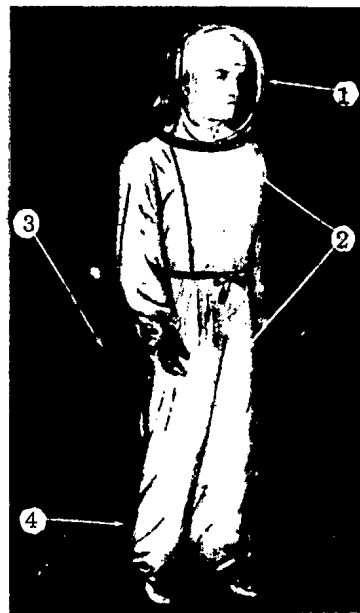


Fig. 4. Pneumatic suit LG-1. 1) helmet (Bell type) of organic glass; 2) plastic coveralls, 3) hose; 4) exhaust valve.

The air intake section of the pneumatic suit consists of a smooth walled hose and a blower.

Pneumatic suit LG-1 (Fig. 4) consists of a transparent plexiglass helmet, plastic coveralls of special design and the air intake section.

The design of pneumatic suit LG-1 ensures air flow over and complete protection of the body and protection of the respiratory organs from radioactive contaminants. However the presence of the rigid helmet limits the uses of pneumatic suit LG-1. For instance when work is conducted in tight and narrow places, where the rigid helmet is inconvenient, it is good practice to use pneumatic suit LG-2.

The pneumatic suits are donned over ordinary cotton paper coveralls, in a clean, uncontaminated area.

Comparative studies of physiological changes in the organism when work is done in a pneumatic suit showed that the suit produces a better environment than other current means of individual shielding (for instance, filtering gas masks and respirators, hose fed gas masks with totally closed coveralls, etc.). In addition it was established that for most favorable working environment, 160-200 l of air are required in the suit each minute, or 10-15m<sup>3</sup> per hour, at a pressure of 50 mm H<sub>2</sub>O at inlet. Under these conditions the person in the suit experiences no body overheating, normal perspiration is not disturbed, and at the same time the air does not excessively inflate the suit. This quantity of air fed into the suit is sufficient for maintenance of some back pressure, and in case of small breaks in the suit prevents penetration by the surrounding contaminated air. The used air is exhausted through valves located in the pants legs.

Because the pneumatic suits are used on the more highly contaminated jobs and become quite heavily contaminated by radioactive substances, they must be cleaned after every work shift. To prevent dissemination of radioactive contamination, the preliminary deactivation is carried out with the suit still on the person. The person wearing the suit enters a shower or is sprayed by a hose with a mesh nozzle. A thorough preliminary deactivation precludes any possible contamination of the hands when the worker removes his pneumatic suit (type LG), and also reduces to a minimum dispersion of radioactive contaminants through the working quarters. The final cleaning of the suits is done in special laundries, set up for deactivation of plastisol protective clothing.

During some types of maintenance work it is necessary to protect only the respiratory organs. Where it is possible to feed air through a hose, the head enclosing helmet of pneumatic suit LG-1 may be used alone. Less convenient, but still feasible, is working with a hose fed gas mask of the type PSh-2.

The use of respirators for protection from radioactive aerosols must be limited for a number of reasons. The filters of most respirators do not guarantee complete filtration of the air (the air that is filtered constitutes only up to 80-97% of the total).

In most cases respirators do not adhere to the face sufficiently hermetically; therefore leaks are possible, and this is inadmissible under the established rigid limits (on the order of 10<sup>-11</sup>-10<sup>-12</sup> curie/l). The materials of the respirators (rubber, cloth) are rapidly contaminated, and their cleaning is difficult.

Simplest and most reliable is the valveless dust respirator of the disposable variety ("The petal") [9], the basis of whose design is the new filtering material FN. The hermetic seal of the new face piece is ensured by the electrostatic properties of the cloth and by dependable fitting of the respirator to the face. The respirator "The petal" is light (10g) and is no less than 99.9% effective for the most penetrating aerosols (with particle radii of 0.15-0.2 μ) offers little resistance to breathing, is convenient and simple to use and does not require special care (Fig. 5).

The respirator ShB-2 (designed by Shatsky et al) is of undoubted interest [13], and can be used successfully for a variety of maintenance jobs under conditions of air contamination by radioactive aerosols. The respirator is designed in the form of a combination filter-helmet-mask, that covers the entire head and face (Fig. 6). The hermetic fit of the respirator on the face, head and the neck is effected by three consecutive seals that ensure filtration of air in three stages which fully compensates for intake of unfiltered air around the edges at seal defects. The effectiveness of the respirator is equal to the effectiveness of the filtering material (99.99%). The light weight (60 g) and the low resistance to breathing (3-4mm H<sub>2</sub>O) make this respirator suitable for use under very high concentrations of radioactive aerosols in the air.

At present other designs for respirators and gas masks are in existence, guaranteeing the filtration of intake air of radioactive aerosols and certain gases (iodine, bromine, etc.). It should be noted that protection from

inert radioactive gases (radon, thoron, etc.) is not afforded by either existing respirators, nor by filtering gas masks. For this reason, when the limits of inert gas content are exceeded, hose fed equipment should be used that isolates the respiratory organs (plexiglass helmet of the pneumatic suit LG-1, gas mask PSh-2), as well as cylinder fed gas masks of the type KIP-5 etc.



Fig. 5. Respirator ShB-1 "The petal."

The proper organization of maintenance work is very significant, and must be based on thorough training of personnel, minimum time spent in areas of possible injury to the organism, and on strict localization of maintenance area (its separation from other quarters).

Preparation for maintenance work must consist of thorough instruction of personnel, and in some cases of prior simulation of the maintenance work. The personnel carrying out the repair must have a thorough picture of the work to be done, in all detail, must know thoroughly the possible dangers involved in the work, must know faultlessly the techniques to be employed in connection with the shielding devices. A rehearsal of the repair work is especially necessary if it must be carried out very rapidly and accurately (for instance in the case of high gamma dose rates, when the time available for performance of the work is measured in minutes). The rehearsal must be carried out with the use of all instruments, devices and shielding means that might become necessary under actual working conditions.

Particular attention must be paid to the methods and sequence of putting on and removal of supplementary individual shielding devices, since carelessness or indifference in this regard leads to contamination of the hands, the cotton paper clothing, the equipment and to dissemination of radioactive substances through clean quarters.

The time spent by workers in areas of possible harm from radioactive substances may be shortened by means of a detailed plan of execution of the maintenance work. It is essential to think through the sequence of individual operations, to accurately distribute responsibilities among the workers, to designate the relatively harmless areas, where workers can await their turns for execution of their particular operations, to prepare in advance all necessary equipment, instruments and shielding devices. Frequent trips after forgotten tools, and the presence in the area of persons not directly engaged in the work, are totally unacceptable. At the same time, in order to avoid accidents involving breathing apparatus (KIP-5, PSh-2, pneumatic suits LG-1 and LG-2, etc.) it is essential to follow a system of working in pairs, that is, the presence at the work site of at least two workers at all times.

The localization of the maintenance area may be effected in several ways, depending on the layout of the

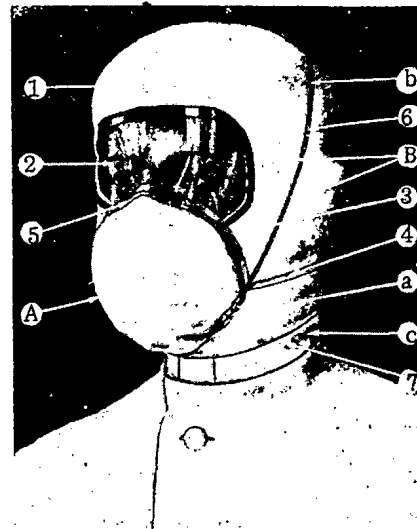


Fig. 6. Respirator ShB-2.

1) body of respirator; 2) viewing window; 3) edge of rubber lace; 4) upper strap; 5) plate; 6) rubber lace; 7) lower strap; A) basic filter zone (effective surface); B) zones of the first and second compensating filters; a) face seal; b) intermediate seal; c) neck seal.



buildings and the equipment. Under normal layouts the borders of the maintenance area are defined by agreement. Upon entering the maintenance area, the workers don the supplementary protective devices: rubber or cotton overshoes, plastic film protective clothing or pneumatic suits, a second pair of gloves, etc. Upon leaving the maintenance area, these supplementary means of individual shielding must be removed.

To minimize the possibility of contaminating surrounding objects and quarters, the individual shielding clothing must receive a preliminary deactivation treatment, before it is removed. For this purpose, at the edge of the maintenance area, a fairly small sized room must be provided, having a water supply, a drain in the floor (for water and the cleaning solutions), and only the most essential furniture (closets and hangers for the protective clothing, chairs). Such a room can be set up for the period of the maintenance work by installing temporary partitions, screens and barriers.

The maintenance of the principle of localization of maintenance work is simplified considerably under the so-called tri-zonal plan, that provides for separation of a special maintenance zone. The advantages of the tri-zonal plan for "hot" laboratories are described in reference [1]. Similar proposals have been made by a number of foreign authors [2, 3].

With tri-zonal plan it is possible to pass from the maintenance area into clean quarters only by passing through a monitor or through double gates that act as a monitor. Thus, conditions are created that operate against dissemination of radioactive contamination to clean quarters ("operational" quarters).

In addition, the creation of special maintenance areas allows the early execution of any necessary protective steps. The maintenance area is piped for clean fresh air supply to the pneumatic suits. In the monitor area, next to the maintenance area, shower installations are made, as are other washing installations for preliminary deactivation of the individual shielding devices, tools, etc. The tri-zonal plan allows execution of emergency repair operations without violation of any of the rules of safety, which is not always possible under common plans of quarters. Finally, time lost to preparation for maintenance work is negligible under the tri-zonal plan.

Working experience in dealing with radioactive substances shows that the proper organization of maintenance in conjunction with skilled use of individual shielding assures dependable protection of workers.

Received December 24, 1956

#### LITERATURE CITED

- [1] V. P. Granilshchikov and G. M. Parkhomenko, Medical Radiology 1, No. 3, 42 (1955).
- [2] R. Spence, An atomic energy radiochemical laboratory design and operating experience (Report No. 438, presented by England at the International Conference on the Peaceful Uses of Atomic Energy, 1955).
- [3] D. R. R. Fair, Brit. J. Industr. Medicine 12, 147 (1955).
- [4] N. G. Gusev, Handbook of Radioactivity and Shielding. [In Russian], (State Medical Press, 1956).
- [5] A. V. Bibergal, U. Ya. Margulis and E. I. Vorobyev, Shielding From X and Gamma Rays. [In Russian], (State Medical Press, 1955).
- [6] P. Zheno, Shielding From Radioactive Elements. (IL 1954).
- [7] V. Fano, Nucleonics 11, 8 and 55 (1953).
- [8] S. M. Gorodinsky, Hygiene and sanitation, No. 1, 27 (1956).
- [9] S. M. Gorodinsky, Medical radiology, No. 5, 84 (1956).
- [10] A. A. Letavet, The effects of radiation on the organism (Reports of the Soviet delegation at the International Conference on the Peaceful Uses of Atomic Energy) Izd. AN SSSR, 1955 p. 3.

[11] Radiation Medicine. Guidebook for Doctors and Students, edited by A. V. Lebedinsky [In Russian], State Medical Press, 1955.

[12] D. I. Zakutinsky, Delayed effects of ionizing radiation damage. (Review of reports of the conference on Delayed Effects of Damage Caused by the Interaction of Ionizing Radiation) [In Russian], State Medical Press, 1955.

[13] C. N. Shatsky, G. A. Vasiliev and P. I. Basmanov, Description of the valveless respirator ShB-2. Moscow, 1956 (manuscript).

## LETTERS TO THE EDITOR

CRITICAL HEAT LOADINGS IN FORCED FLOW  
OF WATER HEATED BELOW BOILING

B. A. Zenkevich and V. I. Subbotin

Works that have been published to date [1 - 5], describing experimental investigations directed to the study of conditions of incipient criticality in boiling regime under forced flow of water that is heated below saturation temperature, cover a range of pressures no higher than 140 atmospheres.

However, the range of pressures above 140 atmospheres is also of interest to power reactor design.

This work is devoted to the study of critical heat loadings, for flow in vertical tubes, of water with bulk heated to below saturation temperature in the range of pressures between 140 and 220 atmospheres.

Installation

A special installation was used for experimental determination of critical heat loadings, the schematic diagram being shown in Fig. 1. The circulating loop (heavy line) has included, in order, the following: centrifugal, greaseless, pump; contact column with working section; main heat exchanger; supplementary heat exchanger; electrical heaters.

The required pressure of up to 220 atmospheres in the circulating loop was created and maintained by means of a pressure compensator, consisting of 4 tanks charged with nitrogen, a piston pump and gas tanks containing nitrogen.

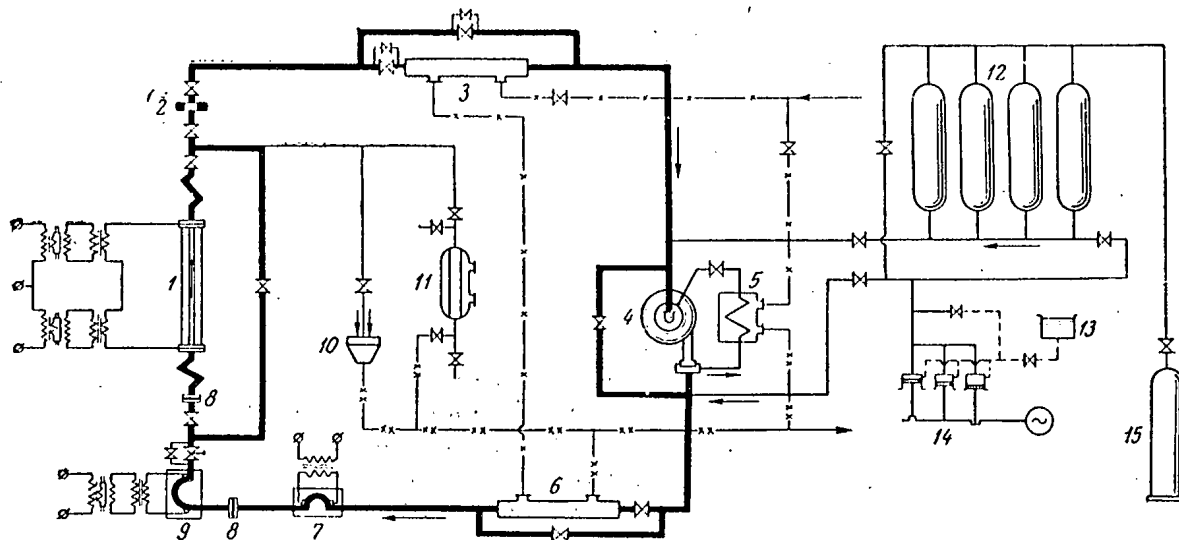


Fig. 1. Principal schematic diagram of the installation.

1) Contact column with working section, load transformer and regulated auto-transformer; 2) flow measuring diaphragm; 3) main heat exchanger; 4) circulation pump; 5) circulation pump cooler; 6) supplementary heat exchanger; 7) electric heater, 30 kw power; 8) flange coupling with electric isolation; 9) electric heater, 80 kw power; 10) overflow funnel for water drainage; 11) sample extractor for analysis of gas content of water samples; 12) pressure compensator; 13) tank with water for system feed; 14) piston pump for system feed; 15) nitrogen gas tank.

All joints, details and piping of the installation, coming in contact with water, are made of stainless steel type 1Kh18N9T.

Figure 2 shows the design of the contact column and working section. The working section is a stainless steel tube (340 or 660 mm long, 4 to 12 mm inside diameter, 0.8 to 2 mm wall thickness) held between two collet type contact jaws. The jaws are made of copper; to decrease contact resistance they were electroplated with silver, and the tube areas enclosed by the jaws were plated with copper.

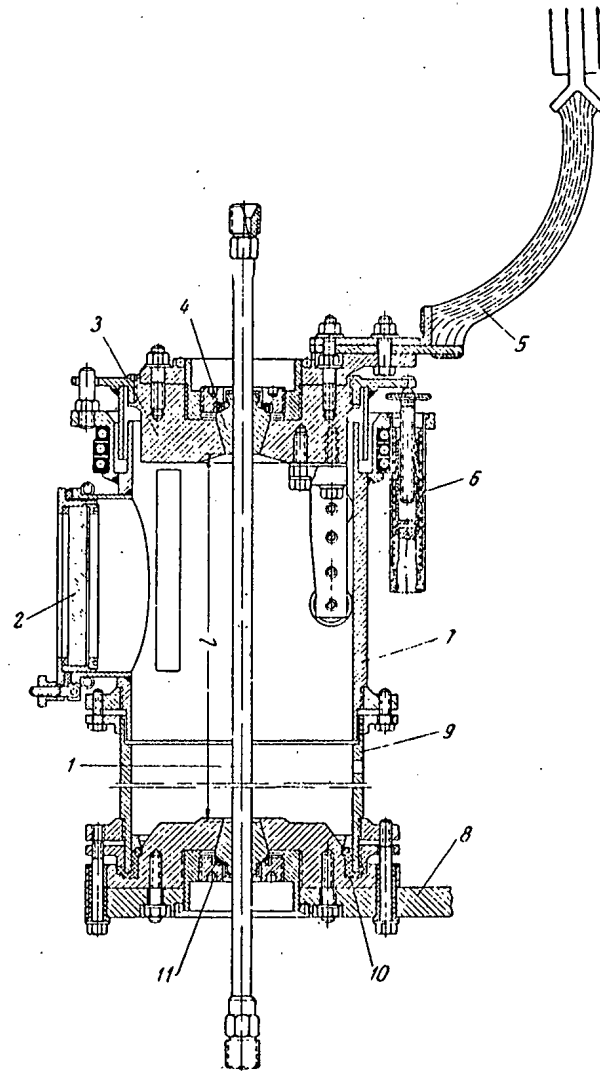


Fig. 2. Contact column with working section.

- 1) Working section; 2) quartz viewing window; 3) movable upper cover - current conductor; 4) collet type contact jaws;
- 5) upper tire (flexible); 6) spring supports of upper cover;
- 7) shell of contact column; 8) lower tire; 9) removable adapter; 10) isolating gaskets; 11) pressure nut.

The working section with the contact column is placed vertically and the water flows through it from bottom to top. Temperature expansion is compensated for by the spring loaded, movable upper cover. The working section is connected into the circulating loop by means of a ball and cone joint. Observation of the tube during experiments is done through a quartz viewing window. Electric current is fed to the contact column through the flexible upper tire and the rigid lower tire.

By means of a special flanged joint, the working section is electrically isolated from the rest of the circulating loop.

Supply of electrical energy to the working section and to the primary electrical heater was done through load transformers, connected to the electric grid through regulating autotransformers.

### Procedure

The installation was put in operation by the following sequence. By means of the piston pump (see Fig. 1), the circulating loop was filled with distilled water, while the pressure compensator was fed compressed nitrogen from the cylinders. By this means, a pressure of 100 to 110 atmospheres was created in the loop. Following this, the water level in the pressure compensator was raised so that the required pressure was maintained in the compensator, and consequently in the loop. As the water pressure in the loop dropped with leakage, water was added through the piston pump.

Following these operations, the centrifugal pump was started, the electric heater was connected into the electric grid, and the loop water temperature rose to the required value.

The critical heat loading  $q_{cr}$  was achieved by slowly increasing electrical power at the working section.

To study the effect of the method of achieving  $q_{cr}$ , several experimental points were taken by means of gradual lowering of water flow velocity with constant heat loading.

The moment of attainment of  $q_{cr}$  was determined by the sharp local increase in wall temperature of the working section, which was determined by a thermo-electric system consisting of a surface thermocouple, attached 5 to 10 mm below the upper contact jaws, and a fast acting automatic, single point, electronic potentiometer of the EPP-09 type. This method came out to be more sensitive than the method of visual observation of reddening of the tube wall in the zone where transition from nucleate to film boiling occurred.

It was established that under certain conditions a transition in the boiling mode does not occur, and instead it exhibits a "degeneration." This degeneration becomes evident, for instance, at a pressure of 200 atmospheres, water velocity  $W = 3$  to 5 m/sec, and subcooling of  $\Delta t_s \geq 60^\circ\text{C}$ ; while at  $\Delta t_s > 100^\circ\text{C}$  the transition does not occur.

Transition of boiling mode also degenerates at pressures above 210 atmospheres (when  $\Delta t_s = 25^\circ\text{C}$  and  $W = 3$  to 5 m/sec).

During the experiments the following parameters were measured:

- a) total potential drop across the working section, by means of a multi-range voltmeter of the 0.5 class;
- b) current strength through the working section, by means of a current transformer of 0.2 class and a dual range ammeter of 0.5 class;
- c) average water temperature at entrance and exit of the working section, by means of a set of mercury thermometers with readable divisions of  $0.5^\circ$ ;
- d) water pressure in the circulating loop, by means of standard manometers of the 0.35 class with scales of 0-250 and 0-400 kg/cm<sup>2</sup>;
- e) quantity of water passing through working section by means of a total flow measuring system consisting of several replaceable chamber diaphragms (for various ranges), a float type, mercury differential manometer and a second manometer.

The degree of subcooling of the water was determined as the difference between the saturation temperature at a given pressure, and the mixed mean water temperature at exit from the working section. The critical heat loadings were calculated from the electric power and were checked by the heat balance of the water flowing through the working section.

The outside diameters and wall thicknesses of the working sections made of standard, off the shelf tubing, were measured accurately. Measurements of tube surface roughness, made by means of a dual Linnick microscope showed that the degree of roughness varied within the limits of 25-35  $\mu$ .

The coolant was a water monodistillate with dry residue content (unfired) of 2-5 mg/l.

The effect of direction of motion of water on  $q_{CR}$  was checked, and for this, part of the experiments were conducted with water flow from top to bottom. Most of the experiments were run with gas content in the water (mainly nitrogen) on the order of 30-130  $\text{ncm}^3 \text{N}_2/\text{kgH}_2\text{O}$ . To study the effect of quantity of gas dissolved in water on the value of  $q_{CR}$ , several series of experiments were run with different velocities and degrees of subcooling, with  $P = 201$  atmos. and gas content in the water up to 1450  $\text{cm}^3/\text{kg H}_2\text{O}$ . The gas content was determined by volume methods by means of a sample extractor.

### EXPERIMENTAL RESULTS

The experiments showed that the transition from nucleate boiling to film boiling is determined by: the weight rate of water flow  $W_g$ , degree of subcooling  $\Delta t_s$  and the pressure. As characteristic of effect of pressure, the ratio  $v''/(v''-v')$ , was chosen, where  $v'$  and  $v''$  are respectively, the specific volume of water and of steam at saturation temperature.

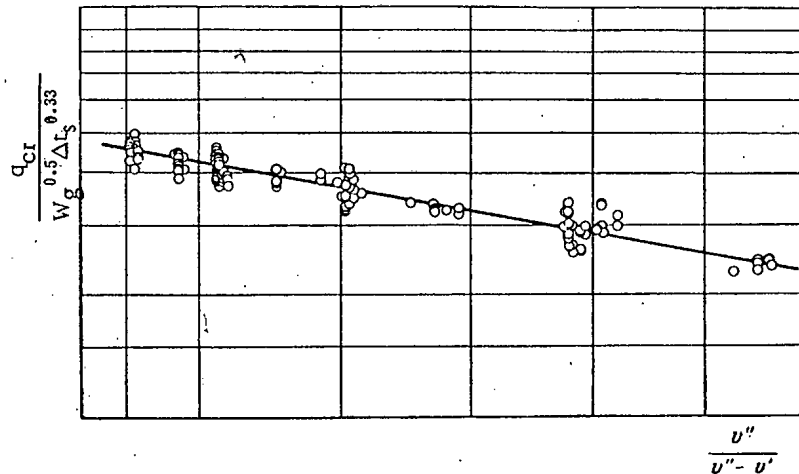


Fig. 3. Variation of the relation  $q_{CR}/(W_g^{0.5} \cdot \Delta t_s^{0.33})$  with the ratio  $v''/(v''-v')$  in the pressure interval 140-210 atmospheres.

It was established that the quantity  $q_{CR}$  is proportional to  $W_g^{0.5}$  and  $\Delta t_s^{0.33}$ . In Figure 3, on log scale, is shown the relationship

$$\frac{q_{CR}}{W_g^{0.5} \Delta t_s^{0.33}} = f\left(\frac{v''}{v''-v'}\right).$$

All experimental points (about 250) fell along one straight line with slope  $-1.8^*$ , from which it follows that

$$q_{CR} = 590 W_g^{0.5} \Delta t_s^{0.33} \left(\frac{v''}{v''-v'}\right)^{-1.8} \text{ kcal/m}^2 \text{ hr};$$

This formula is recommended for calculation of  $q_{CR}$  in the interval of pressures of 140-210 atmospheres, with weight flow rates of water of  $3 \cdot 10^6$  to  $18 \cdot 10^6$   $\text{kg/m}^2 \text{ hr}$ , and subcooling of 10-100°C.

The effect of the following on the value of critical heat loadings was not determined:

- inside diameter of tubing (4-12 mm);
- gas content (nitrogen) in water (30-1450  $\text{ncm}^3 \text{N}_2/\text{kg H}_2\text{O}$ );

\* A significant number of points were coincident on the graph (Fig. 3).

- c) direction of water flow (up and down) with  $W_g > 3 \cdot 10^6$  kg/m<sup>2</sup> hr;
- d) method of achieving  $q_{cr}$  (see above).

The following participated in erection of the apparatus and running the experiments: Engineers O. A. Sudnitsin, O. L. Peskov, V. I. Krotov and N. D. Sergeev. A large amount of work in reducing the experimental data was done by Engineer Z. F. Deryugina and Technician N. A. Gushchina.

Received February 22, 1957

#### LITERATURE CITED

- [1] W. H. McAdams, W. E. Kennel, C. S. Minden, R. Carl, P. M. Picornell, and J. D. Dew, *Ind. and Eng. Chem.* 41, 1945 (1949).
- [2] F. C. Günter, *Trans. ASME*, 73, 115 (1951).
- [3] H. Buchberg, F. Romic, R. Lipkis and M. Greenfield, *Heat Transfer and Fluid Mechanics Institute*, June, 1951, Stanford University Press, Stanford, California.
- [4] W. H. Jens, *Mech. Eng.* 76, 981-986 (1954).
- [5] V. C. Chirkin and V. P. Yurkin, *J. Tech. Phys.* 26, 1542-1555 (1956).\*

---

\* Original Russian pagination. See C. B. translation.

HYDRODYNAMIC RADIATION FROM THE TRACKS OF IONIZING PARTICLES  
IN STABLE LIQUIDS

G. A. Askaryan

When ionizing particles pass through liquids the molecules of the medium are entrained by singly - charged ion aggregates which are pushed apart; in addition, small micro-explosions, due to localized heating, occur close to the tracks of the particles. These processes can lead to the formation of localized cavities and nuclei or "seeds" at which the transition to the vapor or gas phase is possible. (The development of these nuclei into bubbles of visible dimensions, which takes place if the liquid is sufficiently unstable, is used in new devices for studying ionizing radiation - so-called "vapor" and "gas" bubble chambers [1-3].)

The sudden motion of the ion-complexes, the micro-explosive production of the nuclei, the further expansion and contraction and subsequent disappearance or rapid growth (depending on the initial local factors, the properties and state of the medium) should be accompanied by intense localized pulses of radiation of supersonic waves which, in the initial stage, should be quasi-microspherical shock waves. The intensity of this radiation should depend on the properties of the medium which determine the effectiveness of bubble initiation and the dynamics of bubble development (surface tension, stability of the liquid state, etc). It should be noted that similar radiation will occur in solid bodies and compressed gases but its intensity will be considerably smaller than that found in liquids.

When an ionizing particle passes through the liquid, almost instantaneously a system of pulsed sources of compression waves is formed; these are located along the track of the particle at points of highest density of ion production (numerous highly ionizing low-energy  $\delta$ -rays) and in regions of direct Coulomb interactions with nuclei and so on.

In the case of particles which do not have a very high specific ionization (rather large range) the number of regions in which localized energy losses takes place is proportional to the number of effective  $\delta$ -electrons which, just as the number of effective Coulomb collisions, is proportional to  $Z^2/\beta^2$  (here  $Z$  and  $\beta$  are the relative charge and velocity of the ionizing particle). We use the symbol  $n(C)$  to denote the number of bubble nuclei of a given type produced per unit length of track of ionizing particle and  $C$  to denote the group of initial parameters pertaining to the formation of ion "jumps" or cavities (for example, the initial characteristics pertaining to ion aggregates or localized heating processes) which uniquely characterize the radiation process. Then for a wide range of particle velocities we have

$$dn = n(Z, \beta, C) dC \approx \frac{Z^2}{\beta^2} n_1(C) dC,$$

where  $dC = \sum_1 PdC_i$  is the total differential of the production parameters,  $n_1(C)$  is a function which depends on the production parameters and the properties and state of the medium.

We consider the field of supersonic radiation far from the radiation centers. We shall assume that a definite instantaneous state of the system of virtual pulsed-radiation centers is given. We surround each center by a sphere, the radius of which is known to be greater than the amplitude of the pulsations of the radiating cavity. (For definiteness we consider the case of formation and disappearance of the cavity or the initial stage of an arbitrary growth process). The radius  $r_k$  of the  $k$ -th sphere associated with the  $k$ -th source is chosen in



such a way that outside this sphere the amplitude of the radiation field due to the  $k$ -th radiation source is inversely proportional to the distance from the source and the radiation is propagated with constant velocity. Then, at the point of observation  $O$ , the radiation amplitude due to the  $k$ -th source is

$$A_k(O, t) = \frac{1}{R_k} \varphi_k \left( t - \frac{R_k}{v} \right),$$

where  $R_k$  is the distance from the observation point  $O$  to the radiating center,  $v$  is the velocity of propagation of the hydrodynamic radiation,  $\varphi_k(t)$  is the radiation function, which is determined by the initial parameters  $C_k$  and the radius of the sphere  $r_k$ , being equal to the product of the radius and the amplitude of the wave at the surface of the sphere;  $t$  is the time. The Fourier component of the radiation field is

$$A_{k\omega}(O) = \frac{1}{R_k} \varphi_{k\omega}(C_k, r_k) e^{\frac{i\omega R_k}{v}},$$

where  $\omega$  is the radiation frequency.

The total field is obtained by summing the radiation fields of the system of centers

$$A_{\omega}(O) = \sum_k A_{k\omega}(O).$$

If the projection of the dimensions of the region of radiation sources in the direction of observation is considerably smaller than the radiation wavelength which is observed,  $|A_{\omega}(O)| = \sum_k |A_{k\omega}(O)|$  i.e., the radiation from these sources is coherent. The coherent multiplication of the radiation is particularly marked in strongly ionizing, short-range particles, for example, recoil protons and  $\alpha$ -particles (in addition, in these tracks the radiation centers tend to fuse together).

In analyzing a quasi-linear, random distribution of sources we shall distinguish two cases.

If the observed wavelength is rather large, for example, much larger than the projection of the mean distance between radiating centers in the direction of observation, for a quasi-uniform track of length  $L$  we have

$$A_{\omega}(O) \approx \frac{e}{R_0} \frac{i\omega R_0}{v} \int \int n(C) \varphi_{\omega}(C) e^{\frac{i\omega z \cos \theta}{v}} dz dC \approx \frac{e}{R_0} \int n(C) \varphi_{\omega}(C) dC \cdot \frac{\sin \left\{ \frac{\omega \cos \theta \cdot L}{2v} \right\}}{\left\{ \frac{\omega \cos \theta \cdot L}{2v} \right\}},$$

where  $n(C)dC$  is the mean number of radiating centers formed with initial parameters ranging from  $C$  to  $C + dC$  per unit length of track of the ionizing particle. In this case the radiation is predominantly in the direction perpendicular to the track.

If the observed wavelength is much smaller than the mean distance between centers in the direction of observation,

$$|A_{\omega}(O)|^2 \approx \frac{1}{R_0^2} \sum |\varphi_{k\omega}|^2 \approx \frac{1}{R_0^2} \int \int n(C) |\varphi_{\omega}(C)|^2 dC dz,$$

i.e., in this case we have the summation of the angular distributions of the intensities of the radiation centers.

The radiation field close to the track, especially close to the pulsed radiation centers, is of great interest from the point of reaction efficiency since both the amplitude and frequency of the wave are very high in this region.

The suddenness of the cavity production process in liquids and the high density of liquids mean that the radiated energy may be comparable with the energy expended in the formation of the cavity nuclei themselves, i.e., the radiated energy can be a significant part of the energy losses of the particles.

It is characteristic of the process being considered that the zone of strong radiation and, consequently the zone of effective reaction, is considerably larger than the region in which ionization is important. Even at distances from the radiation center of the order of fractions of a micron the amplitude of the compression wave is still high.

It is possible that this local hydrodynamic radiation is the origin of the highly destructive properties of ionizing radiation in the tissues of organisms, cells and microorganisms and that it may be responsible for a number of similar effects which are observed in irradiation by intense supersonic sources. If this is the case, the efficiency of the radiation effect should depend on the physical parameters and the conditions which determine the radiation efficiency of the hydrodynamic waves and the dynamics of formation and growth of cavity nuclei; in particular, the surface tension of the liquid, which depends on the temperature and the concentration of the dissolved gas, the proximity to critical conditions, and so on. The study of this dependence may be useful in determining the optimum conditions for which a particular radiative reaction can be increased or reduced.

Using powerful pulsed or continuous sources of ionizing radiation (radioactive preparations, charged-particle accelerators or special x-ray tubes) and choosing judicious conditions in the liquid, it should be possible to distinguish between sections of the spectrum of supersonic radiation and the comparatively strong background of hydrodynamic radiation which accompanies the passage of particles through dense media.

The effect in question may also be used for detection and measurement of the intensity of ionizing radiation in dense media and other practical purposes.

Received April 9, 1957

#### LITERATURE CITED

- [1] D. Glaser, Suppl. Nuovo Cim. 11, cep. 9, No. 2, 361 (1954).
- [2] G. A. Askaryan, J. Exptl-Theoret. Phys. (USSR) 31, 897 (1956).
- [3] P. Argan, and A. Gigli, Nuovo Cim. 8, 5, 1171 (1956).

## SPARK SOURCE FOR MULTIPLY-CHARGED IONS

A. A. Plyutto, K. N. Kervalidze and I. F. Kvartskhava

Most well-known spark sources for multiply-charged ions make use of weak inductively-coupled sparks which are obtained by means of a Tesla coil [1], [2]. These sources have not been used in charged-particle accelerators because of the small ion current, low charge multiplicity of the ions which are obtained, and general unstable operation.

Starting in 1953 the authors have been carrying out an investigation of "hot" vacuum sparks obtained by the discharge of high-voltage condensers in an effort to obtain intense beams of multiply-charged ions with high charge multiplicities. In 1954 a source was constructed and found suitable for use in pulsed accelerators of multiply-charged ions.

Source and Method of Investigation

A schematic diagram of this source is given in Fig. 1,a. The vacuum spark is produced between the insulated electrodes 1 and 2 by the discharge of a high-voltage condenser. The ions are extracted through aperture 4 in electrode 5. The extraction-accelerating voltage, from a high-voltage high-capacity condenser, is applied to electrodes 5 and 6. Electrodes 2 and 5 are connected together. The operating material, in the form of a solid or thermally stable chemical compound is placed in channel 7 in electrode 1. The walls of the discharge channel are formed by a procelain tube 3 approximately 4 mm in diameter. Below, this type of constraint of the discharge channel will be called "mechanical constriction" of the spark.

The capacity of the condenser which provided the spark was varied between  $10^3$  and  $10^5 \mu\text{mf}$ ; the condenser voltage was varied from 10 to 70 kv and the average spark current from  $10^2$  to  $10^4$  amps. During the spark discharge there is a damped oscillatory current at a frequency of  $10^5$  -  $10^6$  cps. The repetition frequency of the spark could go as high as 50 cps. The capacity of the condenser in the ion extraction circuit was varied between  $10^4$  and  $10^6 \mu\text{mf}$  and the voltage on this condenser was varied from 15 to 70 kv.

The ions were analyzed with a Thomson mass spectrometer (parabola method) [1], [2]. The multiply-charged ions were identified by the method used in these same references. The total ion-electron current flowing between electrodes 5 and 6 was also determined. This current was determined from current oscillograms or from the discharge time of the condenser which supplied the voltage between electrodes 5 and 6.

The source chamber was charged with the operating gas in pulses. Because the charge occupied a rather large volume in the vacuum chamber and the fact that the metallic vapors and vapors of other solid compounds were easily condensed on the cold walls it was not necessary to use high capacity pumps. A vacuum of approximately  $10^{-5}$  mm Hg was easily maintained with 2 TsVL-100 pumps.

The lifetime of the source corresponds to about  $10^6$  pulses. When operating the source at a low duty cycle at a frequency below 50 pulses/sec no supplementary cooling was required.

### Experimental Results. Discussion of the Results

The first experiments indicated that a mechanically constricted spark is more efficient than a free spark. For example, in a mechanically constricted spark it is possible to realize a mode of operation in which there are more multiply-charged ions than singly-charged ions; this situation could not be achieved with an open spark. Hence in the following we will be concerned exclusively with the results obtained with mechanically constricted sparks.

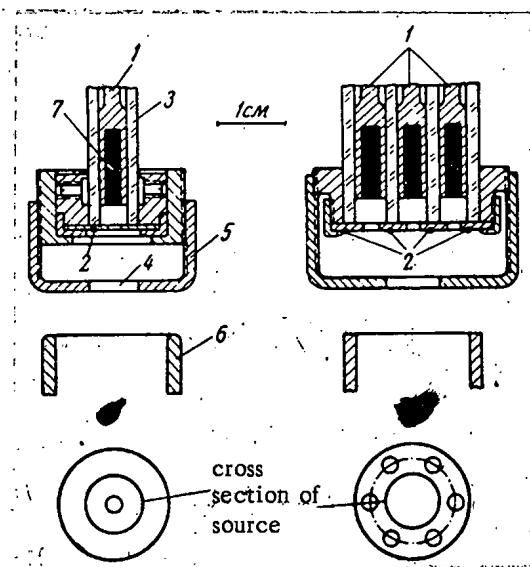


Fig. 1. Section through the spark gap with one (a) and multiple (b) discharge gaps.

Ions of the electrode materials appear in small quantities. The silicon and oxygen ions appear as a result of disintegration of the walls of the porcelain tube which contains the discharge channel.  $H^+$  and  $H_2^+$  ions are produced by ionization of the water vapors and organic compounds which are present at the electrodes and walls of the discharge channel and by ionization of absorbed hydrogen.

All other conditions being equal, in general the relative number of multiply-charge ions increase with increasing amplitude and frequency of the spark current and a reduction of the distance between electrodes 1 and 2 (cf. Fig. 1,a). The latter result means that the region of most intense generation of multiply-charged ions is close to the electrodes.

The total ion current increases with increasing spark power and increasing distance between electrodes 1 and 2 (Fig. 1,a). The density of the ion current was determined by a Faraday cylinder with a secondary-electron suppressor. This cylinder was placed in a plane perpendicular to the beam at a distance of 15 cm from the source. By examining the density of the ion current over the beam cross section the total ion current could be estimated. These measurements yielded a value of approximately 1 amp and higher.

The estimates of the total current due to all the components of the ion beam, in particular, the multiply-charged ions, were carried out indirectly since the focusing conditions were not the same for all components. Photometric methods were used to study the ion spectrum and the total area of all the lines (in arbitrary units) was related to the total ion current; the current associated with each component was determined from the area of the corresponding line on the photometric curve. In this procedure one must take account of the fact that the blackening of the emulsion depends not only on the number of ions which strike a given area, but also on the energy and mass of the ions. The charge multiplicity has no effect on the blackening since the multiply-charged ions capture electrons rapidly in the photoemulsion and then act like singly-charged ions. After introducing corrections for ion energy and mass it was found that the photometric curves reproduced the ratio of current

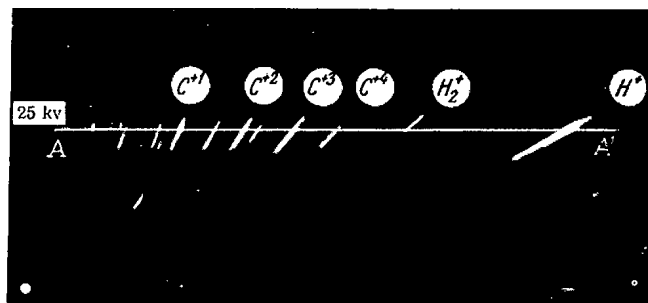


Fig. 2. Carbon ion spectrum.

In Fig. 2 is shown an ion spectrum obtained when the operating material was carbon. Electrodes 1 and 2 (cf. Fig. 1,a) were fabricated from copper and nickel respectively. Similar spectra were obtained for nitrogen, oxygen and other elements from which thermally stable solid compounds could be formed. In Fig. 3 is shown a photometric curve of the ion spectrum in the region AA' (cf. Fig. 2). The spectrum exhibits a high content of multiply-charged ions. With the exception of a small amount of  $H_2^+$ , there were no molecular

components except for  $H^+1$  and  $H_2^+1$ ; these ions produce a blackening which is approximately an order of magnitude greater than that of singly-charged ions of medium mass (for example,  $C^+1$ ). In these cases it was necessary to introduce appropriate corrections.

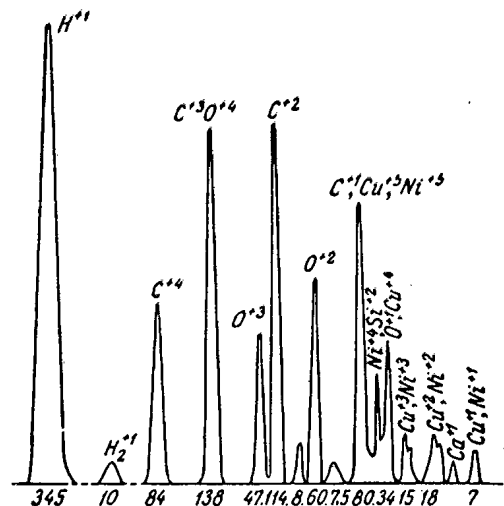


Fig. 3. Photometric curve of the ion spectrum shown in Fig. 2. (The area of the spectral lines is plotted along the abscissa axis in arbitrary units. The total of all areas is 660.)

Considerably greater success was achieved with magnetic focusing, being realized through the use of a system of short lenses. In this case it was also possible to achieve a certain separation between  $H^+1$  and  $H_2^+1$  ions and even between  $C^+3$  and  $C^+4$ . With an extraction voltage of 30 kv it was possible to achieve the following pulsed ion currents:  $H^+1$  - 10 ma,  $H_2^+1$  - 1 ma,  $C^+4$  - 6 ma and  $C^+3$  - 15 ma, on a spot 5-8 mm in diameter. These currents could be increased by increasing the extraction voltage. For example, with an extraction voltage of 70 kv the focused beam of  $H^+$  ions could be increased to 25-30 ma.

The duration of a current pulse from the source is less than several tens of microseconds and the operating cycle of the linear accelerators for which this source was intended is approximately 400  $\mu$ sec. For this reason a multiple spark source was developed; a diagram of this source is shown in Fig. 1, b. Around a central spark gap, at equal distances, there is a series of identical spark gaps which operate independently. Ion extraction, however, takes place through a single aperture which is common to all spark gaps. The authors have investigated a multiple-system consisting of 5 spark gaps fired in succession. The length of the ion current pulse was increased by a factor of five as compared with the source with one spark gap. The yield of multiply-charged ions in each spark remained the same.

It was found in an oscilloscope study of the volt-ampere characteristics that the generation of multiply-charged ions in vacuum sparks occurs in the low voltage region - when the voltage across the discharge gap is 30-40 volts. To explain this effect we must assume that the important process in the generation of multiply-charged ions is the step-by-step ionization of excited states of the ions. A simple calculation shows that this process can be significant at current densities of  $10^6$  amp/cm<sup>2</sup> and above, when the lifetime of the excited state of the ion (approximately  $10^{-7}$  sec) becomes comparable with the mean time in which the ion is excited in the discharge. Densities like these are found in the region of the cathode spot of spark discharges. It has been established at the present time [3] - [5] that at high spark currents the current density in the cathode spot becomes as high as  $10^7 - 10^8$  amp/cm<sup>2</sup>. Thus, the region of intense generation of multiply-charged ions should be close to the cathode; this was directly corroborated by the experiments. Spectrometer investigation of vacuum sparks has also shown intense ion lines, in which as many as four electrons can be excited simultaneously [6].

Using the spark source in pulsed operation it was possible to obtain unfocused  $C^+3$ ,  $C^+4$ ,  $N^+3$ ,  $N^+4$ ,  $O^+3$  and  $O^+4$  ions at from tens to hundreds of milliamps,  $N^+5$ ,  $O^+5$  at hundreds of microamps to several milliamps, and  $O^+6$  at hundreds of microamps. The ion currents due to the electrode materials ( $Cu^+6$ ,  $Cu^+7$ ,  $Ni^+6$ ,  $Ni^+7$  etc.) were of the order of hundreds of microamps. The accuracy with which these currents could be estimated is less than 20-30%.

It was also shown in these experiments that this source can be used to obtain high pulsed currents of protons and deuterons when solid hydrogen compounds are used as the operating material. If an extraction voltage of the opposite sign is applied to electrodes 5 and 6 (cf. Fig. 1, a) electrons can be extracted from the source. With an extraction voltage of 40 kv it was possible to obtain unfocused electron currents of up to 100 amperes in a pulse of 2  $\mu$  sec duration.

It has been found that the well-known methods of electrostatic focusing are not effective at the high ion currents which obtain in this source. Satisfactory focusing could be achieved only when the total ion current was less than approximately 60 ma.

The enhanced content of multiply-charged ions in the mechanically constricted hot sparks as compared with the open sparks can be explained by the higher average current density over the volume of the discharge. In an open hot spark the free expansion of the plasma which is saturated with multiply-charged ions causes the current density to fall off rapidly; thus ionization processes are inhibited and recombination processes tend to dominate. For example, all other conditions being equal the use of mechanical constriction increases the relative number of  $C^{+4}$  ions by a factor of 5-10.

In contrast with other types of ion sources, ion extraction in spark sources takes place in a region far from the spark. In this case use is made of the tendency of a dense plasma to expand in vacuum, thereby forming larger areas for ion extraction [7]. The size and shape of the boundary of the plasma are determined by the ion extraction conditions. The fact that ion currents of approximately 1 amp and higher can be achieved in spark ion sources with comparatively small extraction voltages is explained by the large plasma boundary which appears at aperture 4 (cf. Fig. 1,a).

The rather large energy spread of the extracted ions [3-5 kv (cf. Fig. 2)] is due to oscillations of the ion extraction region and oscillations of the region of penetrating residual field in the expanded plasma; these are produced by oscillations of the plasma density, which start at the spark region and pass through the aperture in electrode 2 (cf. Fig. 1,a).

There are a number of other potentialities for the spark source which have not been utilized. Spectroscopic investigation [8] shows that in hot sparks, more intense than those reported here, there are many  $C^{+5}$ ,  $N^{+6}$ ,  $O^{+7}$  ions as well as  $Mg^{+10}$ ,  $Al^{+11}$ ,  $Cu^{+18}$  and  $Sn^{+23}$  ions. These results point to the possible use of vacuum sparks as a means of obtaining completely ionized atoms of intermediate mass.

In conclusion the authors wish to express their gratitude to A. T. Kapln for help in this work.

Received December 29, 1956

#### LITERATURE CITED

- [1] A. Dempster, Rev. Sci. Instr. 7, 46 (1936).
- [2] Shang-Yi-Chen, Phys. Rev. 50, 212 (1936).
- [3] B. Snoddy, Phys. Rev. 37, 1678 (1931).
- [4] K. Froome, Proc. Phys. Soc. 63-B, 377 (1949).
- [5] R. Craig, Rep. Brit. Electr. Res. Assoc., Ref. L/T 260 (1951).
- [6] Handbook; Landolt-Bornstein, Vol. 1, pp. 50-210.
- [7] M. D. Gabovich and E. T. Kucherenko, J. Tech. Phys. 26, 996 (1956).\*
- [8] B. Edlen, Physica 13, 545 (1947).

\* Original Russian pagination. See C. B. translation.

## SLOW-NEUTRON DETECTOR

T. V. Timofeeva

As is well known, slow-neutron counters make use of scintillators made with a zinc sulfide base with boron additives. The literature [1] - [7] describes two methods for fabricating scintillators of this type; 1) a method in which the components are mixed by mechanical methods, and 2) the fusion method in which a phosphor, prepared in advance, is introduced into the melt containing the boron compound. We have used a third method for fabricating scintillators: in this scheme the materials are sintered. According to our data the efficiency for neutron counting in this method is 5 times greater than that of the first method and 1.25 times greater than the second. In this method boric acid, unenriched in  $B^{10}$ , is introduced into the original phosphor charge and accompanies it through all the fabrication stages. The high efficiency for neutron counting in the phosphor is a strong function of the particular crystalline state of the boric acid.

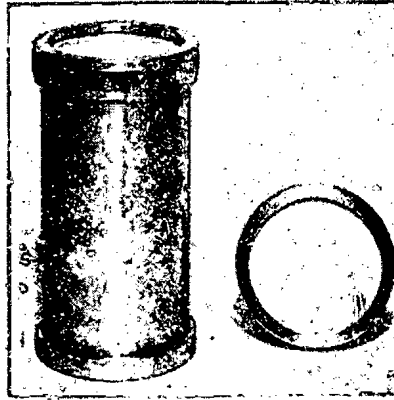
Using this method we have obtained a zinc sulfide, silver activated phosphor, containing boric acid as a fusing material.

The emission spectrum of the phosphor has a maximum at  $4430 \text{ \AA}$ . The neutron counting efficiency of the phosphor is a strong function of the thickness of the layer and the grain size. It increases with increasing grain size and layer thickness. However, there is an optimum value. The optimum layer thickness is equal to 2-3 grain dimensions, regardless of size. If the thickness is increased beyond this value the efficiency either remains constant or falls off slowly. The presence of the maximum is the result of competition between two effects. On the one hand the number of nuclear reactions increases with increasing thickness, thereby giving rise to a greater number of scintillations. On the other hand, the scattering of the luminescence is increased; because of the overlap between the radiation and absorption spectra this situation leads to a reduction in luminescence.

Two neutron detectors in which this phosphor is used have been developed: plane and cylindrical (cf. figure). The plane detector consists of a layer of coarse grain phosphors ( $100\text{-}300 \mu$ ) with a thickness of  $80 \text{ mg/cm}^2$  held between a glass window (4.0 cm in diameter) and an aluminum substrate. The cylindrical detector is fabricated from an aluminum cylinder 9.5 cm high and 4.0 cm in diameter covered on the inside by a similar layer of phosphor and vinyl lacquer, enclosed by a glass protective window. Using the phosphor in a lacquer reduces the counter efficiency by a factor of 2 or 3; however, replacing the plane layer by the cylindrical layer increases efficiency by a factor of 7 or 8.

Both detectors are protected against moisture since the phosphor is rather hygroscopic. The detectors are designed for use with a FEU-19 photomultiplier on the window of which they are applied directly; however, they can be made up in other dimensions. The slow-neutron counting factor in the plane detector is estimated several percent (approximately 5%).\* The results of the foreign authors quoted in Refs. [1], [2], and [4], for a plane detector, vary from 1 to 6%. The neutron counting efficiency in a cylindrical detector is three times greater than the plane detector. The reproducibility of counter efficiency in the phosphors (for different parts) is  $\pm 4\%$  in the plane detectors (for the same part)  $\pm 2\%$  cylindrical detectors (for the same part)  $\pm 6\%$ . The accuracy of the efficiency measurements was  $\pm 2\%$ .

\* The estimate of the counting factor and the efficiency measurements of the counter were carried out by S. P. Khormushko.



General view of the slow-neutron detector.  
Left) cylindrical detector; right) plane detector.

With a  $\gamma$ -background of  $300 \mu r/sec$ , obtained from a radium source, the counter efficiency was reduced by a factor of 4 because of the necessity of distinguishing between neutron pulses and pulses due to the  $\gamma$ -background. The sensitivity of the detectors to fast neutrons is 1% of the slow-neutron sensitivity as obtained by slowing down the fast neutrons in paraffin.

A detailed report of these methods and results will be published shortly.

Received November 26, 1956

#### LITERATURE CITED

- [1] D. Alburger, Rev. Sci. Instr. 23, 769 (1952).
- [2] E. Gatti, E. Germagnoli, A. Persano and E. Zimmer, Nuovo Cimento 9, 1012 (1952); 10 Suppl. 3, 322 (1953).
- [3] T. Kahan, J. Debiesse, R. Champeix and H. Bizot, J. de Phys. 9, 25 (1948).
- [4] P. Koontz, G. Keepin and J. Ashley, Rev. Sci. Instr. 26, 352 (1955).
- [5] K. Sun and W. Shoupp, Rev. Sci. Instr. 21, 395 (1950).
- [6] J. Schenck, Nucleonics 10, No. 8, 54 (1952).
- [7] H. Palevsky, H. Muether and A. Stolovy, Phys. Rev. 93, 920 (1954).



CERTAIN PROBLEMS ASSOCIATED WITH THE USE OF  
SCINTILLATION COUNTERS IN DOSIMETERS

I. B. Keirim-Markus and Z. P. Lisitsina

The use of scintillation counters in dosimeters has a number of important advantages: high efficiency for different types of radiation, wide measurement range, high sensitivity. However, the use of scintillation counters entails a number of difficulties.

Most domestic photomultipliers have photocathodes of small area; this characteristic makes it difficult to use these tubes in scintillation counters intended for measuring surface contamination by  $\alpha$  and  $\beta$  active materials.

Furthermore, a photomultiplier requires a highly stabilized voltage supply. For example, the gain of a FEU-19, operated at a voltage of 1500 volts, is constant to within  $\pm 1\%$  if the high voltage does not change by more than  $\pm 2$  volts.

Since the power supply for a dosimeter must combine a stable high voltage with the contradictory requirement of light weight the usual circuits, in which electronic stabilization is employed, are not very convenient.

I

The literature contains descriptions of a number of special circuits in which stabilization is achieved through the use of the non-linear dependence of photomultiplier gain on the potential difference between any neighboring dynodes [1]-[3]. These circuits, however, do not afford smooth control of the gain and require modification when the photomultiplier is changed [1], [3], or are suitable only for certain types of foreign photomultipliers with asymmetrical dynodes [2] and cannot be used with the majority of domestic photomultipliers.

We have investigated the relation between the gain  $M$  of the FEU-19 and the potential difference  $U$  between neighboring dynodes. The 8th dynode was disconnected from the voltage divider and a potential difference, which could be varied, was applied between the 7th and 8th dynodes. In this procedure the voltage between 8th and 9th dynodes is also changed since the divider voltage, and consequently the voltage between dynodes 7 and 9, remains fixed. The pulse heights produced at the photomultiplier output when the cathode was exposed to flashes from a neon tube relaxation oscillator were measured as a function of the voltage  $U$ . In Fig. 1 are shown the results obtained with three different voltages  $V$  across the photomultiplier.

As is to be expected, the gain is a maximum when the potential difference between the 7th and 8th dynodes and between the 8th and 9th dynodes is the same.

A similar relation between the gain  $M$  and the voltage  $U$  applied between the "smoothing" dynode and the neighboring dynode can be obtained analytically.

As a rough approximation it may be assumed that the multiplication factor of the dynode is proportional to  $U^{1/2}$  when electrostatic focusing is used (cf. for example, Fig. 7 in Birks [4]). If we neglect the effect of the voltage change on the photocathode and collector system in an FEU-19 with 13 dynodes,  $M \sim U_0^{13/2} \sim V^{13/2}$  where  $U_0$  is the potential difference between neighboring dynodes when the voltage is equally distributed

between dynodes and  $V = nU_0$  is the high voltage applied to the photomultiplier ( $n = 15$  is the number of electrodes in the photomultiplier).

If a voltage  $U \neq U_0$  is maintained between the "smoothing" dynode and one of the neighboring dynodes, the voltage between the "smoothing" and the opposite neighboring dynodes is  $2U_0 - U$ . Then

$$M \sim U_0^{1/2} U^{1/2} (2U_0 - U)^{1/2}. \quad (1)$$

The function  $M(U)$  has a maximum at  $U = U_0$ . A curve showing this relation is given in Fig. 2.

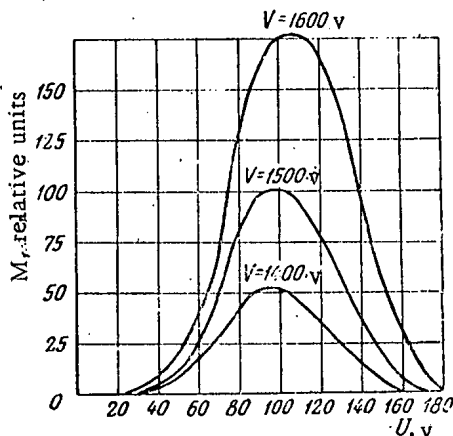


Fig. 1. Experimental curves showing the relation between the gain of the FEU-19 photomultiplier and the voltage applied between the "smoothing" dynode and the neighboring dynode.

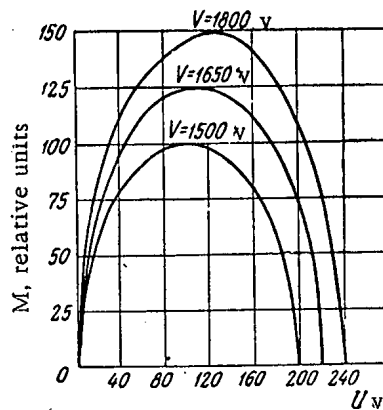


Fig. 2. Calculated curves showing the relation between the gain of the FEU-19 photomultiplier and the voltage applied between the "smoothing" dynode and the neighboring dynode.

The difference between the curves in Fig. 1 and Fig. 2 indicates that our assumed relaxation between the gain and dynode voltage  $M \sim U^{1/2}$  is incorrect. However, in the qualitative analysis which follows this discrepancy is not important.

From Equation (1) we have

$$U = U_0 (1 \pm \sqrt{1 - M^2 K U_0^{-13}}), \quad (2)$$

where  $K$  is a constant.

When  $M = \text{const}$  the curve showing the dependence of the potential difference between the "smoothing" dynode and the neighboring dynode as a function of the high voltage (proportional to  $U_0$ ) is a part of a hyperbola with branches asymptotically approaching the line  $U = 0$  and  $U = 2U_0$ .

The inflection point, which corresponds to the minimum value of the high voltage for which a given gain  $M$  can be obtained, is found from  $U = U_0 = \sqrt[13]{KM^2}$ .

The curves  $U(U_0)$  are plotted for two values of  $M$  in Fig. 3.

When  $M = \text{const}$  the function  $U(U_0)$  is essentially linear over a wide variation of the high voltage. This fact suggests the possibility of a simple circuit for stabilizing the gain of the photomultiplier.

Similar curves can be plotted on the basis of the experimental data given in Fig. 1. Such curves were taken with the FEU-19.

In Fig. 4 we show curves obtained when the voltage was changed between the 7th and 8th dynodes at three values of  $M$ . The gain  $M$  increases in going from left to right. A comparison of Fig. 3 and Fig. 4 indicates that a relation of the kind given in (2) actually applies.

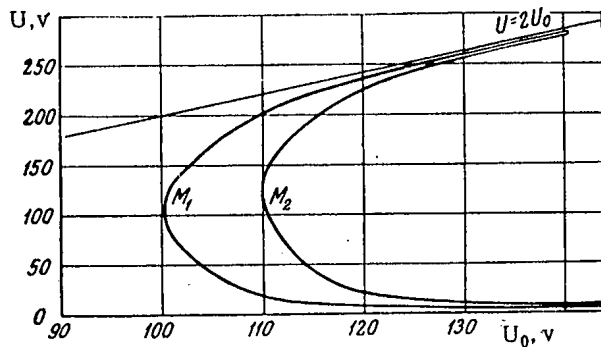


Fig. 3. Calculated curves of the function  $U(U_0)$  for  $M = \text{const}$  ( $M_2 > M_1$ ).

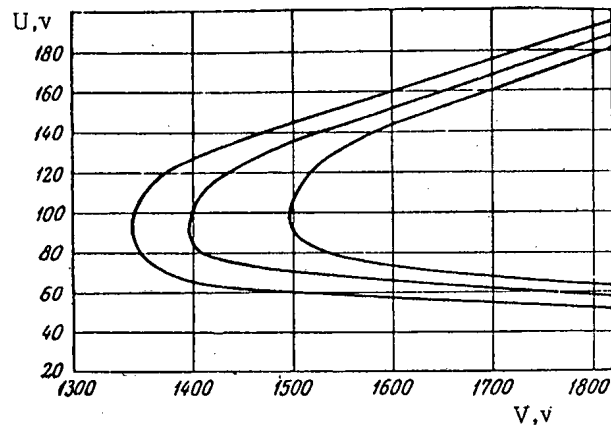


Fig. 4. Relation between  $U$  and  $V$  for  $M = \text{const}$  (experimental curves).

Similar curves were obtained when the 6-th, 7-th, 10-th, 12-th or 13-th dynodes were used as the "smoothing" dynode. With asymmetrically arranged electrodes (diaphragm, first and last emitters) the curves are different.

The curves in Fig. 4 indicate that with  $M = \text{const}$  the function  $U(V)$  is linear for segments of as much as 450 volts for both the upper and lower branches.

The linear sections of the curves can be considered in terms of a circuit consisting of an ohmic resistance and a constant voltage element (Fig. 5).

Any of the dynodes from No. 6 to No. 12 can be used as the smoothing dynode  $x$ .

It is convenient to use a voltage regulator tube as the constant voltage element. Neon tubes are not suitable for this purpose because of their poor stability.

The parameters for the FEU-19 circuit can be easily computed from the formulas

$$R = \frac{R_2}{R_1 + R_2} = \frac{16-x}{15} \frac{U_2 - U_1}{V_2 - V_1}, \quad (3)$$

$$U_R = U_{R0} \frac{16-x}{15} - U_2 + (V_2 - U_{R0}) \frac{U_2 - U_1}{V_2 - V_1}, \quad (4)$$

where  $U_1$  and  $U_2$  are the voltages between the  $x$ -th and the  $(x-1)$ -th dynodes with  $V$  equal to  $V_1$  and  $V_2$  respectively;  $U_R$  is the voltage taken from the voltage regulator;  $U_{R0}$  is the total voltage on the voltage stabilizer.

These formulas apply in the case in which the curves (cf. Fig. 4) represent the potential differences between the  $x$ -th and  $(x-1)$ -th dynodes. The values of  $U_1$  and  $U_2$  can be obtained from curves similar to those given in Fig. 4.

The theoretical analysis and experimental work indicate that good gain stabilization in the FEU-19 can be achieved with the following values of the circuit parameters:

$R_1 = 1.2$ megohm	$R_1 = 1.1$ megohm
$r_1 = 2.2$ megohm	$r_1 = 2.2$ megohm
$R_2 = 560$ kohm	$R_2 = 720$ kohm
$r_2 = 220$ kohm	$r_2 = 220$ kohm
$U_{R0} = 300$ v (two VR-150)	$U_{R0} = 150$ v (VR-150)
$U_R = 244$ v	$U_R = 118$ v.

When the voltage in the circuit varies by + 10 or -15%, the total change in gain of the FEU-19 is  $\pm 1\%$ .

The relation between the gain of the FEU-19 and  $V$  in this stabilization circuit is shown in Fig. 6.

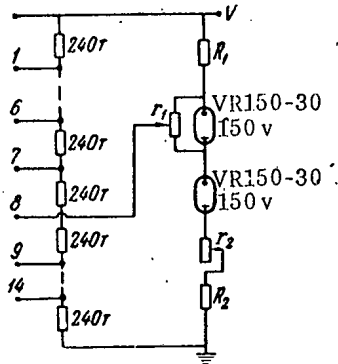


Fig. 5. Stabilization circuit for the FEU-19.

According to the instructions from the manufacturing plant the VR 150-30 tubes used as voltage regulators should be operated at currents of 5-30 ma. K. S. Kalugin has shown that gas tubes can also provide good voltage stabilization when  $I_{reg} = 1$  ma. This value was used in calculating the circuit parameters although it is not necessary that the VR 150-30 tube be used this way.

The fact that the circuit has two variable resistances,  $r_1$  and  $r_2$ , makes it possible to adjust the FEU-19 stabilization at different values of the gain.

The slope of the linear sections of the curves in Fig. 4 is established by  $r_2$ . The other resistance  $r_1$  changes the total gain of the multiplier.

The circuit can be modified for operation with any photomultiplier of the FEU-19 type. In this case  $R$  is varied from tube to tube within the limits 0.400 to 0.425 (as shown by our experience with 14 FEU-19 tubes). This change is completely provided for when  $r_2 = 220$  kohms.

Since the slopes of the linear sections of the curves in Fig. 4 are almost identical, the correct setting of the arm can be found in one trial: it is chosen in such a way that the signal at the output does not change when the voltage  $V$  on the FEU changes within the required limits. After this setting is found the gain is adjusted using  $r_1$ .

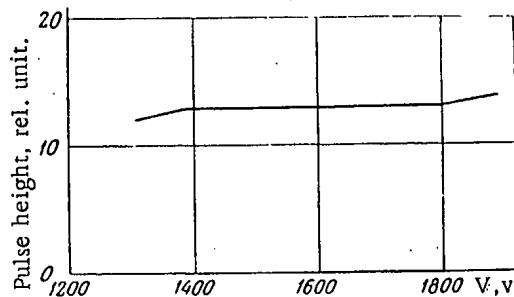


Fig. 6. Gain of the FEU-19 as a function of voltage with the stabilization circuit in use.

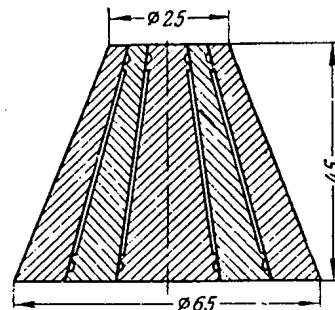


Fig. 7. Section of light-pipe.

The considerations given above also apply to other types of photomultipliers with similar dynode configurations. Thus, Shishkina has shown that this power supply arrangement is suitable for the FEU-25, with 9 multiplier dynodes. The use of a smoothing dynode (any dynode from No. 2 to No. 7) provides constant gain when  $V$  varies from 400 to 500 volts if the following circuit parameters are used (Fig. 5):

$$\begin{aligned} R_1 &= 630 \text{ kohm}, & U_R &= 23 \text{ v}; \\ \gamma_1 &= 2.2 \text{ megohm}, & U_{R0} &= 150 \text{ v}; \\ R_2 &= 700 \text{ kohm}, & r_2 &= 220 \text{ kohm}. \end{aligned}$$

When scintillation counters are used in dosimetry instruments difficulties arise because of the small dimensions of the sensitive area of the photocathode.

The use of photomultipliers with large photocathodes improves the situation but we must take account of the fact that these tubes have large dark currents and that their use leads to an increase in the size of an instrument. Hence, it is necessary to consider the use of a light-pipe to provide uniform light collection between the large surface and a small surface, without appreciable loss.

The simplest solution to this problem is a light-pipe in the form of a truncated cone. A light-pipe of this type, made from organic glass, is used in a scintillation attachment (type P-3492-2) issued by a domestic manufacturer.

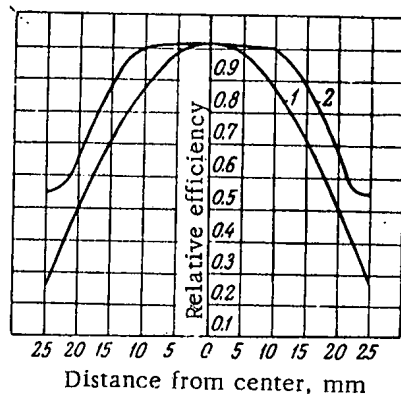


Fig. 8. Efficiency of various points of a light-pipe with a large base.

1) light-pipe in the P-349-2 attachment; 2) light-pipe shown in Fig. 7.

We have constructed a light pipe consisting of an assembly of hollow cones of organic glass, one nesting inside the other (Fig. 7).

A comparison of the relative efficiency of a light pipe using this construction and the light pipe in the scintillation attachment is given in Fig. 8.\* It is apparent from the curve that the sectional light pipe yields a somewhat more uniform sensitivity area distribution. If the area of the large base of the cone is increased a still more favorable ratio is obtained.

Because of reflection losses and absorption in the organic glass the pulse amplitudes are reduced as much as 50%. However, in detecting  $\alpha$ -radiation or thermal neutrons, which produce strong scintillations, this absorption is not important. It may, however, be much more important in measurements of other types of radiation.

The authors wish to express their gratitude to R. D. Vasilev, K. S. Kalugin, V. V. Markelov, L. N. Uspensky and V. A. Shishkina for advice and help in this work.

Received July 5, 1956.

#### LITERATURE CITED

- [1] N. O. Chechik, S. M. Fainshtein and T. M. Lifshits, *Electron Multipliers*, State Tech. Press, (1954) p. 182.
- [2] G. L. Gvernsey, G. R. Mott, B. K. Nelson and A. R. Roberts, *Rev. Sci. Instr.* 23, 476 (1952).
- [3] *Methods of Experimental Electronics*. Collection, IL (1949) pp. 85-87.
- [4] G. Birks, *Scintillation Counters*, IL (1955). [Russian Translation]
- [5] V. A. Shishkina. Candidate's Thesis, MIFI (1956).

\* The measurements were carried out without a reflector; hence the results obtained for the manufactured light pipe differ from the standard specifications.

## SCIENTIFIC AND TECHNICAL NEWS

### THE USE OF RADIOACTIVE AND STABLE ISOTOPES AND OF RADIATION IN THE NATIONAL ECONOMY AND FOR SCIENTIFIC PURPOSES IN THE USSR

During April 1957 at the M. V. Lomonosov Moscow State University an All-Union Scientific Technological Conference was held on the use of radioactive isotopes and radiation in the national economy and in science. The conference was attended by more than 3000 representatives of 1016 scientific institutions and industrial enterprises of the Soviet Union and by 94 scientists from foreign countries.

A total of 444 reports were heard at the conference and were discussed by about 500 delegates. The conference provided both a review of work involving isotopes and radiation for industrial and scientific purposes and an exposition and discussion of new and promising directions and methods of application of such isotopes and radiation.

The conference was divided into four sections: 1) technological sciences and the industrial utilization of isotopes; 2) chemistry; 3) biology, medicine and agriculture; 4) the production of isotopes and the design of gamma-irradiation facilities.

The plenary sessions of the conference were devoted to various aspects of the production of radioactive isotopes (Yu. S. Frolov, V. V. Bochkarev and E. E. Kulish) and their use in the prospecting and development of mineral resources (V. N. Dakhnov), in the control and automatization of technological processes (N. N. Shumilovskiy and L. V. Meltser), in agriculture (V. M. Klechkovsky) and clinical medicine (A. V. Kozlova). A. V. Lebedinsky reported on the sources and peculiar effects on the organism of small doses of ionizing radiation.

In view of the impossibility of mentioning here even briefly all of the papers that were presented we shall confine ourselves to only a small portion.

At the chemical sessions 40 reports were heard which touched on the following fields: 1) the study of the mechanism and kinetics of the most important chemical reactions; 2) radiation chemistry; 3) analytic chemistry and production controls; 4) radiochemistry and 5) chemical methods of producing isotopes.

In all of the investigated cases of oxygen isotope exchange in inorganic and organic acids and their salts, as well as in aldehydes and ketones, it was shown that oxygen exchange takes place through reversible hydration and the intermediate formation of the ortho form. A similar mechanism exists in sulfur exchange between  $H_2S^{35}$  and compounds containing the sulfide group  $-SH$ . In polysulfides and polythionates sulfur isotope exchange is accompanied by breaking of the  $S^{II}-S^{II}$  bond and preservation of the  $S^{II}-C$  and  $S^{II}-S^{VI}$  bonds. The valence of the sulfur is preserved. The study of sulfur isotope exchange in compounds containing the  $C=S$  group, such as 2-mercaptobenzthiazole, showed that exchange with elementary sulfur in  $C=S$  bonds occurs more easily as this bond is more strongly polarized; this is in agreement with the exchange mechanism involving the intermediate compounding of elementary sulfur with the formation of polysulfide chains (A. I. Brodsky, N. A. Vysotskaya, I. I. Kukhtenko, L. L. Strizhak and L. V. Sulima).

For the determination of the types of vulcanized structures a method has been developed which is based on their different capacities for isotope exchange with elementary sulfur and sulfur-containing compounds. A way was found of establishing the relation between the rate of sulfur exchange in vulcanized rubber and such factors as the degree of vulcanization, strain relaxation, fatigue etc. This is of great practical importance for the study of vulcanization processes (B. A. Dogadkin, Z. P. Tarasova, and M. Ya. Kaplunov).

There is great practical value in the utilization of ionizing radiation to accelerate the polymerization of various not easily polymerized monomers such as ethylene. Radiation can be used to polymerize monomers

such as hexafluoropropylene which have not been polymerized by other methods. For monomers in which the radiation yield of free radicals is small it is advantageous to produce the polymerization in solutions, using solvents which supply a large number of radicals that can induce polymerization. Thus, for example, in methyl alcohol, acetone, cyclohexane and n-heptane solutions the yields of solid polyethylene are 40-50 times greater than from the polymerization of ethylene in the gaseous phase under similar conditions. There are also very promising methods of emulsive polymerization which are very fast and produce polymers of high molecular weight (S. S. Medvedev).

Investigations of radiation-chemical transformations of high molecular compounds show that irradiation often gives polymers new and valuable properties. The most promising development in this field is the radiation vulcanization of polyethylene, various rubbers etc. Rubbers produced by radiation vulcanization show improved properties such as higher thermal stability, dielectric constant, wear-resistance etc. (V. L. Karpov, Yu. S. Lazurkin and A. S. Kuzminsky).

For the purpose of determining the effect of dispersed petroliferous rocks on the formation of gases from petroleum a determination was made of the relative amounts of hydrogen and methane that are formed when  $\text{Co}^{60}$  gamma rays are used to irradiate pentane adsorbed on dispersed silica gel, aluminum oxide, iron oxide etc. It was found that iron oxide has considerable effect in increasing the  $\text{CH}_4$  : H ratio. This enables us to explain the relative absence of hydrogen in petroleum gas and supports the hypothesis that petroleum has been formed from complex organic substances by radiation from uranium (A. O. Allen, USA).

By utilizing a photonuclear ( $\gamma, n$ ) reaction it is possible to determine the oxygen content of various metals and semiconductors. The sensitivity of the method is as much as 1%. For 20-25 Mev bremsstrahlung the sensitivity of the method can be brought to 0.01% (A. Kh. Breger).

The use of radioactive isotopes of various elements in spectral analysis has furthered the development of a method of separate investigation of evaporation and excitation of elementary atoms in a source, as well as the experimental study of the effect of various factors which characterize a substance and the exciting source during both processes. The use of stable isotopes has opened a path to the development of a more highly perfected method of spectral analysis marked by greater accuracy and universality. This is called the method of isotopic additions. It is based on two phenomena, the great similarity of the physical and chemical properties of isotopes and the isotope shift in atomic spectra (E. E. Vainshtein).

There is great practical value in a method of measuring the moisture penetrability of synthetic materials such as polyethylene, polytrichlorethylene, rubber, etc. by using water that is tagged with tritium. This method has permitted 1) reduction of the period of the tests from 2-6 weeks to 2-10 days; 2) an approximately tenfold increase in accuracy (E. E. Finkel).

A new radioelectrochromatographic method can be used successfully to analyze some solutions containing radioactive products of uranium fission. This method is based on the ability of ions to move along a paper strip moistened with an electrolyte when acted upon by an electric field. The method does not require isotope carriers and can function with solutions of low radioactivity ( $10^{-3}$  microcuries per gram) (P. V. Zimakov, A. G. Bykov and I. A. Usacheva).

An electrochemical method based on radioactivity has permitted the study of a number of chemical properties of some elements such as Po and of their compounds (valence, solubility etc.) at concentrations of  $10^{-7}$  -  $10^{-14}$  moles per liter. In the case of radioactive silver it was shown that the character of binary systems can be determined from the electrode potentials (D. M. Ziv and G. S. Sinitsyna).

A method has been suggested for synthesizing some very important basic organic compounds tagged with  $\text{C}^{14}$ . The yield of all tagged compounds from the original substance is  $\sim 70\%$ . The specific radioactivity of the synthesized compounds is  $\sim 10^{-6}$  -  $10^{-7}$  pulses per minute per millimole.

The utilization of isotopes and radiation in biology, medicine and agriculture presents two principle aspects at present: 1) the action of radiation on the living organism for the purpose of producing directed changes in plants and animals and the curing of human illnesses and 2) the utilization of isotopes as tagged atoms in the study of vital processes.

The basis of the first line of investigation is a relatively new branch of science - radiobiology.

The mechanism of the biological effect of radiation has attracted additional attention recently also because in connection with the use of atomic energy in industry and science and especially the testing of nuclear weapons the natural radioactive background has been increased. And although the increase of the background is still not great it is possible to determine changes in the human environment and to study the effect of small doses on the human organism (A. V. Lebedinsky).

An understanding of processes in the living organism which are induced by ionizing radiation is impossible without an analysis of the biological mechanism involved. The primary ionization and excitation of molecules in living matter give rise to a chain reaction that is self-accelerating. The existence of such a chain reaction can be judged from a mathematical analysis of the relation between the effect of the radiation and the dosage (B. N. Tarusov).

Primary ionization and excitation have their greatest effect on the high polymers of the living organism, especially the nucleoproteids, by disrupting their ordered structure (A. M. Kuzin).

Special experiments have made it possible to some extent to determine the direct physico-chemical mechanisms which are at the basis of radiation effects such as hemolysis of the erythrocytes (G. M. Frank).

With regard to changes produced in the organism as a whole by ionizing radiation the attention of the conference was mainly focused on two lines of research, the change of the internal fluids and the reaction of the nervous system to radiation.

An investigation of the biological properties of blood in irradiated animals established the existence of biologically active substances which have different effects on the functions of the organism at different periods after irradiation (P. D. Gorizontov).

Among such biologically active substances is histamine, which is found in higher concentrations in the tissues after irradiation (E. I. Krichevskaya).

Impairment of the penetrability of the barriers between the blood and the tissues results in a number of changes of the composition and properties of the tissue fluids, thus also affecting the functions of the organs (L. S. Shtern, M. M. Gromakovskaya and S. Ya. Rapoport).

In the treatment of radiation sickness it is important to combat increased hemophilia. It has been shown that increased hemophilia results from a reduction of the thromboplastic activity of the blood and that shielding of the liver during irradiation aids the survival of animals who thus maintain thromboplastic activity at a relatively high level (Kudryashov et al.). A small part is also played in this process by the change in permeability and disturbance of hemodynamics (N. V. Butom et al.).

In radiation sickness there is disturbance of the normal nervous regulation of the functioning of internal organs (I. T. Kurtsin). The degree to which the nervous system is affected depends on the type of nervous action of the irradiated animal (L. I. Kotlyarevsky et al.). Disruption of the activity of the central nervous system results from the change of oxidizing processes in the brain tissue (A. D. Snezhko) and of electrical activity of the cerebrum (N. A. Anadzhhalova); direct morphological changes have also been observed as a result of sub-lethal doses (M. M. Aleksandrovskaia).

Important practical results have been obtained from an investigation of the course of various infectious diseases in irradiated animals. It has been shown that resistance to grippe (O. S. Peterson and V. P. Emaikina), pneumonia (P. N. Kiselev et al.) and anaerobic infections (R. V. Petrov) is considerably reduced, whereas polio and yellow fever have the same course in irradiated and non-irradiated organisms (O. S. Peterson).

Experiments in the therapy of radiation sickness have produced nothing essentially new. There is some interest in experiments with choline, which in prolonged prophylactic treatment gave only 2% mortality after doses of 1000 r (M. L. Eleazarova).

In clinical medicine for the diagnosis and treatment of patients radioactive isotopes have been used in the Soviet Union for more than 8 years (A. V. Kozlova). For diagnosis  $I^{131}$  and  $Na^{24}$  are most extensively used. The speed of the entrance of radioactive iodine into the thyroid gland permits accurate diagnosis of the various disturbances of its functioning. The same test can successfully be used for the diagnosis of other diseases (K. G. Nikulin and L. N. Kazakova).



$\text{Na}^{24}$  has been used to investigate the rate of blood flow and the volume of circulating blood. The determination of the speed of blood flow in the tissues has revealed the state of cardiovascular decompensation in those stages where this was not possible by other means (A. L. Syrkin).

$\text{I}^{131}$  has been used with great success for the curing of thyroid diseases. According to A. V. Kozlova a single treatment with  $\text{I}^{131}$  results in a cure in 81-90% of the cases.

There are some prospects, especially in the treatment of malignant neoplasms in the female genital region, that colloidal radioactive gold ( $\text{Au}^{198}$ ) will be useful (L. A. Novikova et al.).

An important problem in the use of radioactive isotopes for diagnosis and treatment is safety of the patient during treatment. In the Soviet Union only the short-lived isotopes  $\text{Na}^{24}$ ,  $\text{I}^{131}$  and sometimes  $\text{P}^{32}$  are used (A. V. Kozlova).

There are two principal directions in the application of radioactive isotopes to agriculture.

First is the use of tagged atoms for the study of the most important biochemical processes.

Radioactive  $\text{C}^{14}$  has played a decisive part in investigations of photosynthesis; at the present time the study of photosynthesis is proceeding principally along the lines of a detailed analysis of intermediate products and the investigation of their subsequent history (N. G. Doman, E. A. Boichenko and N. I. Zakharova).

The stable isotope  $\text{N}^{15}$  has been used to establish that atmospheric nitrogen is not fixed by bacteria living on the nodules of leguminous plants but by the nodules themselves (F. V. Turchin et al.). The isotopes  $\text{P}^{32}$  and  $\text{Ca}^{45}$  have been used in an investigation of the effect of atmospheric electricity on the rate of flow of cations and ions from the soil into plants. It was shown that in the presence of a positive atmospheric electric charge the quantity of transferred phosphorus increases up to 220% above the normal rate while the flow of calcium is reduced as much as 45% (Z. I. Zhurbitsky).

Radioactive isotopes, especially  $\text{P}^{32}$ , have been used to solve a number of practical agricultural problems such as the time and place to fertilize the soil, the most favorable physical conditions for fertilizing etc. Thus, for example, a reduction of the size of superphosphate granules permitted a reduction of the cost of fertilizer without impairing its efficiency (P. A. Dmitrienko).

A second line of research has been concerned with the improvement of harvests by the use of radioactive fertilizers. At present no clear results have been obtained; however, any increase of radioactivity in plants, which must result from radioactivity in fertilizers, is undesirable in so far as it may affect human health. Radioactive substances in plants can enter the human organism either directly through foods or through milk and meat (V. M. Klechkovsky).

A number of reports were concerned with the method of preparing and separating radioactive isotopes and the construction of powerful gamma radiation facilities for radiation-chemical, biological and other studies.

Among the facilities for radiation-chemical studies there is the very interesting K-20,000 developed at the Karpov Institute (A. Kh. Breger et al.). This facility has a source with a strength of 20,000 grams equivalent of radium that enables us to irradiate 0.5 liters at the rate of 1000 r/sec and 100 liters at about 100 r/sec. The control of the facility is completely automatic, thus eliminating the possibility of affecting the operating personnel.

The construction of powerful gamma-ray sources opens broad possibilities for irradiation of foods and agricultural products as a method of sterilization. E. S. Pertsovsky et al., described a semi-industrial experimental facility with a 32,000 radium gram-equivalent source which can sterilize 450 kg of grain per hour. There was also a discussion of the possibility of utilizing uranium fission fragments in the construction of industrial irradiators.

The 180 reports at the section of technical sciences and industrial utilization of isotopes were heard in subsections.

The reports at the subsection on metallurgy and metallography were grouped as follows: the theory and practice of ferrous metallurgy (blast-furnace and open-hearth smelting), nonferrous and rare metals, diffusion in metals and its practical use, the effect of radiation on metals.

Among the more interesting papers on these subjects we may mention the following: the determination of the thermodynamic activity of sulfur in the systems Fe-S-C, Fe-S-Si and Fe-S-P (V. K. Zhuravlev and A. A. Zhukhovitsky), providing a new treatment of solutions of metalloids in liquid iron; the obtaining of new data regarding the motion of materials of furnace charges and the deterioration of refractory linings (I. P. Bardin, P. L. Gruzin and S. V. Zemsky); a study of the melting of ore and limestone in 380 ton furnaces of the Magnitogorsky Metallurgical Combine (V. F. Aganov, A. P. Varshavsky and A. I. Dyakonov) with acceleration of the melting; a study of the distribution of sulfur impurities in the crystallization of steel (V. M. Tageev and Yu. D. Smirnov) and the improvement of the distribution by the addition of cerium, lanthanum and zirconium.

In ferrous metallurgical plants it is possible that considerable numbers of workers will come into contact with radioactive substances. To insure safety a hygienical survey of the working conditions is made (N. I. Volkova) and special radiation laboratories are established.

An investigation of the behavior of impurities in the production of ammonium molybdate and paratungstate (K. T. Koneva and S. L. Savalsky) was the basis of technological schemes for the production of very pure  $WO_3$  and  $MoO_3$ .

From among the large number of investigations of diffusion in metals we may choose a very important theoretical report concerning the effect of hydrostatic pressure on self-diffusion in polycrystalline zinc (S. D. Gertsriken and M. P. Pryanishnikov). These workers showed that when the pressure is increased to 80 atmospheres the self-diffusion coefficient in the range 270-380°C increases by the factor 1.5-2.5. An investigation of the diffusion, solubility and segregation of silver, iron, tin and antimony in germanium (A. A. Bugai, V. N. Vasilevskaya, V. E. Kosenko and E. G. Miselyuk) led to a determination of the limit of solubility of these admixtures at the crystallization point.

Tritium was used to determine the amount of hydrogen in metals (A. I. Chizhikov and V. K. Boyarinkov). An investigation of the influence of neutron irradiation on martensite transformation (O. P. Maksimova and A. I. Zakharov) is of interest as a method of investigating the nature of phase transformations.

The work of the subsection on machine design, the control of technological processes and the measurement and dosimetry of nuclear radiation showed that considerable progress has been made in this field during recent years.

In machine design radioactive isotopes are being used mainly for the study of wear of machine parts and instruments (V. I. Dikushin). This considerably reduces the time required by other methods of study and increases accuracy, as was shown in a study of metal cutting (N. F. Kazakov). Wear is accompanied by the transfer of metal (G. M. Zamoruev and Ya. N. Levin) from one rubbing part to another, and depends on the stresses at areas of contact, the friction path, lubrication etc; the degree of wear varies with different conditions. It was established that the quality of lubricating oils (V. E. Zavel'sky and K. S. Ramaiya) and of special additives (Yu. S. Zaslavsky, G. I. Shor and I. A. Morozova) affects the wear of engine cylinders and pistons.

As technological processes in industry become more complicated and are automatized they must be continuously controlled and regulated without introducing internally any sensitive devices that will make contact with the fluids which are to be controlled. This problem can be solved by using nuclear radiation for the measurement of thermal power parameters (G. G. Jordan and K. S. Furman). Among the numerous control instruments extensive use has been made of gamma level gauges (V. K. Latyshev, V. V. Landin, S. V. Medvedev, Yu. S. Pliskin, L. K. Tatochenko and V. I. Shul'ga) different forms of which have been used to measure and regulate the level of liquid metal etc. Excellent results are obtained from the use of radioactive isotopes in safety technology (I. S. Reizen and V. S. Medvedeva) for the construction of necessary emergency switches and protection from static electricity. This is also important for the textile industry in connection with synthetic fibers (P. L. Polotin, L. V. Mel'tser and N. I. Panyukov) where during the warping of caprone static charges can be successfully removed by soft  $S^{35}$  beta rays.

Control of the soil content in a water-and-soil mixture in dredging equipment by a gamma-ray densimeter (E. T. Kardash) has been practised by industry for several years, and new devices of this type have now been developed.

Automatic control of the weight of a moving paper strip (E. A. Nekhaevsky) has resulted in the saving of approximately 660 thousand rubles annually from a single paper-making machine by eliminating paper of improper weight.

Radioactive isotopes have been used to locate leaks in underground gas mains (V. I. Kuznetsov) and the separations between different petroleum products pumped successively through pipelines (B. Z. Votlokhin, A. Z. Dorogochinsky and N. P. Melnikova).

A large number of enterprises in the Soviet Union utilize gamma-ray inspection of materials. Thick steel parts are inspected and continuous control is effected by a new method of betatron flaw detection employing scintillation counters (I. G. Fakidov, A. A. Samokhvalov, N. I. Davidenko, M. D. Avramenko). Welded and cast parts are inspected by the use of  $\text{Co}^{60}$  and even more conveniently and efficiently with isotopes which yield soft radiation ( $\text{Cs}^{137}$ ,  $\text{Ir}^{192}$  and  $\text{Se}^{75}$ ). The seams of welded pipes and thick-walled parts are penetrated by using a special facility with  $\text{Tm}^{170}$ \* (S. V. Rumyantsev) which has increased sensitivity by a factor of 2 to 4. There has been an improvement of pocket radiation gages and dosimeters for gamma and hard beta radiation used in geological and field work (G. R. Golbek and A. N. Vyalshin).

There has been considerable success with methods of increasing sensitivity and with new methods of measuring radioactivity. A diffusion chamber permits the determination of alpha activity in gases of the order of  $10^{-13}$  curies per liter (V. K. Lyapidevsky). It has been shown experimentally that there is a possibility of photocaloric beta dosimetry of doses of the order of  $10^{-7}$  -  $10^{-8}$  curies per millileter and even smaller doses, and calculations have shown that a galvanic method of measuring beta activity is possible (M. F. Lantratov, V. E. Manoilov and O. A. Myazdrikov). For the recording of radioactive radiation a method has been developed of preparing transparent scintillating plastics using terphenyl with admixtures of 1,4-di-[2-(5-phenyloxazole)] benzene (N. A. Adrova, M. M. Koton and Yu. N. Panov).

The mining section discussed the principal trends in the utilization of the radioisotopes which are used most widely in the USSR:

- a) Neutron methods of logging based on the study of slowing-down and succeeding capture of neutrons by rocks;
- b) The study of scattering by rocks of gamma radiation from a source lowered into a bore-hole;
- c) The measurement of gamma radiation from radioactive materials introduced into the substance under investigation (V. N. Dakhnov).

These methods have been developed and put into extensive practical use by the petroleum industry for the prospecting and exploitation of oil and gas deposits. Radioactive methods have considerably increased the efficiency of coreless drilling. More exact logs have been obtained for wells through highly resistant rock and in drilling in highly mineralized liquids. In some regions of the USSR radiometrical methods have been used in conjunction with electrical measurements for a clear delineation of the gas-bearing layers in the logs.

In the working of oil deposits with flooding it is very important to develop neutron methods of distinguishing oil-bearing layers from water-bearing layers, based on the fact that the cross section of chlorine for neutron capture (32 barns) is considerably larger than the capture cross sections of other elements in the rocks of oil deposits (0.0002-0.5 barns). These methods make it possible to distinguish the water-bearing from the oil-bearing portions of rock layers and to determine the progress of water during exploitation (A. I. Kolin and V. N. Dakhnov). For water with a relatively small quantity of chlorine methods have been developed for separating oil-bearing and water-bearing rocks by sodium activation (F. A. Alekseev). Considerable progress has been made in the development and industrial testing of a method that uses scattered radiation for the logging of coal bore-holes. The distinguishing of coal-bearing layers by study of scattered gamma radiation from a source containing  $\text{Co}^{60}$  provides a determination of coal-bearing layers in bore-hole logs which is much more accurate than that attained by other methods (Yu. P. Bulashevich, A. P. Fisenko, I. N. Senko-Bulatny and E. P. Davidenko).

In recent years radioactive methods have been found to be effective in the logging of water borings. The measured intensities of natural and neutron gamma radiation can not only be used to increase the accuracy of distinguishing water-bearing rocks but also in some instances to provide an estimate of probable productivity (V. A. Ryapolova).

In addition to the development and utilization of various radiometric methods for the prospecting and exploitation of different kinds of natural resources considerable attention has been devoted to the construction of radiometric logging devices. Among the recently developed instruments one must mention oil-well equipment

\*[As in original; probably  $\text{Tm}^{170}$  — Translator's note.]

which includes proportional neutron counters for the determination of thermal neutron densities; instruments for measurements in wells up to temperatures of 150°C; logging equipment with scintillation counters; a two-channel instrument with a boron envelope for determining the position of the oil-water surface and for neutron gamma-ray sounding of rocks (V. M. Zaporozhets, Ya. Ya. Gorsky, V. P. Mikhailovsky, Yu. I. Sitnitsky and D. F. Bespalov).

The principal direction in the improvement of radiometric apparatus was determined by the conference as the development of small neutron generators for bore-holes.

The conference also noted the very inadequate utilization of possible radiometric methods for reconnaissance and prospecting of deposits of boron, manganese, mercury, aluminum, wolfram, cesium and certain lanthanides, for which these methods may be effective.

Those who attended the conference saw displays of dosimetric and radiometric apparatus and became acquainted with the technical literature concerning the utilization of isotopes, as well as making a trip to an atomic energy power plant.

G. A. Nekrasova, S. V. Levinsky, O. E. Orlov and  
M. M. Konstantinov

AT THE ATOMIC PAVILION OF THE ALL-UNION INDUSTRIAL EXPOSITION  
(SECTION ON THE UTILIZATION OF RADIOACTIVE ISOTOPES IN INDUSTRY)

Modern industrial production imposes high requirements on the instruments for the control and regulation of technological processes because of the great increase in the speed of such processes, the high temperatures and pressures which prevail, the extensive utilization of vacuum techniques, etc.

Instruments and apparatus which meet these requirements are displayed in the section on the Utilization of Radioactive Isotopes in Industry.

One of the booths demonstrates the utilization of radioactive isotopes in blast-furnace operations by means of diagrams and charts; these include the effects of different factors on the movement of the furnace charge, gas velocity in the blast furnace and control of lining and well erosion. On display are a device for determining gas velocity and the DR-1 instrument for radiometric measurements of the motion of materials in the furnace charge (Fig. 1).

This section also contains a display of instruments for non-contact measurements of densities and concentrations: a PZhR liquid densimeter and a gamma-ray ground gage. There are photographs and diagrams of instruments designed for such purposes: a PZhR-2 liquid densimeter with modulated radioactivity and a scintillation counter, and an RKM radioactive concentration meter.

The displayed gamma-ray ground gages are used to equip dredges, to provide continuous remote control of the ground composition of the slurry and thus maintain optimum operating procedures. During 1956 the dredges of the River Ministry alone used 36 of these gages; considerable economy resulted.

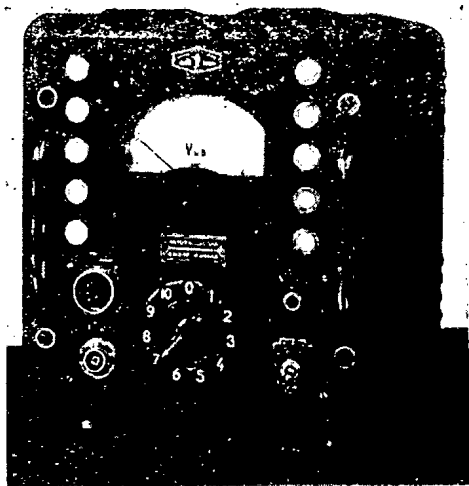


Fig. 1. VPU unit of a ten-channel DR-1 remote-control radiation gage.

There is a display of instruments, circuits (with photographs under industrial conditions) for non-contact measurements of thickness and weight: ITU-495 gages for the measurement of the thickness of rolled steel, an ITP-476 meter for measuring the thickness of tin plating and an R-3 wall-thickness gage (Fig. 2).

The pavilion contains a display of other operating instruments designed for the solution of similar problems. One of these is a non-contact weight gage (BIV) for material passing through a machine and also for materials applied to fabrics (Fig. 3). Another instrument measures and records irregularities in textile products, using a differential measuring scheme and providing automatic calculation of a variation index.

All of these devices provide the possibility of accelerating processes and reducing spoilage. Thus the use of devices for the control of the thickness of rolled stock at the Leningrad steel rolling plant, the Zaporozhstal plant and others has, according to

incomplete data, cut in half the amount of metal rejection because of improper thickness and has reduced the stoppage time of machines to one-tenth.

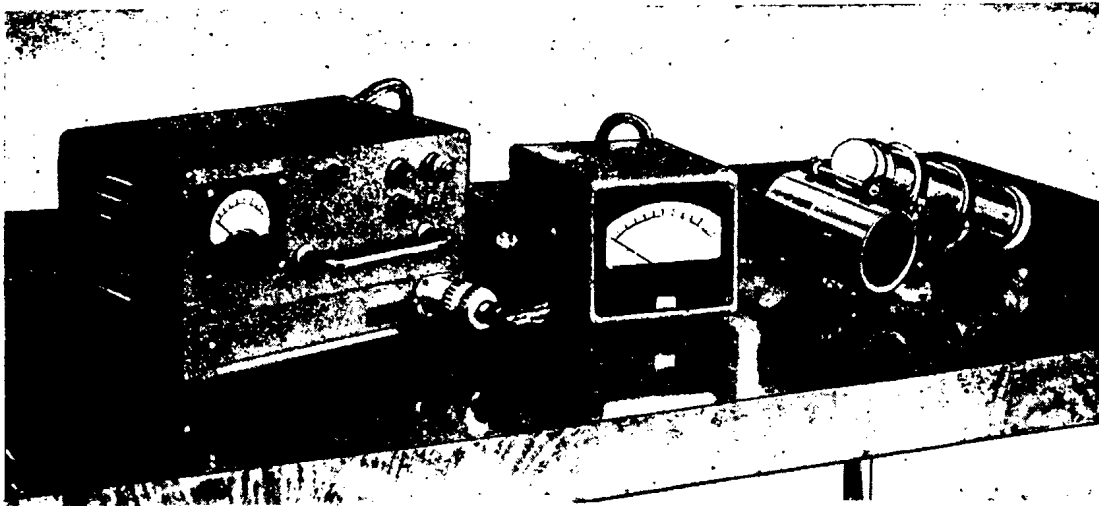


Fig. 2. R-3 wall thickness gage.

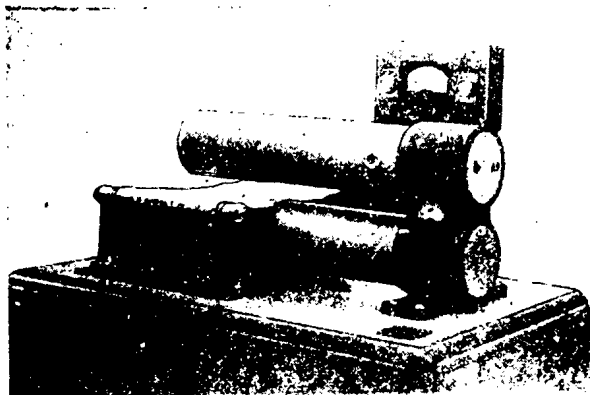


Fig. 3. BIV non-contact weight gage.

Level gages utilizing radioactive emissions find application in the control and automatization of technological processes involving aggressive, toxic, viscous, friable and boiling substances as well as processes which take place at high pressures and temperatures.

One section of the pavilion displays various types of level gages; the UR-4 gage with a tracking system; the IU-3, RU-2 and IU-2a radioactive liquid metal level gage, regulator and indicator; a RIU-3 float-type radioactive level indicator; and the scheme of a radioactive level indicator for drum boilers.

In the petroleum industry radioactive isotopes and radiation are employed to determine the location of water-bearing and oil-bearing layers and the oil-water surface in wells with steel cas-

ings; in such wells to determine the layers which are saturated with gas or liquid (oil and water); to determine the gas-liquid surface; to determine the hydraulic ruptured zone of a layer and to control the technological condition of wells etc. A display shows one of the means of radiometric control of the successive flow of petroleum products in pipe lines and the radiometric regulation of oil refineries. An adjacent display shows sectional apparatus for radioactive logging (RARK, NGGK-55, LS-2 and NNK-57 models).

The pavilion also contains various types of apparatus, such as the GUP-Co-0,5-1 (Fig. 4), GUP-Co-5-1 (Fig. 5) etc., for flaw inspection of industrial products.

The application of gamma radiation to the control of the quality of industrial products has been one of the most effective forms of the utilization of nuclear radiation. At the present time various factories in the Soviet Union are using more than 1000 gamma-ray flaw detectors.

The demonstrated MIR-2 ionization pressure gage, which is based on the ionization of gases by radioactivity, permits pressure measurements from 0.1 micron to 1000 mm Hg.

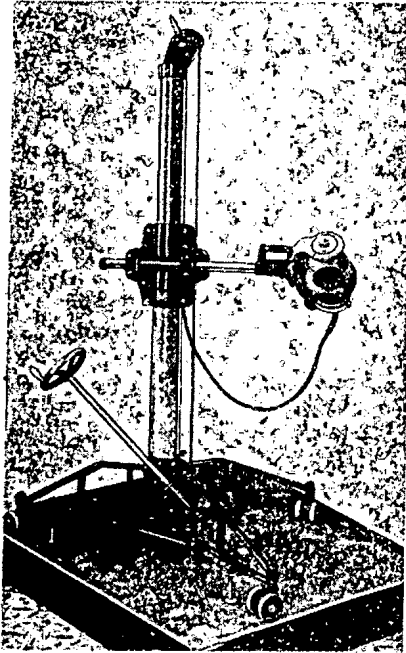


Fig. 4. GUP-Co-0.5-1 apparatus for gamma-ray flaw detection.

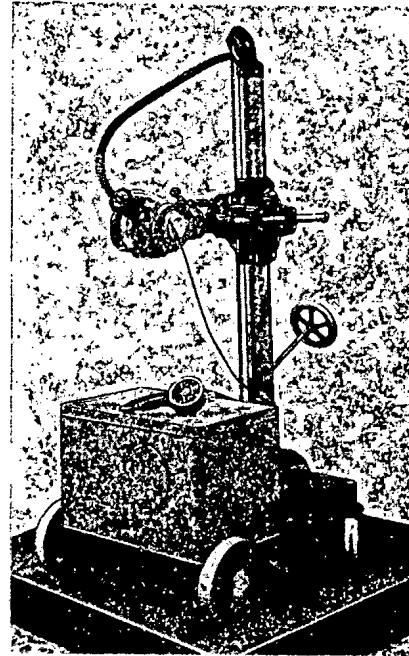


Fig. 5. GUP-Co-5-1 apparatus for gamma-ray flaw detection.

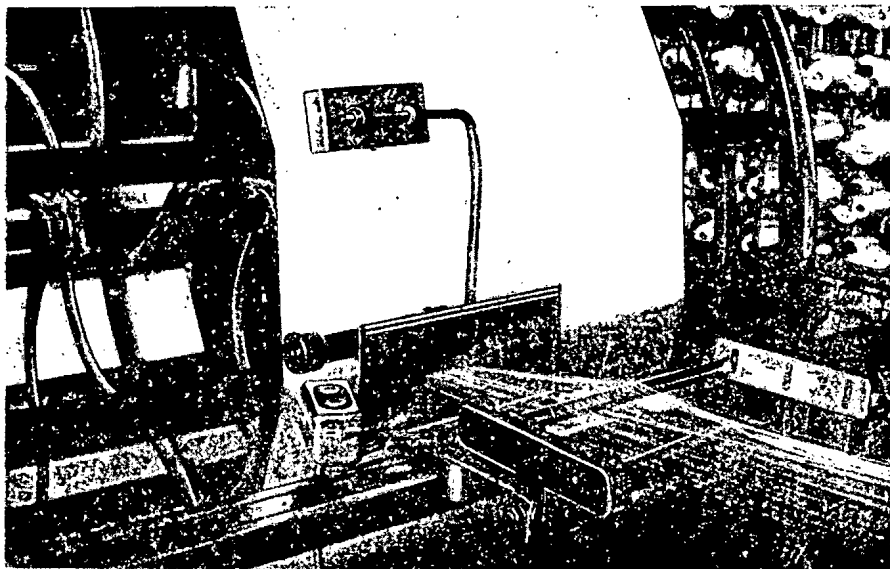


Fig. 6. Device for removing static electricity from a warp machine.

A functioning model demonstrates the use of radioactivity for removing static electric charges; this is very important in the branches of industry where the rapid motion of dielectric materials leads to an accumulation of static charges (the moving-picture film, silk, rubber, glass industries etc.).

The use of this method to neutralize static charges at the Shcherbakov Textile Combine (Fig. 6) has made it possible to increase the speed of a warp machine by a factor of four.

Some exhibits show how radiation is used in relay devices. The functioning devices are: a device for the marking of rolled steel stock, a radioactive counter (RSP-7) of objects on a conveyor, a radioactive heat regulator,

a signalling frequency regulator, a signalling device for storage battery voltage in telephone stations etc.

All of the exhibits at the exposition are evidence of the great attention devoted in the Soviet Union to the peaceful applications of atomic energy.

S. Perepletchikov

### NEW DATA ON NEUTRON CROSS SECTIONS

The Brookhaven National Laboratory(USA) recently issued a supplement [1] to its earlier compilation "Neutron Cross Sections" [2].

The supplement contains new data on neutron cross sections, obtained up to October 1, 1956. The first section is devoted to thermal neutron cross sections. The end of this section contains the best values of the parameters of the fissionable isotopes  $U^{233}$ ,  $U^{235}$  and  $Pu^{239}$  for neutrons with a velocity of 2200 m/sec, which were obtained in several countries, especially the USSR, USA and England. The table contains the absorption cross sections  $\sigma_a$ , the fission cross sections  $\sigma_f$ , their ratios  $\sigma_a/\sigma_f = (1 + \alpha)$ , the number of secondary neutrons per absorbed neutron  $\nu_{eff}$  and the number of secondary neutrons ejected per fission event  $\nu$ . The average values for the world are given, obtained by averaging the data from the different countries, as well as adjusted world values obtained from the average world values through small corrections made for the purpose of adjusting the individual parameters among themselves.

Iso- tope	Constants	Mean world values	Adjusted world values	f
$U^{233}$	$\sigma_a$ barns	$591 \pm 7$	$588 \pm 7$	1.001
	$\sigma_f$ barns	$532 \pm 6$	$532 \pm 6$	1.006
	$1 + \alpha$	$1.100 \pm 0.004$	$1.105 \pm 0.007$	0.995
	$\nu_{eff}$	$2.29 \pm 0.02$	$2.28 \pm 0.02$	1.005
	$\nu$	$2.51 \pm 0.03$	$2.52 \pm 0.03$	1.000
$U^{235}$	$\sigma_a$ barns	$697 \pm 6$	$694 \pm 10$	0.974
	$\sigma_f$ barns	$579 \pm 5$	$582 \pm 10$	0.977
	$1 + \alpha$	$1.189 \pm 0.008$	$1.192 \pm 0.008$	0.997
	$\nu_{eff}$	$2.070 \pm 0.015$	$2.07 \pm 0.02$	1.003
	$\nu$	$2.47 \pm 0.03$	$2.47 \pm 0.03$	1.000
$Pu^{239}$	$\sigma_a$ barns	$1025 \pm 13$	$1025 \pm 13$	1.077
	$\sigma_f$ barns	$740 \pm 9$	$738 \pm 9$	1.052
	$1 + \alpha$	$1.38 \pm 0.02$	$1.39 \pm 0.03$	1.024
	$\nu_{eff}$	$2.085 \pm 0.016$	$2.09 \pm 0.02$	0.976
	$\nu$	$2.91 \pm 0.04$	$2.91 \pm 0.04$	1.000

The last column of the table gives the factors  $f$  by which the corresponding parameters must be multiplied to obtain their values in the Maxwellian neutron spectrum for the mean velocity 2200 m/sec [3].

Other sections give new data on the resonance parameters of nuclei and their cross sections as a function of neutron energy.

After the supplement [1] appeared some papers were published containing still later measurements of neutron cross sections.



K. L. Aitken and his collaborators [4] measured the absorption cross section of reactor neutrons for  $\text{Sm}^{149}$ , obtaining the value  $74\,500 \pm 1100$  barns, which is somewhat higher than the value given in [1].

Leachman and Schmitt [5] measured the fission cross section of  $\text{U}^{238}$  by neutrons of the fission spectrum, obtaining the value  $0.307 \pm 0.005$  barns.

T. S. Green and his collaborators [6] measured the thermal neutron absorption cross section of  $\text{U}^{233}$ , obtaining the value  $578 \pm 17$  barns, which is in agreement with [1].

P. K.

#### LITERATURE CITED

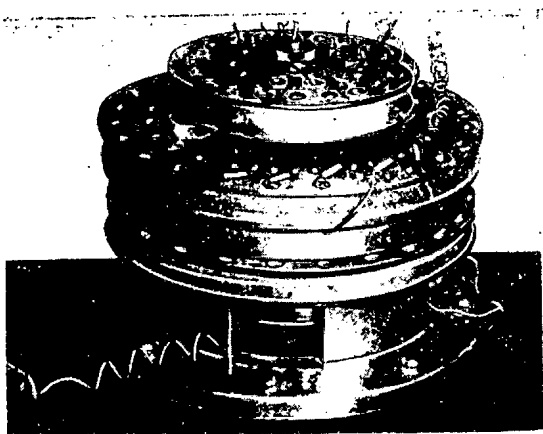
- [1] D. J. Hughes and R. B. Schwartz, Neutron Cross Sections, BNL-325, Suppl. 1, BNL, 1957.
- [2] D. J. Hughes and J. A. Harvey, Neutron Cross Sections, McGraw-Hill Co, 1955.
- [3] D. J. Hughes, Private communication.
- [4] K. L. Aitken, D. J. Littler, E. E. Lockett and G. H. Palmer, J. Nucl. Energy 4, 33 (1957).
- [5] R. B. Leachman and H. W. Schmitt, J. Nucl. Energy 4, 38 (1957).
- [6] T. S. Green, V. G. Small and P. E. Glanville, J. Nucl. Energy 4, 409 (1957).

#### IRON-FREE DOUBLE-FOCUSING $\beta$ SPECTROMETER

The Moscow Institute of Engineering Physics has designed, constructed and tested a magnetic double-focusing  $\beta$  spectrometer with  $\pi\sqrt{2}$  central angle, using a magnetic field excited by iron-free coils.

The magnetic field in the plane of specular symmetry follows the field calculated by P. Pavinsky within 0.2% over a broad range of the radial coordinate. This field effects exact focusing of a broad flat electron beam and first order focusing for a three-dimensional beam. A simple readjustment of the instrument permits us to obtain in the median plane, in addition to the Pavinsky field, other fields which are characterized in the

approximate theory of double focusing by the coefficients  $1/8$ ,  $1/4$  and  $3/8$ . Since the magnetic field is excited by a set of coreless coils, the topography of the field is preserved when the electric current through the coils is changed, and there is strong linear dependence between the field strength and the magnet current. This makes it relatively easy to obtain precise measurements of the electron energy distribution. The radius of the equilibrium orbit of the spectrometer is 100 mm. The maximum angles of divergence of the electron beam in the radial and axial directions are  $\pm 10^\circ$  and  $\pm 6^\circ$ , respectively.



Photograph of the  $\beta$  spectrometer.

The spectrometer can analyze electrons with a maximum energy of 0.3 Mev. The half-width

obtained for the F line of ThB was 0.58% with an 0.6% relative solid angle. The width of the source was 1.5 mm and the width of the rectangular receiving slit was 1.2 mm. The spectrometer is shown in the photograph; its maximum diameter is 400 mm, height 280 mm and weight about 40 kg.

On the basis of the results obtained with the instrument described here we have designed a similar spectrometer with an equilibrium orbit of 200 mm radius, which will analyze electrons up to 3 Mev.

V. F. Baranov

## DEVELOPMENT OF ATOMIC ENERGY IN FRANCE

The difficulties in the French economy occurring at the end of 1956 caused by the events of the Suez Canal once more emphasized the dependence of the economic life of France upon fuel import. This dependence cannot be eliminated by expanding the power generating establishment of France at the expense of the common energy sources. At the present time, coal production has almost attained the maximum: about 50% of the hydroelectric resources are being utilized, and although the supply of oil and natural gas has increased substantially, it is hardly sufficient for fulfilling the demand. For this reason, the French Planning Commission has in view a rapid expansion of atomic energy. It is proposed that the electric power output of atomic power stations be doubled every 3 or 4 years; by 1975 they should comprise 15 to 35% of the power industry [2], depending upon the rate at which the costs of "atomic electricity" are lowered.

Before undertaking the construction of atomic power stations, the French Atomic Energy Commission realized an extensive program of experimental operations. The majority of the experimental operations are being conducted at a research center in Saclay established 8 years ago, and some in Chatillon. Experiments are also being conducted in 38 scientific research organizations of the country which are associated with the Commission by contract. A research center in Grenoble will become active in the near future.

Of the experimental reactors, note should be made of the EL-2, which is designed for research purposes, particularly for radiation testing of materials, and also for producing radioisotopes and a small amount of plutonium. For a long time, this was the only reactor in the world in which compressed gas was used as the coolant. For experimental checking of design calculations on power and industrial reactors, there have been and are being built several zero-power reactors: "Aquila," "Minerva," "Prozerpine" (see Table 1).

Along with the program of research in the area of atomic energy, the Commission is planning the study of problems associated with elementary particles. For this purpose, in Saclay, in addition to four small particle accelerators, there is under construction a synchrotron with a maximum proton energy of 3 Bev, the size and characteristics of which are comparable to the well-known Brookhaven Bevatron. The majority of its subassemblies will be manufactured in France. It will become active at the end of 1957, and will be the largest accelerator in Western Europe (including England).

A characteristic of reactor development in France is the preference for producing plutonium in a production center in Marcoule, instead of separating uranium isotopes. The creation of this center, which is provided for in the first five-year plan, will be near completion this year. At the present time, the Commission is forced to import enriched uranium for experimental purposes (for example, low enriched uranium rods for the reactor EL-3 were obtained from England). In June of last year, an agreement was made with the USA to sell to France 40 kg of  $U^{235}$ .

In January of 1956, the first of three Marcoule series "G"(graphite) reactors - G-1\* became active, with a productivity of 15 kg of plutonium per year (Fig. 1). The output of electrical energy (5 Mw) from this reactor serves for strictly experimental purposes, and does not even satisfy its own requirements. This series of reactors will employ natural uranium; the moderator will be graphite, and the coolant,  $CO_2$ . The selection of this type of reactor is due to a tendency to employ raw materials produced in France, and also to its relative simplicity of construction and ease of operation. In addition, the use of a gaseous coolant decreases the possibility of radioactive contamination of the area, which is especially important for France with its large population density.

\* See Atomic Energy, 1, 2, 108 (1956). [See C. B. translation.]

TABLE 1  
French Reactors [1]

Reactor and purpose	Date Critical	Moderator	Coolant	Fuel	Power, thermal/electrical	Place constructed
1. ZOÉ (research)	1948	D <sub>2</sub> O	None	3 tons UO <sub>3</sub>	5 kw /0	Chatillon
2. ZOÉ (improved, research)	1953	D <sub>2</sub> O	D <sub>2</sub> O	2 tons natural uranium	150 kw /0	"
3. FL-2 (research)	1952	D <sub>2</sub> O	Nitrogen - then CO <sub>2</sub> at 10 atmos.	3 tons natural uranium	2.5 Mw /0	Saclay
4. "Aquila" (research)	August 1956	D <sub>2</sub> O or H <sub>2</sub> O	None	Various types of fuel elements in various arrangements	1 watt/0	"
5. EL-3 (material testing)	1957	D <sub>2</sub> O	D <sub>2</sub> O	low enriched uranium	10-15 Mw /0	"
6. Swimming pool reactor No. 1 (for training personnel and shielding research)	1958	H <sub>2</sub> O	H <sub>2</sub> O	About 5 kg U <sup>235</sup> in uranium enriched 20%	1 Mw /0	Grenoble
7. Swimming pool reactor No. 2 (for shielding research)	1958	H <sub>2</sub> O	H <sub>2</sub> O	About 5 kg U <sup>235</sup> in enriched uranium	1 Mw /0	Chatillon or Saclay
8. "Minerva" (for reactivity study)	1958	H <sub>2</sub> O, possibly BeO <sub>2</sub>	None	About 3 kg U <sup>235</sup> in enriched uranium	1 watt/0	Chatillon
9. "Proserpine" (homogeneous, research)	1957	H <sub>2</sub> O	H <sub>2</sub> O	Plutonium sulfate solution (several hundred grams)	1 watt/0	Saclay
10. "Marin" (for ocean vessel propulsion)		No data available				
11. "Chaud" (for aircraft propulsion)		No data available				
12. G-1 (for plutonium production)	Jan. 1956	Graphite	Air	100 tons natural uranium	40 Mw /5 Mw	Marcoule
13. G-2 (for production of plutonium and electric power)	1957	"	CO <sub>2</sub> at 15 atmos.	100 tons natural uranium	150 Mw /30 Mw	"
14. G-3 (for production of plutonium and electric power)	1958	"	CO <sub>2</sub> at 15 atmos.	100 tons natural uranium	150 Mw /30 Mw	"
15. EDF-1 (for production of plutonium and electric power)	1959	"	CO <sub>2</sub> at 25 atmos.	130 tons natural uranium	300 Mw /60 Mw	Avoigne

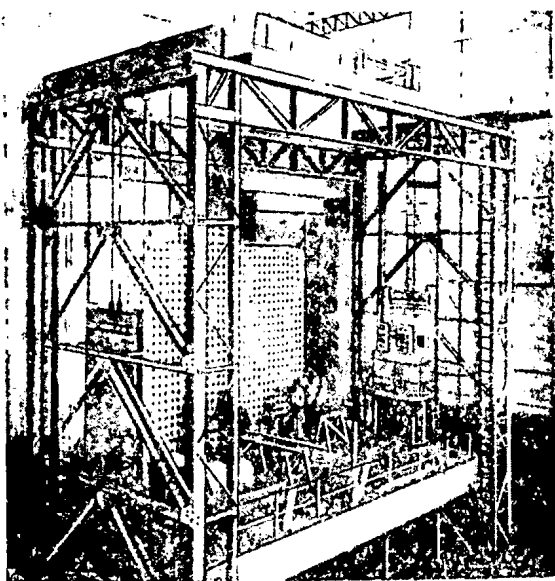


Fig. 1. Reactor G-1. Loading face.

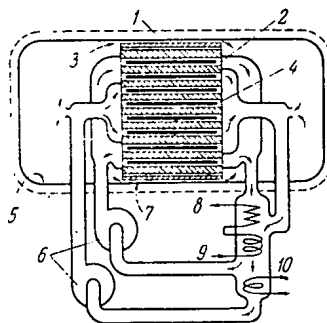


Fig. 2. Schematic diagram of reactor G-2.  
 1) Combination shield and concrete high-pressure shell; 2) fuel channels; 3) gas which cools the high-pressure chamber; 4) uranium rods; 5) thin steel lining; 6) gas blower with steam drive; 7) cast iron shield for thermal neutrons; 8) superheated steam; 9) feed water; 10) economizer.

The type G-2 (Fig. 2) and G-3 [4] reactors have a dual purpose, i.e., in addition to producing plutonium, electric power will be generated (30 Mw each).

French reactor designers have created a reactor of original design, which in many respects differs from operating English reactors (Calder-Hall). The shell of the French reactors, which is designed for pressure, consists of concrete lined with sheet steel on the inside (for a better hermetic seal). It is cooled by carbon dioxide gas circulating between a cast iron screen for thermal neutrons and the steel lining. The fuel (about 100 tons of natural uranium mixed with a small amount of aluminum) is in the form of cylinders 300 mm in length and 28 mm in diameter (the aluminum protects the cylinders from distortion). Each cylinder is encased in a ribbed tube consisting of an alloy of zirconium and magnesium, and is mechanically attached to the tube. The cylinders are located in 1200 horizontal channels (70 mm in diameter) at a spacing of 200 mm apart. The coolant - carbon dioxide gas under a pressure of 15 atmospheres - in contradistinction to the Calder-Hall reactor cools two different zones, in which connection the temperature in the exterior zone is greater than in the interior zone. The reactor is reloaded during operation.

A chemical plant is under construction in Marcoule for extraction of plutonium from irradiated uranium.

The first installation designed mainly for the production of electrical energy will be the reactor EDF-1, the construction of which was undertaken in Avoigne (Loire River Valley) by the company "Electricité de France." The reactor of this station will be made of the same materials as those of the G-2 and G-3 series, but for the purpose of decreasing the cost of electrical energy, certain modifications will be introduced into the design of this reactor. In particular, it is designed for greater pressure and temperature of carbon dioxide gas. The second five-year plan for development of atomic energy in France, for which French specialists are completing the planning at the present time, makes provision for the creation in Avoigne of an atomic energy center with a total power of 300 Mw. In accordance with this plan, an atomic electrical station will be set into operation every year; the power of each new station will be greater than that of each preceding station. The locations of other atomic energy stations are as yet unknown. Realization of the plan will start at the end of 1957, although 10 billion francs allotted for this purpose will have been spent by this time.

According to a statement by George Guillet, the French government secretary who is responsible for problems on atomic energy, 200-300 billion francs are required for fulfillment of the second five-year plan. For purposes of comparison, it is noted that capital investments in the atomic industry toward the end of 1957 will comprise 150 billion francs, whereas in 1945 they comprised 0.5 billion francs. Apparently, the materials used in reactors of series G and EDF-1 will not necessarily be used in future reactors. The new five-year plan does not provide for the construction of a reactor with a greater breeding of fuel, although it is assumed that a decision will be made on its construction.

Mention should be made of France's intention to construct two atomic submarines [8]. A training center has been created in Cherbourg to train their crews [9]. The new ocean liner "France," which has a displacement of 55,000 tons, is being constructed with the view that in the future its power installation can be replaced by an atomic installation [5]. The research reactor "Marin" is a proto-type reactor for ocean vessels. Another research reactor, "Chaud," of which little is known except that it operates "at a very high temperature" and is not designed for the production of electrical energy, apparently is a prototype reactor for airplanes.

Successful fulfillment of the atomic energy development program depends to a great extent upon the degree to which France will be able to provide the installations with the necessary materials. The most important problem is fuel. For this reason, nearly one-third of the personnel of the Atomic Energy Commission work in the Mining Administration. The resources of France itself (50,000-100,000 tons of uranium) [6] make it possible for the country to attain first place in Western Europe in supply of uranium. In addition, in Madagascar there has been discovered about 1,000 tons of thorianite containing 10-20% uranium and 60-70% thorium. Searches for new deposits are being conducted in the Sahara Desert, French Equatorial Africa, French West Africa and in Guiana.

In 1957 it is planned to obtain 380 tons of concentrate [7] containing 60% uranium, 300 tons of reactor grade uranium and 300 tons of reactor grade thorium nitrate. It is planned to increase future production of uranium as follows: in 1958 - 500 tons; 1961 - 1,000 tons; 1970 - 2,500 tons; 1975 - 3,000 tons.

TABLE 2  
Plants Which Process Uranium Ore [3]

Location of plant	Ore processed, tons/ year	Uranium content in ore, %	Uranyl yield, tons/ year
Gueugnon (Département de Saone-et-Loire)	50,000	0.1-0.8	300
Escarpere (Département de Vendée)	300,000	0.11-0.15	400
Bessines (Département de Haute-Vienne)	200,000	0.11-0.25	450

In order to obtain a concentrate containing 60% of uranium, it is planned to process low-content uranium ore in three enriching plants (see Table 2), one of which has already become active (in Gueugnon). Construction of a plant for extracting reactor-grade uranium is near completion in Boissy, near Paris. The cost of obtaining chemical concentrate in the enterprises of the Commission is 12,000 francs per kilogram, while extraction of uranium from concentrate in the plant in Boissy costs 5,000 francs per kilogram. It is expected that in the near future the cost of processing will be decreased to 10,000 and 4,000 francs per kilogram for uranium and concentrate, respectively.

Reactor grade graphite (cross section less than 4.5 m barns, density of 1.7) is being produced in sufficient quantities by the firm "Pechine." Heavy water is not being produced commercially in France; various methods are being tested at the present time for producing it. In particular, the firm "French Heavy Water Co," constructed a research installation for producing heavy water by means of distillation of liquid hydrogen. France is still receiving heavy water from Norway and the USA. Reactor grade beryllium and beryllium oxide (density of latter is 2.95, which is higher than that in the USA) are being produced in large quantities in the country. The production of hafnium-free zirconium is increasing rapidly. The greater part of special equipment for atomic energy, including electronic equipment, is being manufactured in France. It is expected that soon all the materials required for the atomic industry will be produced in France. A very important exception to the above, however, is the fact that France does not have an industrial installation for separating uranium isotopes.

The rapid development of atomic energy has given rise to a revival in the activity of French industry [10]. In the course of several years, industrial firms have evolved from the position of simple contractors to

associates of the Commission. In 1955, there were 25 firms working with the Commission under contract. At the present time, the number of firms participating in the operations of the Commission is so great that it was found more convenient to create associations of firms, such as "Indatom" (9 firms), "Francatom" (19 firms), "Occiatom," and the "Technical Association for the Utilization of Atomic Energy" (50 firms).

The problem of providing the French atomic energy industry with trained personnel is even more complex than the problem of supply of materials, even though France has been conducting investigations in this area for 12 years. At the present time, in the enterprises and apparatus of the Commission, disregarding the working force employed in the overseas mining industry of France, there are about 6,000 workers, including approximately 2,000 people with a higher and secondary education.

To upgrade the qualifications of the personnel of private firms, in the research center in Saclay courses have been organized in nuclear physics, theoretical and experimental physics, radiobiology, biophysics, radio-isotopes and metallurgy of reactor materials. The training is accompanied by three months of practice in the enterprises of the Commission. In 1956, 40 engineers of private companies completed these courses. It is planned to offer similar courses in the new research center in Grenoble, where up to 200 engineers will be trained every year.

V. A.

#### LITERATURE CITED

- [1] Nucleonics 14, 12, 9-10 (1956).
- [2] Atomics and Nucl. Energy 8, 1, 15-19 (1957).
- [3] Atomics and Nucl. Energy 8, 2, 51 (1957).
- [4] A. Ertaud, Atomics and Nucl. Energy 8, 2, 52-59 (1957).
- [5] Nucleonics 14, 9, 11 (1956).
- [6] Nucleonics 15, 1, 9 (1957).
- [7] Nucl. Power 2, 10, 40 (1957).
- [8] Newsweek 48, 25, 42 (1956).
- [9] Nucl. Engineering 2, 12, 125 (1957).
- [10] Bull. d'information économique et technique 5, 4-8 (1956).

## PROGRESS IN THE STUDY OF PHASE DIAGRAMS OF METAL SYSTEMS

A conference devoted to problems of the study of phase diagrams of metal systems was held from 17th to 21st of May, 1957 in the Baikov Institute of Metallurgy of the Academy of Sciences of the U.S.S.R.

O. S. Ivanov read a paper on "Progress and future in the study of phase diagrams of metal systems" in which he discussed problems relating to the study of metals and alloys, particularly beryllium, niobium, zirconium, uranium and plutonium used in atomic power engineering.

In the search for alloys possessing important practical properties and in determining the methods for their treatment, a knowledge of their phase diagrams is of great importance in providing the broadest concept of the interaction between two, three or more metals as a function of concentration, temperature and pressure.

The application of thermodynamic calculations based on models of regular solutions and a study of the electronic structure of alloys permit a wider visualization of the way in which the phase diagram of a given metal depends upon its chemical nature and the position of its alloying components in the periodic system.

For producing strongly reactive metals, atomic power engineering is making use of new methods: arc melting on cooled hearths and crucibleless melting. Research on radioactive metals, which are very rare or are dangerous to life (plutonium, polonium, etc.) is carried out on a microscale, for which methods of microthermal, microdilatometer, x-ray and magnetic analysis of specimens of fractions of cubic millimeters and weights of the order of one milligram have been developed. For specimens of high radioactivity, "hot" cells with remote-controlled manipulators have been designed. Thermocouples of high-melting metals and perfect optical micropyrometers have been produced, but investigations in the temperature range from 200 to 3000°C are inadequate in both quantity and quality.

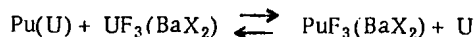
The scale of research carried out by many organizations in different countries is quite considerable. According to published data, 22 binary systems based on uranium, 12 based on thorium and 7 based on plutonium have been fully investigated, while 3 ternary systems based on thorium and 5 based on uranium have been partly investigated. Detailed data are also available on the structure of more than 70 intermetallic compounds of plutonium.

O. E.

DISTRIBUTION OF PLUTONIUM AND FISSION PRODUCTS BETWEEN  
MOLTEN URANIUM AND  $UF_3$ - $BaCl_2$  ( $F_3$ ) MIXTURES\*

In the experiments, 20 g of irradiated uranium (plutonium content  $50 \mu g/g$ ) and a mixture of uranium trifluoride and barium halides was used.

At a temperature of 1200-1400°C, the plutonium and fission fragments are extracted in the melt, passing from the metal phase to the salt phase according to the reaction:



\*F. S. Martin and E. W. Hooper, J. Inorg. Nucl. Chem. 4, 2, 93, (1957).



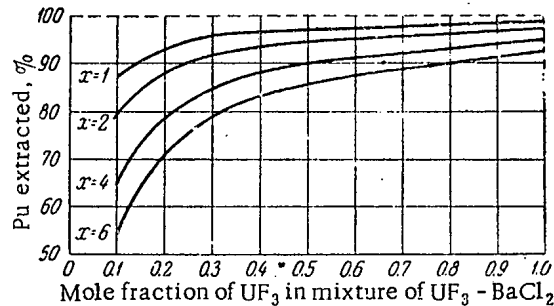
The time for establishing equilibrium (without mechanical mixing of the phases) is not less than 1 hour. The equilibrium constant for the plutonium distribution is written in the following form:

$$K = \frac{\% \text{ Pu}}{100 - \% \text{ Pu}} \cdot \frac{\text{moles of U}}{\text{moles salt}} \cdot \frac{1}{N_{\text{UF}_3}}$$

where % Pu is the plutonium extracted from the metal into the salt;  $N_{\text{UF}_3}$  is the mole fraction of  $\text{UF}_3$  in the salt mixture;  $N_{\text{U}} = 1$ , mole fraction of U in the metal.

It was found that K for  $1200^\circ\text{C}$  was  $72 \pm 50\%$ . The free energy change for the reaction, calculated for  $K = 72$ , was 12.8 kcal. Using a given value for the equilibrium constant, curves were calculated for the extraction of plutonium for different compositions of the salt phase (see figure).

It is easy to see that increasing the mole fraction of  $\text{UF}_3$  above 0.4 does not result in any material increase in the percentage of plutonium extracted. It is preferable to use multistage extraction with a small quantity of salt phase. For example, when  $x = 6$  and  $N_{\text{UF}_3} = 0.4$  for the first extraction stage, the plutonium extraction will be 83%, for the second stage, it will be 97.1%. The mean concentration factor is then  $(0.97/2) \times (6/0.4) = 7.3$ . For other conditions, when  $x = 1$  and  $N_{\text{UF}_3} = 0.4$ , the concentration factor is  $0.97 \times (1/0.4) = 2.4$ , i.e., only one-third of the previous value.



Calculated curves for extraction of plutonium from uranium by a  $\text{UF}_3 - \text{BaCl}_2$  mixture at  $1200^\circ\text{C}$  (x is the mole ratio of metal phase to salt phase).

The fission products were extracted from the irradiated plutonium to more than 99% for different experimental conditions. Complications associated with oxidation effects, however, prevented calculation of the equilibrium constant of the reaction. In addition, at temperatures of  $1200-1400^\circ\text{C}$ , about 80% of the caesium and 20% of the strontium are volatilized.

V. P.

#### SOME PROPERTIES OF NEPTUNIUM METAL

In the research laboratory of the Windscale Works (England), a small piece of neptunium has been obtained by bomb reduction [1].

The percentages of impurities present were:

Ca	U	Ni	Mg	Cr	Pu	Al	Mo	V
0.34	0.22	0.06	0.03	0.03	0.03	0.02	0.05	0.06

Probably small quantities of fluorine and oxygen were also present (no analysis was made).

A powder photograph of unannealed filings showed that neptunium metal has the rhombic structure of the  $\alpha$ -phase stable at room temperature [2]. Theoretical density 24.45 g/cm<sup>3</sup>; density at 20°C, 20.2 g/cm<sup>3</sup>. Specific heat in the range 29-99°C is 0.0319 cal/g°C and lies between published figures for the specific heat of uranium and plutonium.

Microscopic investigation of a metallographic specimen prepared in a dry chamber showed that it has two types of inclusion in a volume amounting to 3%. After oxidation for some hours in air of the mechanically polished specimen, grains of a mean diameter of about 0.3 mm could be seen in polarized light. Like the grains in cast uranium, the grains in neptunium have a very irregular shape and differ considerably in size, although no clear evidence of the presence of sub-grains was obtained.

Near hardness impressions long, thin parallel deformation twins were observed, the systems of which were restricted by the given grain.

A Mayer [3] hardness analysis with a 1 mm steel ball under loads from 1-120 kg gave the following relationship:  $L = 360 d^{2.19}$  ( $L$  is the load in kg;  $d$ , diameter of impression in mm). Vickers hardness (diamond pyramid, load 10 kg) was 355, i.e., considerably harder than bomb-reduced uranium.

The ultimate tensile strength of neptunium, determined from the stress-strain curve and the empirical relationship between hardness and tensile strength lies within the limits of 124-138 kg/mm<sup>2</sup>.

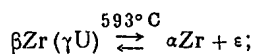
G. Z.

#### LITERATURE CITED

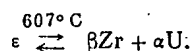
- [1] V. W. Eldred and G. C. Curtis, Nature 179, 4566, 910 (1957).
- [2] W. H. Zachariasen, Acta Cryst. 5, 660 (1952).
- [3] D. Tabor, The Hardness of Metals, Oxford, (1951).

#### URANIUM - ZIRCONIUM ALLOYS

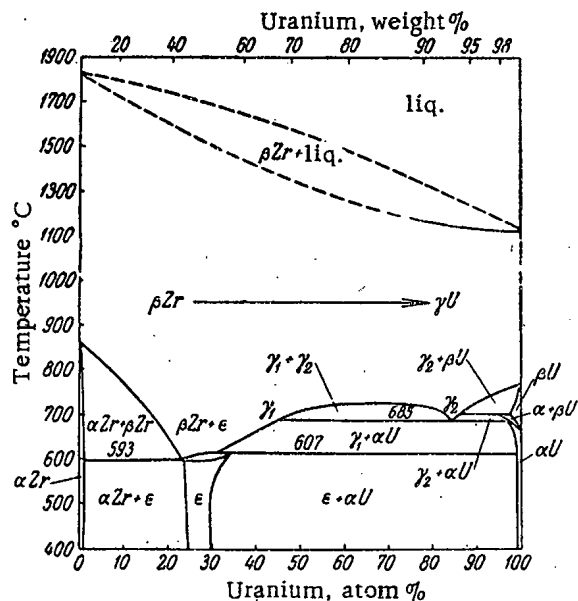
Published investigations of the uranium-zirconium system [1, 2] differ in some of the details of  $\epsilon$ -phase formation. The stability of this phase has been open to doubt, since it has not always been possible to discover it in the alloys, and on etching it exploded. Recent investigations of this system [3] have shown that the  $\epsilon$ -phase is stable. A more exact phase diagram (see figure) has been constructed on the basis of these investigations.  $\gamma$ -uranium and  $\beta$ -zirconium, isomorphous at high temperatures decompose according to the eutectoid reaction



The  $\epsilon$ -phase is stable up to approximately 610°C, when it is decomposed according to the peritectoid reaction



The presence of the  $\epsilon$ -phase has been firmly established in experiments on the diffusion of vapor from a uranium ingot placed in a zirconium cylinder, carried out at temperatures below the stability temperature of a solid solution of uranium in  $\beta$ -zirconium. Metallographic evidence of the stability of the  $\epsilon$ -phase was obtained by annealing a specimen (50% by weight U) of cold-worked and recrystallized  $\epsilon$ -phase in a furnace having a temperature gradient. The existence of the two-phase region  $\beta\text{Zr} + \epsilon$  in a narrow temperature interval has been established by high-temperature x-ray examination [4].



Uranium-zirconium phase diagram.

The data quoted show that uranium-zirconium alloys, prepared from crystalline zirconium rod (0.005% oxygen) and zirconium sponge (0.1% oxygen) will behave differently. In particular, for quenching alloys made from sponge with conversion to solid solution of  $\beta$  Zr, much higher temperatures will be required than for the same alloys made from crystalline zirconium rod.

G. Z.

## LITERATURE CITED

- [1] Nuclear Reactors, Vol. III. Materials for Nuclear Reactors. II., Moscow, 1956, p. 301.
- [2] H. A. Saller and F. A. Rough, BMI - 100, USA, 1955.
- [3] H. A. Saller, F. A. Rough and A. A. Bauer, Second Nucl. Eng. and Sci. Conference, pap. 57 - NESC - 20, 1957.
- [4] F. A. Rough, A. E. Austin, A. A. Bauer and J. R. Doig, BMI - 1092, USA, 1956.

## URANIUM CONCENTRATING WORKS IN CANADA

Until 1953, the only large source of supply of uranium concentrates in Canada was the concentrating works on the well known uranium deposit of Eldorado in the Great Bear Lake region. In 1953, a plant was started up in a new uranium region, near Beaverlodge Lake, where the large hydrothermal deposits of Ace-Fay and Gunnar were discovered, together with numbers of small deposits. In the same year, intensive prospecting was commenced in the Blind River region, where uranium mineralization was found in conglomerates [1]. This was followed by the development of mines and works in this region. Somewhat later, industrial exploitation was commenced of the deposits in the Bancroft region, where the uranium ore is associated with pegmatites. Years of prospecting for uranium deposits in British Columbia resulted in the discovery of the uranium fluorite deposit of Rexspar.

In addition, a partial investigation of the uranium-zirconium-oxygen phase diagram has shown the following:

1) Solubility of oxygen in the  $\epsilon$ -phase is less than 0.05% and small quantities of oxygen abruptly restrict the region of its existence;

2) On further increase in the oxygen content, the  $\epsilon$ -phase exists simultaneously with  $\alpha$ -uranium and  $\alpha$ -zirconium, and with still greater quantities of oxygen it disappears altogether.

3) The  $\beta$  Zr region likewise contracts when oxygen is added to the alloy, as shown by an experiment in which alloys with 40% by weight of uranium and different oxygen contents were annealed for 100 hours at 660°C.

Oxygen content, % by weight	0.005	0.1	0.3
Vol. of $\alpha$ Zr phase, % (determined metallographically)	2.87	10.70	19.80

TABLE

Name of region and mine	Daily production, tons of ore	Yearly production value, thousands of dollars	Operating costs per ton of ore, dollars	Content, %
BLIND RIVER Algom (nordic and Quirk)	6 000	49 300	8.50	0.08— —0.11
Can. Met Exploration Consolidated	2 500	20 500		
Denison	6 000	49 300	10.00	
Milliken Lake	3 000	24 600		
Northspan	9 000	73 900		
Pronto	1 500	12 300		
Stanleigh	3 000	24 600		
Stanrock	3 300	27 100		
BEAVERLODGE	34 300	281 600		
Eldorado	2 000	31 000	12.00	0.13— —0.22
Gunnar	1 650	24 000		
Lorado	500	7 300		
BANCROFT	4 150	62 300		
Bicroft	1 000	9 100	10.00	0.08— —0.13
Cavendish	750	6 800		
Dyno	1 000	9 100		
Faraday	750	6 800		
Greyhawk	600	4 900		
NORTHWEST TERRITORY	4 100	36 700		
Rayrock			35.00	0.3
(Marian Lake)	150	3 800		
Eldorado (Port Radium)	200	3 000		
BRITISH COLUMBIA	350	6 800		
Rexspar	750	5 500	—	0.08
Grand Total	43 650	392 900	—	—



Chart showing location of the principal regions of uranium exploitation in Canada.  
 1) Eldorado (Great Bear Lake); 2) Marian Lake; 3) Beaverlodge; 4) Blind River;  
 5) Bancroft; 6) Rexspar (British Columbia).

Thus, in the course of the last 3 or 4 years, due to the discovery of new deposits and the construction of plants, uranium sources in Canada have undergone considerable development with a substantial change in the part played by the various regions in their exploitation.

The location of uranium works in Canada (operating and completing construction in 1957) and their fundamental productivity data are shown in the table [2].

These data show that the Blind River region, covering more than 70% of the total uranium production of Canada, is the most important. The Great Bear Lake region (Eldorado), judging by the published data, does not have a very high productivity. The high productivity of the Bancroft works, where the ore is associated with pegmatites, is striking. Evidently, this is the only region in capitalist countries, where the pegmatite type gives appreciable uranium concentrates.

M. K.

#### LITERATURE CITED

- [1] Atomic Energy 1, 2, 112 (1956).\*
- [2] South Afr. Min. and Eng. Journal 68, 3346, 565 (1957).

\*[See C. B. translation.]

RADIOBIOLOGICAL WORK AT THE INSTITUTE OF BIOPHYSICS,  
ACADEMY OF SCIENCES OF THE USSR, IN 1956

Work on the mechanisms by which ionizing radiations affect plant and animal organisms was carried out at the Institute of Biophysics, Academy of Sciences of the USSR, in 1956.

Most attention was paid to the inapparent physicochemical changes occurring in cells immediately after irradiation, before appreciable morphological changes are observed. Using radioisotopes it was shown (A. M. Kuzin, N. B. Strazhevskaya) that the permeabilities of plant cells to various ions dropped sharply immediately after irradiation, this being due to changes in the surface polar groups of the biocolloids. Polar group changes are also indicated by isoelectric point measurements on the proteins isolated from the cells (A. L. Shabadash, S. O. Enenko, N. L. Samoilina); considerable shifts in the isoelectric points to the acid side being observed during the first 24 hours after irradiation. The exact shift varies with the dose and time after irradiation, and with the particular function and metabolism of the organ. The acid-side displacement is always found on irradiation, and may prove useful in elucidating the detailed mechanism of radiation reaction (A. L. Shabadash, S. O. Enenko, N. L. Samoilina and L. V. Orlova).

The physicochemical changes in living structures after irradiation have also been studied by measuring tissue absorption of radiocolloids (A. M. Kuzin, E. A. Ivanitskaya). Colloidal Ag<sup>110</sup>, P<sup>32</sup>-tagged chromic phosphate and I<sup>131</sup>-globulin were used to demonstrate changes in liver absorption in generally irradiated animals at 2 and 24 hours after irradiation.

Work on nucleoproteins separated from irradiated plant tissues (S. D. Chigirev) showed that the physicochemical properties (structural viscosity, tendency to polymerize) changed markedly while the chemical composition remained constant.

Fluorescence studies on living tissues (Meisel) showed that considerable changes occurred in the nuclear matter even by 1-1½ hours after irradiation (A. V. Gutkina). The changes in the nuclei of bone-marrow cells were even found after 100 r. These changes were clearly focal in character and varied regularly with dose and time after irradiation. These observations are very important for further work on radiation reactions. The changes are all due to direct radiation action on the cells since they do not occur on general irradiation when particular tissue is carefully screened (V. A. Sondak).

Changes in the mucopolysaccharide content of intestinal epithelium in irradiated animals were also demonstrated (Shabadash, L. V. Orlova); these materially affect recovery processes.

New data on the important part played in retarding cell division by toxic factors produced on irradiation were produced (N. M. Berezin); on removing the irradiated spermatozoa plus endosperm and cultivating them on artificial media the growth retardation produced by irradiation can to a considerable extent be reversed.

Factors depressing cell division were observed in extracts from irradiated tissues (G. N. Saenko, V. A. Yazykova). A new method, using plants uniformly labeled with radiocarbon, was developed for this purpose (A. M. Kuzin, V. I. Tokarskaya).

New methods of recording the ultraslow EEG oscillations were developed for work on radiation effects on the central nervous system, as well as new ways of determining free oxygen in tissues polarographically in long-term experiments.

The EEG work above showed that changes in the oscillations are among the earliest radiation reactions in

the nervous system. The changes were shown related to the dose and site of irradiation. Hence it was supposed that relatively low doses (400-500 r) caused the subcortical centers to react with a prolonged and stable increase in activity, the initial depression indicating temporary inhibition in the central nervous system produced by direct radiation action (N. A. Aladzhhalova).

The early disturbances in tissue respiration, and the specific actions produced on irradiating certain sites, are of special importance in understanding the mechanism of radiation action on the brain. It is found that in the first post-irradiation hours oxidation in the cortex is depressed, this being due to direct action (G. M. Frank, A. D. Snezhko).

Fresh data on the morphological changes on nerve cells in the early phases of radiation sickness at non-lethal doses have also been obtained (A. L. Shabadash).

Work has also been done on the duration of radiation sickness in animals with parts of the CNS removed, particularly the cerebellum; this had indicated alterations in the development of leucopenia (P. F. Minaev).

In the physiology laboratory (L. S. Shtern) the effects of irradiation on blood-tissue barrier permeabilities and on tissue metabolism have been studied. Among other things it was found that irradiated animals survive longer if given low doses of alcohol. This occurs because the catalase is protected from anticatalase, the usual reduction in the catalase activity occurring much later (S. R. Zubkova, A. L. Platonov).

E. I. Krichevsky developed a quantitative method for estimating histamine in tissues and body fluids which was used to demonstrate increased histamine soon after irradiation, and decreased histamine later on, in many organisms.

The role of neural factors in permeability changes on irradiation was elucidated as regards the early changes, and possibilities of preventing them by injecting neurotropic materials, such as novocaine, atropine and morphine were discovered (M. M. Gromakovskaya, S. Ya. Rapoport).

The work on ionizing radiation and mammal fertility was continued in 1956 (I. O. Shapiro, N. I. Nuzhdin, O. N. Petrova and O. N. Kitaeva). Mouse ovaries were found particularly radiosensitive: fertility was much reduced at 25 r, and ovulation was irreversibly disturbed at 50 r. Studies of radiation sterilization produced by general x-irradiation are of particular interest. It was shown that this is produced only by local irradiation of the ovaries, while the hormonal system (including the hypophysis) is not disturbed. The marked difference in the radiosensitivities of sex cells may be very important in extending radiobiological (and radiogenetic) data from one type of animal to another.

Prolonged irradiation of plants at low dose-rates throughout the growing period showed that the reproductive organs became large at very low doses (10-100 r). Hence it might be possible to increase plant yields in zones of increased activity (L. P. Breslavets, N. M. Berezina).

The Institute also had pointed out that increased yields might be obtainable by irradiating the seeds with  $\gamma$ -rays prior to sowing: this was verified under agricultural conditions. Experiments carried out in the Krasnodar region on an area of 2 hectares gave an increase in carrot carotene of 35%. An experiment with radishes (carried out on 1.5 hectares at market garden No. 2 Combine of the Ministry of Agricultural Produce) gave a yield increase of 11% (L. P. Breslavets, N. M. Berezina).

In 1956 the first radio-ecological studies on the role of insects in the self-purification of artificial lakes contaminated with long-lived radioisotopes were carried out, as well as work on the distribution of activity from radioactive fallout and on radiation genetics.

A. M. Kuzin

## BRIEF COMMUNICATIONS

USSR. In 1958 it is planned to complete the construction of a three-story laboratory building at the Moscow Order of Lenin Power Institute. This building will house the Department of Thermal Engineering Physics together with the Department of Atomic Power Stations of the Institute, which was established in July 1956. The research plans of this department include a study of the corrosion resistance of metals, problems concerning the hydrodynamics and properties of steam and the hydrodynamics of the water in a boiling water reactor.

During the next school year the instruction provided by the Department of Atomic Power Stations of the Institute will be expanded. At present it is planned to offer courses of lectures on such subjects as Atomic Power Stations, Steam Generators of Atomic Power Stations, Heat Transfer Agents in Nuclear Power Installations, Materials of Nuclear Power Installations and Corrosion. (V. Parkhitko of the editorial staff.)

England. A prototype of a pressurized water reactor for an English atomic submarine will be constructed on land in Dounreay where a fast-neutron reactor is being built. [Nucl. Eng. 2, 14, 215 (1957)].

England. A few hundred annular fuel elements in the center of the fast-neutron breeder reactor at Dounreay are encased in niobium. Niobium was chosen because of its high melting point and good resistance to the effects of hot uranium and the sodium coolant. [Nucl. Power 2, 14, 226 (1957)].

England. The tank for the fast-neutron reactor which is being constructed at Dounreay was shipped to the site during April, 1957. The construction of the tank required 18 months. The welded seams of the tank were checked by x-rays. [Nucl. Power 2, 13, 171 (1957)].

France. The UNESCO conference at Paris, September 9-20, 1957 will discuss the utilization of radioactive isotopes in scientific work. More than 1000 delegates will attend [Nucl. Eng. 2, 14, 215 (1957)].

France. Work on an atomic submarine has begun. A spokesman for the atomic center at Saclay reports that the first French atomic submarine (the Q-2444) will be launched within 4 years. [Nucl. Eng. 2, 14, 215 (1957)].

Sweden. At the Nobel Institute in Stockholm a joint Swedish-American-British team has produced element 102. Its halflife is about 10 minutes and it emits alpha particles of 8.5 Mev. [Engineering, July 26, (1957), p. 124].

Denmark. The Foreign Affairs Ministries of Sweden, Denmark, Norway and Finland have announced that their governments will conduct joint investigations in the field of atomic energy. For this purpose a joint research institute will be established in Copenhagen. [Nucl. Eng. 2, 14, 214 (1957)].

USA. The American reactor APPR-1 at Fort Belvoir (near Washington) reached the critical stage in April, 1957 and supplied electric power. The reactor will be tested for a week, after which it will be stopped for inspection and then operated at full strength. [Atom. Industry Reporter 98, 3 (1957); Atom. Energy Guideletter 114, 8 (1957)].

USA. At Quincy, Massachusetts construction of the first American atomic cruiser "Long Beach" will soon begin. The cruiser will cost 87.5 million dollars. Completion is scheduled for the end of 1960. [Army, Navy and Air Force Register 78, 4030, 8 (1957)].

USA. The California Mining Journal of February 1957 (p. 13) contains a list of current prices of reactor materials in the USA, as follows: uranium metal \$40. per kilogram; thorium metal \$43. per kilogram, U<sup>235</sup> \$16.



per gram,  $U^{233}$  \$15. per gram, plutonium \$12. per gram, heavy water \$62. per kilogram, beryllium metal \$230. per kilogram, zirconium \$51. per kilogram.

USA. Plans have been formulated to build at Erwin, Tennessee, the first privately-owned plant in the country for the production of materials utilized in the fuel elements of nuclear reactors - uranium, thorium, rare-earth alloys and metals. The plant will include units for solvent extraction to produce pure uranium and thorium salts, for the reduction of these salts to metallic powder or sponge and for the melting and casting of metals. [ Atomic Energy Newsletter 17, 4, 2 (1957)].

South Africa. According to the Atomic Energy Council of the Union of South Africa the total uranium ore reserves of South Africa (in uranium-gold conglomerates), containing 375,000 tons of uranium oxide, are estimated at 1100 million tons. [Uranium Magazine 4, 4, 12 (1957)].

Australia. A few months ago high-grade primary uranium ore was discovered in Tasmania near Rossarden in Chalezky's Lease. [Mining World 19, 3, 107 (1957)].

Brazil. Recently a new type for Brazil of uranium mineral was discovered in the form of a disseminated deposit in Triassic sandstone. The deposit is located near the city of Aguazdo Prata in the state of Sao Paulo. The ore is found in the contact between sandstone and nephelinic rocks. A few chemical analyses indicate 0.5% of uranium. [ Mining World 19, 3, 9 (1957)].

Argentina. Within the country 150 uranium deposits and occurrences have been found. Twelve uranium minerals have been discovered. At the present time uranium is going from 12 mines to concentrating mills at Cordoba and Mendoza. The principal uranium deposits are located at Santa Brigida and San Victorio near Sanogasta in La Rioja. The uranium content of these ores exceeds that from other parts of the country. [ Mining World 19, 3, 9 (1957)].

Japan. In recent months 8 uranium veins have been discovered on the island of Honshu, which are considered to be the most important uranium discoveries in Japan up to the present time. The uranium zone extends along the boundary between the prefectures of Okayama and Tottori. [Mining World 19, 3, 107 (1957)].

## BIBLIOGRAPHY

### NEW LITERATURE

#### Books and Symposia

The Biochemical and Physico-chemical Bases of the Biological Action of Radiation. Theses of reports of Mezhvuzovsk scientific conference, 25-28 February 1957. Moscow Univ. Press, 1957, pp. 44, unpriced.

The 1st All-Union Conference on Radiation Chemistry. Moscow, March 25 - April 2, 1957 (Theses of reports). Izd. AN SSSR, 1957, 76 pp., unpriced.

Zaslavsky, Yu. S. and Shor, G. I., The Use of Atomic Energy in the Petroleum Industry, Gostoptechizdat, 1956, 88 pp., 2 r 25 kop.

Ivanov, I. I., Balabukha, V. S. et al., Metabolism During Radiation Sickness. Edited by Prof. I. I. Ivanov. Medgiz, 1956, 251 pp., 8 r 50 kop.

Kazakov, N. F., The Use of Radioisotopes for the Study of Cutting-tool Wear. AN SSSR Inst. tech.-econ. information, 1956, 35 pp., illust., 10 r.

MacLine, Stewart, Lectures on Reactor-building Practice. Trans. from Eng. Ed., with preface, by A. A. Kanaev, Sudpromgiz, 1957, 212 pp., 17 r 90 kop.

Melkov, V. G. and Pukhalsky, L. Ch., Uranium Prospecting, Ed. by E. M. Yanishevsky. Gosgeoltechizdat, 1957, 219 pp., 12 r 55 kop.

XI Scientific and Technical Session on Refractory Alloys and Metalloceramic Materials. Moscow, April 1-6, 1957. (Theses of reports). Baikov Inst. of Metallurgy AN SSSR, 1957, 110 pp., unpriced.

Pavlov, A. S. and Zubovsky, G. A., Prophylaxis and Treatment of Radiation Sickness, Review of foreign literature. Medgiz, 1957, 69 pp., 2 r.

Pobedinsky, M. N., Radioisotopes in Medicine. Min. of Health RSFSR. Gos. Sci. Res. Inst. of Hygiene and Occupational Diseases, Leningrad, 1957, 26 pp., unpriced.

Rabinovich, M. S., Charged-particle Accelerators, Izd. "Znanie," 1957, 47 pp., 1 r 20 kop.

Strashinin, A. I., Radioactive Materials in Medicine. Medgiz., 1957, 76 pp., 1 r 35 kop.

Khlopin, V. G., Selected Works. Ed. by B. A. Nikitin and A. P. Ratner, Vol. 1. Works in Radiochemistry, Izd. AN SSSR, 1957, 372 pp., 23 r 25 kop.

Nuclear Reactors for Research. Trans. from Eng. Foreign Lit. Press, 1956, 485 pp., 35 r 90 kop.

#### Articles in Journals

Abrikosov, A. A. and Khalatnikov, I. M., "New Symmetry Properties of the Elementary Particles." Nature, No. 5 (1957).

Alimarin, I. P. and Gibalo, I. M., "The Analysis of Beryllium in Alloys and Concentrates by Radiometric Titration." Factory Laboratory, No. 4 (1957).

- Aidarkin, B. S. and others, "On the Method of Identifying Beryllium in Ores using Photoneutrons." Proc. Khlopin Radium Inst., 5, No. 2, 1957.
- Aikhipova, O. P. and Kozulitsina, T. I., "The distribution of  $P^{32}$ -labeled Tuberculosis Microbacteria in Guinea pigs with Subcutaneous Infection." Comm. 1. Problems of Tuberculosis, No. 2 (1957).
- Alpert, Ya. L., "Some Problems in Ionosphere Physics. 1. The Fluctuation of Electron Density and Radio-wave Scattering." Progress of Physical Sciences, LXI, No. 3 (1957).
- Askaryan, G. A., "A Method for Preserving Corpses by Radioactivity." Avt. Document No. 107250, 1957.
- Bazhanov, E. B. and others, "The Energy and Angular Distributions of Photoprotons from Ni and Al." DAN SSSR, 113, No. 1 (1957).
- Bazazyan, G. G., "On the History of the Development of Soviet Radiology and Radiobiology." Bull. Moscow University, No. 1 (1957).
- Baranov, V. I., "The Use of a Compensation Method for the Determination of Actinium in Small Quantities." Proc. Khlopin Radium Inst., 5, No. 2 (1957).
- Barkov, L. M. and Nikolsky, B. A., " $\pi$  Mesons (A Review of Experimental Data)." Progress of Physical Sciences, LXI, No. 3 (1957).
- Belousov, S. A. and others, "Photoproduction of  $\pi$  Mesons in Complex Nuclei." DAN SSSR, 112, No. 6 (1957).
- Blokhintsev, D. I., "Non-local and Non-linear Field Theories." Progress of Physical Sciences, LXI, No. 2 (1957).
- Vinogradov, A. P., "The Isotope  $K^{40}$  and its Biological Role." Biochemistry 22, Nos. 1-2 (1957).
- Voskoboinikov, G. M., "Theoretical Foundations of Selective Gamma-gamma Oil-well Logging." Izvestia AN SSSR. Geophys. ser., No. 3 (1957).
- Gerling, E. K. and others, "The Argon Method for Determining Age and Its Applications." Bulletin of the Commission for Determining the Absolute Age of Geol. Formations. AN SSSR, No. 2 (1957).
- Grebenshchikova, V. I., "The Adsorption of Radium on Lead Sulfate." Proc. Khlopin Radium Inst. 5, No. 2 (1957).
- Grishin, S. I., and others, "The Demonstration of the Assimilation by one Bacterial Form of the Break-down Products of Another Form by the Method of Labeled  $P^{32}$  Atoms." Questions of Borderline Pathology. AN Uzbek. SSR, No. 8 (1956).
- Golfand, Yu. A., "Fermi Fields and Spinors of an Infinite Space." DAN SSSR, 113, No. 1 (1957).
- Ignatiev, O. M. and Andreev, I. I., "The Use of Iridium-192 for the Defectoscopy of Welded Pipe Seams." Factory Laboratory, No. 4 (1957).
- Katsnelson, M. U. and others, "An Integral Method for the Determination of the Quantity of a  $\gamma$ -emitting Substance." Factory Laboratory, No. 4 (1957).
- Kirakosyan, Z. A., "Mean Free Paths for Proton Absorption in Graphite and Lead." DAN Arm. SSR 23, No. 5 (1956).
- Coffinberry, Waldron, "Plutonium Metal Working." Trans. by N. P. Zverovoy. Problems of Modern Metallurgy. Collection of translations and reviews of foreign periodicals, No. 2 (1957).
- Kuznetsov, V. I., "The Main Features of the Geological Formation of Tantalum and Niobium Deposits Associated with Granite Pegmatites." Sci. Reports of the Lvov Polytech. Inst. No. 46, Series geologorazved., No. 1 (1956).
- Lavrukhina, A. K., "The Use of Radioisotopes in Quantitative Analysis." (Review). Factory Laboratory, No. 3 (1957).

- Malashenko, I. V., "The Design of a Laboratory for Work with Radioisotopes," Factory Laboratory, No. 3 (1957).
- Malysheva, T. V., "Investigation of the Absorption of  $\beta$ -radiation in Matter," Factory Laboratory, No. 3 (1957).
- Moroz, E., "The Bubble Chamber." Science and Life, No. 5 (1957).
- Pavlovskaya, T. E. and Pasynsky, A. G., "On the Action of Ionizing Radiations on Albumin Solutions in Air and Vacuum." Biochemistry 22, Nos. 1-2 (1957).
- Perfilov, N. A. and others, "Triple Fission of Uranium by Fast Particles." DAN SSSR 113, No. 1 (1957).
- Poznyak, L. A., "The Methodology of Radiographic Analysis of the Distribution of Elements in Welded Seams." Factory Laboratory, No. 4, (1957).
- Ratner, A. P. and others, "On the Colloidal Solutions of the Radioelements." Proc. Khlopin Radium Inst. 5, No. 2 (1957).
- Ross, Yu. K., "On the Measurement of Radiation by the Yanishevsky Pyranometers." Izvestia AN Eston. SSR 6, Tech. and phys.-math. series, No. 1 (1957).
- Soltitsky, B. P. and Kartuzhansky, A. L., "The Measurement of Very Small Concentrations of  $\alpha$ -Emitters in Vegetable Matter with the Help of Thick Photographic Plates." Journal Tech. Phys. 27, No. 3 (1957).
- Spivak, G. V. and others, "The Observation of the Domain Structure of a Ferromagnetic with the Help of Photoelectrons." DAN SSSR 113, No. 1 (1957).
- Starik, I. E. and Starik-Smagina, A.S., "Polarographic Determination of Uranium." Proc. Khlopin Radium Inst. 5, No. 2 (1957).
- Starik, I. E., "The State of Micro-quantities of radioactive Elements in Liquid and Solid Phases." Progress of Chemistry XXVI, No. 4 (1957).
- Teller, E., "The General Problem of Controlled Thermonuclear Reactions." Progress of Physical Sciences LXI, No. 3 (1957).
- Tugarinov, A. I., "On the Determination of the Time of Metamorphosis of Uranium Minerals by the Method of Measurement of the Age of Witwatersrand Ores." (Review). Bulletin of the Commission for Determining the Absolute Age of Geol. Formations. AN SSSR, No. 2 (1957).
- Unkovskaya, V. A., "The Identification of Small Quantities of Uranium by the Fluorescence Method." Proc. Khlopin Radium Inst. 5, No. 2 (1957).
- Tsfasman, A. Z., "Some Features of Radioiodine Metabolism with Inadequate Blood Circulation." Clin. Medicine 35, No. 4 (1957).
- Cherdyntsev, V. V., "On the Fission and Stability of Heavy Nuclei." Proc. Khlopin Radium Inst. 5, No. 2 (1957).
- Shapiro, I. S., "On the Non-conservation of Parity in  $\beta$  Decay." Progress of Physical Sciences LXI, No. 3 (1957).
- Sherstnev, E. A., "The Production of Starch Containing Radiocarbon  $C^{14}$  by Photosynthesis." Botanical Journal 42, No. 3 (1957).
- Shepotyeva, E. S., "The Measurement of an Active Deposit of Radium and Actinium Using  $\beta$  Rays." Proc. Khlopin Radium Inst. 5, No. 2 (1957).
- Shcherbakov, M. Ya., "The Evaluation of the Resolving Power and the Choice of Cycles for a Three-stage Radiofrequency Mass-spectrometer." Journal Tech. Physics 27, No. 3 (1957).

FOREIGN LITERATURE PRESS

SUBSCRIPTIONS ARE NOW DUE

FOR 1958

FOR THE COLLECTED TRANSLATIONS OF FOREIGN

PERIODICAL LITERATURE

"PROBLEMS OF NUCLEAR ENGINEERING"

(VOLUME 2)

A series of translated papers and reviews edited by AN SSSR member-correspondent Prof. M. A. Styrikov.

The more interesting papers on the problems associated with nuclear engineering which appear in the foreign scientific and technical journals will be published in these translations. Particular attention will be paid to the problems of the design and construction of nuclear power reactors, the design of atomic power stations, the investigation of new fuel elements and various forms of constructional and other materials, the design of heat exchange, control, measurement and various types of auxiliary equipment, the problem of shielding and technical and economical aspects.

The translations are aimed at specialists in the field of nuclear engineering and related branches of nuclear technology, as well as a wide circle of scientific and technical workers interested in nuclear technology and its further development.

Each issue will consist of 10 folios.

There will be six issues a year. The annual subscription is 42 r.

Subscriptions are payable at city and regional branches of "Soyuzpechat," communication offices and sections, as well as to representatives at institutes and organizations.

## CONTENTS

	<u>Page</u>	<u>Russ. Page</u>
1. The Lenin Prize for the Construction of the First Atomic Power Station. <u>Yu. K.</u> . . . . .	847	87
2. Nuclear Multiplets in Light Odd-Odd Nuclei and their Manifestation in $\gamma$ -Transitions Occurring After Thermal Neutron Capture. <u>L. V. Groshev and A. M. Demidov</u> . . . . .	853	91
3. Determination of the Intensity of Short Fast-Neutron Pulses. <u>V. M. Gor- bachev and Yu. S. Zamyatnin</u> . . . . .	863	101
4. Angular Distribution of Elastic and Inelastic Scattering of 2.34 Mev Neutrons from Chromium, Iron and Lead. <u>O. A. Salnikov</u> . . . . .	869	106
5. Spectroscopic Quantitative Analysis of the Isotopic Composition of Gas Mix- tures Containing Hydrogen, Deuterium and Tritium. <u>M. N. Oganov and A. R. Striganov.</u> . . . . .	875	112
6. Analysis of Natural Radioactive Elements by Means of Laboratory Radio- metric Measurements. <u>I. M. Nazarov</u> . . . . .	885	121
7. Phosphate-Hydroxyquinoline Method for Separation and Volumetric De- termination of Zirconium. <u>A. V. Vinogradov and V. S. Shpinel</u> . . . . .	895	130
8. Natroautunite. <u>A. A. Chernikov, O. V. Krutetskaya and N. I. Organova</u> . . . . .	901	135
9. Individual Shielding During Maintenance Operations Under Conditions of Radioactive Contamination. <u>S. M. Gorodinsky and V. L. Shcherbakov</u> . . . . .	907	141

## Letters to the Editor

10. Critical Heat Loadings in Forced Flow of Water Heated Below Boiling. <u>B. A. Zenkevich and V. I. Subbotin.</u> . . . . .	915	149
11. Hydrodynamic Radiation from the Tracks of Ionizing Particles in Stable Liquids. <u>G. A. Askaryan.</u> . . . . .	921	152
12. Spark Source for Multiply-Charged Ions. <u>A. A. Plyutto, K. N. Kervalidze and I. F. Kvartskhava</u> . . . . .	925	153
13. Slow-Neutron Detector. <u>T. V. Timofeeva</u> . . . . .	929	156
14. Certain Problems Associated with the Use of Scintillation Counters in Dosimeters. <u>I. B. Keirim-Markus and Z. P. Lisitsina</u> . . . . .	931	157

## Scientific and Technical News

The Use of Radioactive and Stable Isotopes and of Radiation in the National Economy and for Scientific Purposes in the USSR. (937). At the Atomic Pavilion of the All-Union Industrial Exposition (Section on the Utilization of Radioactive Isotopes in Industry). (944). New Data on Neutron Cross Sections. (947). Iron-free Double-Focusing  $\beta$  Spectrometer. (948). Development of Atomic Energy in France. (950). Progress in the Study of Phase Diagrams of Metal Systems. (955). Distribution of Plutonium and Fission Products Between Molten Uranium and  $UF_3 - BaCl_2 (F_3)$  Mixtures. (955). Some Properties of Neptunium Metal. (956). Uranium-Zirconium Alloys. (957). Uranium Concentrating Works in Canada. (958). Radiobiological Work at the Institute of Biophysics, Academy of Sciences of the USSR, in 1956. (961).

CONTENTS (continued)

	<u>Page</u>	<u>Russ. Page</u>
15. Brief Communications .....	963	180
<b>Bibliography</b>		
16. New Literature .....	965	182

SIGNIFICANCE OF ABBREVIATIONS MOST FREQUENTLY  
ENCOUNTERED IN SOVIET PHYSICS PERIODICALS

AN SSSR	<i>Academy of Sciences, USSR</i>
FIAN	<i>Physics Institute, Academy of Sciences USSR</i>
GITI	<i>State Scientific and Technical Press</i>
GITTL	<i>State Press for Technical and Theoretical Literature</i>
GOI	<i>State Optical Institute</i>
GONTI	<i>State United Scientific and Technical Press</i>
Gosenergoizdat	<i>State Power Press</i>
Gosfizkhimizdat	<i>State Physical Chemistry Press</i>
Gozkhimizdat	<i>State Chemistry Press</i>
GOST	<i>All-Union State Standard</i>
Goztekhizdat	<i>State Technical Press</i>
GTTI	<i>State Technical and Theoretical Press</i>
GUPIAE	<i>State Office for Utilization of Atomic Energy</i>
IF KhI	<i>Institute of Physical Chemistry Research</i>
IFP	<i>Institute of Physical Problems</i>
IL	<i>Foreign Literature Press</i>
IPF	<i>Institute of Applied Physics</i>
IPM	<i>Institute of Applied Mathematics</i>
IREA	<i>Institute of Chemical Reagents</i>
ISN (Izd. Sov. Nauk)	<i>Soviet Science Press</i>
I YaP	<i>Institute of Nuclear Studies</i>
Izd	<i>Press (publishing house)</i>
KISO	<i>Solar Research Commission</i>
LETI	<i>Leningrad Electrotechnical Institute</i>
LFTI	<i>Leningrad Institute of Physics and Technology</i>
LIM	<i>Leningrad Institute of Metals</i>
LITMiO	<i>Leningrad Institute of Precision Instruments and Optics</i>
Mashgiz	<i>State Scientific-Technical Press for Machine Construction Literature</i>
MATI	<i>Moscow Aviation Technology Institute</i>
MGU	<i>Moscow State University</i>
Metallurgizdat	<i>Metallurgy Press</i>
MOPI	<i>Moscow Regional Institute of Physics</i>
NIAFIZ	<i>Scientific Research Association for Physics</i>
NIFI	<i>Scientific Research Institute of Physics</i>
NIIMM	<i>Scientific Research Institute of Mathematics and Mechanics</i>
NII ZVUKSZAPIOI	<i>Scientific Research Institute of Sound Recording</i>
NIKFI	<i>Scientific Institute of Motion Picture Photography</i>
OIYaI	<i>Joint Institute of Nuclear Studies</i>
ONTI	<i>United Scientific and Technical Press</i>
OTI	<i>Division of Technical Information</i>
OTN	<i>Division of Technical Science</i>
RIAN	<i>Radium Institute, Academy of Sciences of the USSR</i>
SPB	<i>All-Union Special Planning Office</i>
Stroiizdat	<i>Construction Press</i>
URALFTI	<i>Ural Institute of Physics and Technology</i>

NOTE: Abbreviations not on this list and not explained in the translation have been transliterated, no further information about their significance being available to us.—*Publisher.*



*Announcing . . . .* A *NEW* expanded program for the translation and publication of four leading Russian physics journals. *Published* by the American

Institute of Physics with the cooperation and support of the National Science Foundation.

Soviet Physics - Technical Physics. A translation of the "Journal of Technical Physics" of the Academy of Sciences of the U.S.S.R. 12 issues per year, Vol. 2 begins July 1957, approximately 3,000 Russian pages. Annually, \$90.00 domestic.

Soviet Physics - Acoustics. A translation of the "Journal of Acoustics" of the Academy of Sciences of the U.S.S.R. Four issues per year, approximately 400 Russian pages. Annually, \$12.00 domestic. Vol. 3 begins July 1957.

Soviet Physics - Doklady. A translation of the "Physics Section" of the Proceedings of the Academy of Sciences of the U.S.S.R. Six issues per year, approximately 800 Russian pages, Vol. 2 begins July 1957. Annually, \$25.00 domestic.

Soviet Physics - JETP. A translation of the "Journal of Experimental and Theoretical Physics" of the Academy of Sciences of the U.S.S.R. Twelve issues per year, approximately 3,700 Russian pages, Vol. 5 begins August 1957. Annually, \$75.00 domestic.

Back issues are available, either in complete sets or single copies.

All journals are to be complete translations of their Russian counterparts. The number of pages to be published represents the best estimate based on all available information now on hand.

Translated by competent, qualified scientists, the publications will provide all research laboratories and libraries with accurate and up-to-date information of the results of research in the U.S.S.R.

Subscriptions should be addressed to the

## AMERICAN INSTITUTE OF PHYSICS

335 East 45 Street

New York 17, N. Y.